SIMULATION AND OPTIMISATION OF A DRYING MODEL FOR A FORCED CONVECTION GRAIN DRYER

BOOKER ONYANGO OSODO

A Thesis Submitted in Partial Fulfillment of the Requirements for the Award of the Degree of Doctor of Philosophy (Renewable Energy Technology) in the Department of Energy Technology in the School of Engineering and Technology of Kenyatta University

KENYATTA UNIVERSITY

NOVEMBER 2018

DECLARATION

This thesis is my original work and has not been presented for award of any diploma or degree in any other University.

Signature ……Date ……

BOOKER ONYANGO OSODO

(REG NO: J98/25749/2011)

This thesis has been submitted for examination with our approval as the University supervisors.

Signature ……Date ……

Prof. Daudi M. Nyaanga

Associate Professor, Department of Agricultural Engineering, Egerton University

Signature ……Date ……

Dr. Jeremiah K. Kiplagat

Director, Institute of Energy studies and Research, Kenya Power, Nairobi

DEDICATION

This thesis is dedicated to my parents, and to my dear wife Rose and children Joel, George and Kennedy.

ACKNOWLEDGEMENT

My heart felt gratitude goes to my supervisors, Prof. Daudi Nyaanga and Dr Jeremy Kiplagat, for their guidance during the entire research process and thesis writing. Special thanks are due to Prof. Nyaanga for his encouragement and ever timely guidance through the entire process. I wish to thank Dr George Owino for his invaluable assistance in the simulation process, and for availing me the simulation software ComsolMultiphysics. Thanks are also due to Dr Joseph Muguthu for his assistance in the use of Minitab and Origin softwares, and to late Mr Runyiri for his assistance during the data collection period. Further thanks are due to Dr Njue, Dr Manene, Mr Kagucia, Mr Kobia and Silla for their technical assistance in fabrication and in electrical wiring of the Proportional Integral Derivative (PID) system. I would also wish to acknowledge the Higher Education Loans Board (HELB) for their tuition grant, and the National Council for Science, Technology and Innovation (NACOSTI) for funding my research.

TABLE OF CONTENTS

LIST OF TABLES

LIST OF FIGURE

LIST OF PLATES

LIST OF SYMBOLS / ACRONYMS

A	Area
A_c	Collector area
c_{pa}	Specific heat capacity of air
d_p	Particle Diameter
E	Energy
H_v	Latent Heat of Vaporisation
L_p	Length of Bed
P	Rate of Permeation
P_f	Fan power
ΔP	Pressure Drop
$\dot{m}$	Mass Flow rate
m_a	Mass of drying air
m_w	Mass of moisture evaporated
Q	Volume Flow Rate
T	Temperature of air
$T_{d,o}$	Air temperature at dryer outlet (K)
$T_{d,i}$	Air temperature at dryer inlet
I_g	Rate of total radiation incident on the absorber surface
$\frac{dM}{dt}$	Drying rate at any time
E	Energy consumed by dryer
X	Moisture content of wet material
X_r	Moisture Ratio
X_0	Initial moisture content
X_{eq}	Equilibrium moisture content
X_{cr}	Critical moisture content
MRR	Moisture Removal Rate
OSD	Open sun drying
DSD	Direct solar drying
ISD	Indirect solar drying

EUR	Energy Utilisation Ratio
HVAC	Heating Ventilation and Air Conditioning
MS	Mild steel
S/N Ratio	Signal to Noise Ratio

GREEK SYMBOLS

μ	Viscosity of Fluid (Drying Air)
u_o	Fluid Superficial Velocity
ε	Void Space of Bed
ρ	Density of drying Air
η	Efficiency

Subscripts

A	Air
c	Collector
cb	Drying cabinet
d	dryer
drg	Drying
f	Fan

ABSTRACT

Forced convection grain dryers are more efficient and achieve greater drying rates than natural convection dryers. However, it is necessary to provide an appropriate solar air heater in order to achieve the required drying air temperature. Well sized fan and drying cabinet, as well as an optimal combination of air velocity, temperature and grain layer thickness are also essential for improved performance of such a dryer. In order to predict variation of moisture content with time during the drying process, it is necessary to have an appropriate drying model. In this study carried out at Njoro, Nakuru County in Kenya, an experimental grain dryer was sized, fabricated and its performance investigated under different drying conditions. Simulation of air flow within an initial model of the dryer was done and the results used to size the fan and drying cabinet. The effect of air velocity, grain layer thickness, number of trays and temperature on drying efficiency (ratio of energy used in removing moisture to sum of energy lost by drying air and that used for running fan) and moisture removal rate (ratio of mass of moisture removed to mass of wet grain per unit time) was investigated. The Taguchi approach was used to determine the optimal combination of drying air velocity, temperature and grain layer thickness that could be used to ensure greatest drying efficiency and Moisture Removal Rate (MRR). Analysis of Variance (ANOVA) and Least Square Differences (LSD) tests were used to determine whether change of air velocity and grain layer thicknesses significantly affected drying efficiency as well as MRR. The best fitting drying model for drying maize grain was selected and subsequently used to develop a computer simulation model for predicting drying time. On the basis of simulation results, number of trays and mass of grain to be dried per batch, the experimental grain dryer developed was of dimensions 0.5 m x 0.5 m x 1.0 m and was equipped with a 0.039 kW centrifugal fan. MRR was found to decrease with increase in grain layer thickness as long as air velocity was kept constant. For example, at 0.41 m/s air velocity, as grain layer thickness increased from 0.02 to 0.08 m, MRR decreased from 0.061 to 0.022 kg moisture / (kg wet grain. hour). Drying efficiency decreased with increase in drying air temperature where-as MRR increased with rise in air temperature as long as air velocity and layer thickness remained constant. For an air velocity of 0.41 m/s and 0.04 m grain layer thickness, drying efficiency was 23.5% at 40 °C and reduced to 10.1 % at 55 °C. On the other hand, MRR increased from 0.045 to 0.058 kg moisture / (kg wet grain. hour) over the same temperature range. It was found that when drying a given grain layer thickness, use of two trays did not significantly improve MRR as compared to the use of one. As a result of the optimisation process, it was also determined that when drying was done under laboratory conditions, a combination of 0.41 m/s air velocity, 45 °C air temperature and 0.02m layer thickness resulted in greatest MRR and drying efficiency. The drying model that best describes the drying curve was found to be the Midilli model. The optimal drying parameters, if applied by the user of the dryer, will result in optimal drying rate and drying efficiency, and this in turn will lead to reduced post-harvest grain loss. The computer simulation model developed will enable the farmer to plan drying schedules. Application of simulation to size the fan and dryer cabinet should be emulated by those who seek to size dryers. It is recommended that further study be carried out to determine the effect of grain porosity on dryer performance. Investigations should also be done to find ways of utilizing the warm exhaust air from the dryer.

CHAPTER ONE: INTRODUCTION

1.1 Background

Food security of a nation is basic to the well-being of the nation's people, since access to quality, nutritious food is fundamental to human existence (USDA, 2018). However, a large proportion of food product is often lost between harvesting and consumption. The problem of food loss is particularly significant in developing countries. In these countries, food losses are estimated to be of the order of 40%, but can rise to be as high as 80% under very adverse conditions. A significant percentage of these losses is related to improper and or untimely drying of foodstuffs such as cereal grains, meat, tubers and fish (Bolaji and Olalusi, 2008). One reason for loss of grain after harvesting is spoilage resulting from high moisture content. Postharvest loss of maize in Kenya in 2007 was 21.1% (Hodges, 2009). Drying of the grain is necessary to avoid loss between harvesting and consumption. Moist and partly moist crop is prone to fungus infection, which renders it unusable. High moisture content also encourages loss due to attacks by insects, pests and increased respiration (Tiwari, 2002; Twidell and Weir, 2006). According to Barawal and Tiwari (2008), drying of crop helps to achieve better product quality, longer safe storage and reduction of post-harvest loss hence ensuring more food is available for the growing world population. Also, drying using solar energy leads to conservation of conventional energy sources.

Grain drying may be carried out using different sources of energy. However, solar energy is preferred to other alternative sources of energy such as wind and shale since it is abundant and freely available, inexhaustible and non-polluting (Akinona *et al.,* 2006; Lingayat *et al*., 2017). Traditionally, crop drying is done by placing it in the open, where it is exposed to the sun. In open sun drying, the absorbed radiation is converted to thermal energy, thereby increasing the temperature of the crop. This leads to evaporation of moisture from the grain, hence drying it. Although inexpensive and easy to adopt (El-sabaii and Shallaby, 2013), this mode of drying has several disadvantages. The grain is lost to rodents, birds and other pests since it is exposed. Unexpected rain may worsen the situation by further increasing the moisture content of the grain. Over drying, insufficient drying, contamination by

foreign materials such as dust, insects and micro-organisms are other problems associated with open sun drying (Tiwari, 2002; Tiwari, 2016). In addition, it results in loss of quality (Sharma and Wadhawan, 2018).

Other modes of grain drying are direct solar drying otherwise known as cabinet drying, and indirect solar drying. Direct solar drying utilizes the greenhouse effect to dry crop placed in an enclosure covered with a transparent cover, the crop being directly exposed to solar radiation. This mode of drying is, however limited to small scale applications due to its small capacity. The crop is also prone to discoloration due to direct exposure to solar radiation. Moisture condensation inside the glass cover reduces the transitivity of the glass. Some of the limitations of direct solar dryers are addressed by indirect solar dryers, in which heated air from a separate solar collector is passed through the crop, placed in a separate chamber (Tiwari, 2002). A mixed mode solar dryer utilises hot air from the solar collector, but at the same time the drying chamber absorbs energy directly through transparent walls and roof (Bolaji and Olalusi, 2008). According to Simate (2003), for the same quantity of grain dried, the mixed mode solar dryer is shorter in length than the indirect mode dryer, resulting in savings in construction material. This is because it receives extra energy through drying chamber transparent cover, reducing on energy demand from the collector. The drying cost in the mixed mode solar dryer is 26% lower than for indirect mode dryer. Also, there is more uniform moisture content distribution due to the additional drying from the direct radiation at the grain bed.

A natural convection solar dryer is the most appropriate where electricity is not available. Determination of an optimum design that will ensure best ventilation for any particular application is essential to ensuring best performance (Afriyie *et al*., 2011). However, natural convection solar dryers are limited due to inadequate air flow, leading to low drying rates and sometimes rotting of the crop. The grain layer thickness is also limited for similar reasons. In Forced convection solar drying, a fan is used to force the air through the grain in order to enhance the circulation of the heated air. Such dryers produce greater drying rates and it is easier to control the drying process (Mercer, 2012; Sallam *et al*., 2013). The resultant nutrient quality from a Forced Convection Solar Dryer is also superior to that from a Natural

Convection Dryer (Sharma and Wadhawan, 2018). The performance of a dryer may also be evaluated based on other criteria such as drying and dryer efficiency, uniformity of drying and quality of final product (extent of cracking and discoloration of grain) as well as total drying time (Mohanraj and Chandrasekar, 2009; Kassem *et al*., 2011).

Good performance of a dryer leads to desirable properties of dried product, such as low and uniform moisture content, minimal proportion of broken or damaged grain, low mold count and high nutritive value. High dryer efficiency is also desirable (Tiwari, 2016). The process of optimisation may be used to manipulate parameters that affect dryer performance characteristics, so that a combination of parameter levels that result in minimum or maximum performance measures, whichever is desired is determined. According to Sevik (2013) and Alqadhi *et al*. (2017), factors affecting drying rate include air temperature and velocity, product type, layer thickness and moisture content of product, method of drying, moisture diffusivity and drying kiln structure. Others are crop porosity and humidity of the surrounding air. The surface area of the crop exposed is yet another factor that affects drying rate (Twidell and Weir, 2006; Bolaji and Olalusi, 2008). Efficiency of a dryer, however, is affected by air flow rate and drying air temperature (Aissa *et al*., 2014; Balbine *et al*., 2015).

Simulation, which is the imitation or reproduction of the behavior of a system or process (Frangopoulos and Sciubba, 2002), is useful in the design, as it saves on the time and resources that would otherwise be required to obtain optimal performance. Modelling of solar drying curves involves describing variation of moisture ratio as a function of drying time (Kamenan *et al.,* 2009) and various researchers have developed different such drying models for a variety of products. According to Eterkin and Firat (2015), various statistical tools, such as Coefficient of Determination (R^2), Root Mean Square Error (RMSE), Modelling Efficiency (EF), Root Mean Square Deviation (RMSD), Reduced Chi Square (χ^2) may be used to select the best suitable model for describing drying behavior of a product.

1.2 Statement of the Problem

Forced convection solar dryers achieve greater drying rates than natural convection dryers (Harun *et al*., 2016). However, their performance is often not optimal. One reason for this is inadequate distribution of air flow, resulting in inadequate drying air in some sections of the dryer and hence uneven drying of the grain. Sometimes, the fan is undersized, leading to insufficient air flow (and velocity), or oversized, leading to excessive energy consumption and in extreme cases grain being blown upward. Also use of inappropriate grain layer thickness leads to poor performance. If the grain layer is too thick, some sections do not dry uniformly as they receive air which is saturated with moisture. If too thin, air exits while still having capacity to remove moisture, leading to low thermal efficiency. Very high air flow rates do not give the air enough time to absorb moisture, and may lead to low thermal efficiency while very low flow rates lead to low drying rate. Non-optimal layer thickness and air flow rate leads to poor dryer performance on the basis of drying efficiency, moisture removal rate and total drying time. Inability to predict drying time for different initial grain moisture content makes it impossible to plan drying schedules. Design of dryers that meet these criteria, without use of simulation, would require troublesome development stages, involving iterations and continued testing and use of prototypes, a process which would be expensive and time consuming.

1.3 Justification

Use of simulation to develop a dryer helps avoid the lengthy and expensive development stages that would otherwise be required in dryer design. Well distributed air flow ensures adequate air in all sections of the drying cabinet and therefore enables even drying of grain. Proper sizing of the fan leads to sufficient air flow, while avoiding excessive energy consumption by the fan, as well as the cost of an unnecessarily bigger fan. Use of an appropriate grain layer thickness ensures that all grain receive drying air which is not saturated with moisture, resulting in proper drying. Knowledge of the grain layer thickness also enables proper sizing of the drying cabinet to fit the grain to be dried. Adequate air velocity enables air penetration, allowing time for the air to remove moisture and achieve proper drying of the grain. Drying efficiency as well as moisture removal rate are thus improved.

The ability to predict drying time is of essence to the farmer, and will enable the farmer to plan a drying schedule. This is enabled by the computer simulation model developed as a result of the research.

1.4 Objectives of the Study

The broad objective of this research was to simulate, optimise and select a drying model for an experimental forced convection grain dryer.

The specific objectives were:

1. To simulate the grain quantity, fan and solar collector sizes for an experimental forced convection grain dryer
2. To establish the effect of air velocity, grain layer thickness, number of trays and drying air temperature on the performance of an experimental forced convection grain dryer
3. To optimise the performance of an experimental forced convection grain dryer and verify a selected drying model for it

1.5 Research Questions

1. What are the simulated grain quantities, fan and solar collector sizes for the experimental forced convection grain dryer?
2. How do air velocity, grain layer thickness, number of trays and drying air temperature affect the performance of the experimental forced convection grain dryer?
3. What is the optimal combination of drying air velocity, temperature and grain layer thickness that should be used for the grain dryer and which drying model best describes the drying curve it?

1.6 Scope and Limitations

This research dealt with a forced convection grain dryer, utilizing solar air heating on one hand and electrical air heating on the other. Simulation of air flow through the drying cabinet using ComsolMultiphysics software was carried out and used to size the drying cabinet and fan. The study sought to optimize drying efficiency as well as moisture removal rate. The dryer used a centrifugal suction fan to facilitate

forced convection and operated between 40 °C and 60 ºC. Air velocity ranged between 0.21 m/s and 0.41 m/s and grain layer thickness between 0.02 m and 0.08 m. The dryer performance was evaluated using maize grain, and experiments carried out in the open sunshine as well as in laboratory conditions.

CHAPTER TWO: LITERATURE REVIEW

This chapter outlines literature on crop drying, especially the application of solar energy in the grain drying process. It reviews the application of simulation in the development and optimisation of a forced convection solar grain dryer as well as selection and fitting of various drying models for different products.

2.1 Solar Crop Drying

A great proportion of crop is often lost between harvesting and consumption. The problem of post-harvest loss is particularly significant in developing countries. In these countries, these losses are estimated to be of the order of 40%, but can rise to be as high as 80% under very adverse conditions (Bolaji and Olalusi, 2008). According to Adebayo *et al.* (2014) loss of crop occurs in the field (15%), during harvesting (13-20%), as well as during processing and storage (15-25%). Post-harvest loss of crop may be attributed to different causes. Pests, such as large grain borer account for 10-20% loss, while 5-10% of the losses may be attributed to poor storage facilities. Diseases, on the other hand, contribute to 5% of post-harvest crop loss (Bett and Nguyo, 2007). Also, a significant percentage of the losses is related to improper or untimely drying of foodstuffs such as cereal grains, meat, tubers and fish (Bolaji and Olalusi, 2008). Incidences of post-harvest product loss in Kenya have been estimated at 30%, and can rise to be as high as 100% with the advent of afflotoxin (Irungu, 2010). Maize is usually harvested with moisture content of between 18 % and 24 %. Drying maize to below 13.5% moisture content increases storage life and maintains quality by decreasing growth of fungi and insect infestation during storage. It also prevents germination (FAO, 1998; Irungu, 2010).

2.1.1 Solar thermal collectors

A Solar thermal collector serves the purpose of trapping solar radiation which is then used for heating the working fluid. It usually consists of a black surface, the absorber, and a transparent cover. The absorber does not trap all the incident energy from the sun. It incurs losses due to reflection by the encapsulation (cover) or the absorber itself, convection as a result of exchange with the surrounding air, as well as radiation from the hot absorber surface. The efficiency of the collector depends

on two factors: the extent to which solar radiation is converted to heat, and the extent of heat losses to the surroundings (Klaus *et al*., 2014).

Solar collectors are classified into three categories: uncovered, covered and vacuum collectors. Uncovered collectors have no transparent cover hence the radiation is directly incident on the absorber surface. Reflection losses are minimized due to absence of reflective cover. Covered collectors have a transparent covering material, providing extra insulation, but there is also increase in reflective losses. In vacuum collectors, also called Evacuated Tube Solar Collectors (ETSCs), the absorber is encapsulated in vacuum tubes hence there is little loss to the surroundings. They can therefore be used for high temperature applications. Another way of classifying solar collectors is according to their shape, hence flat plate and concentrating collectors. Flat plate collectors have flat absorbers, and can deliver moderate temperatures, up to around 100 °C. Concentrating collectors have their performance optimized by decreasing the area of heat loss. An optical device with a smaller area is placed between the source of radiation and the absorber. They find use in higher temperature applications (Klaus *et al*., 2014).

In a solar air heater, air is circulated in contact with a black radiation-absorbing surface, above which there is usually one or more transparent covers to reduce heat loss. Although solar air heaters come in various forms, a typical one consists of an absorbing plate, a rear plate with insulation below it, and the transparent cover on the exposed side. The air may flow above, below or both above and below the absorber plate. The absorber plate may be flat, corrugated (with rounded or v-troughs), finned or of the matrix type. In the matrix type, an absorbing matrix is placed in the air flow path between the glazing and the absorber plate. Another type of absorber plate is the overlapped transparent plate type, composed of a staggered array of partially blackened transparent plates. The transpiration collector, also called porous bed collector, is a variation of the matrix type, in which the matrix is closely packed, and the back absorber plate is eliminated (Garg and Prakash, 2005).

One limitation of flat plate solar collectors is convection heat loss, which reduces their thermal efficiency considerably. An evacuated solar collector reduces

convection heat losses by removing air between the absorber and the glass cover, leaving radiation as the only remaining mechanism for heat loss. Because it is difficult to maintain vacuum in a flat plate collector, Evacuated Tube Solar Collectors (ETSC) were invented. Umayal *et al*. (2013) reported that evacuated tube solar collectors have many advantages over the flat plate collectors mostly used in solar dryers. These include high efficiency in performance as well as ability to perform even in bad weather. Dabra *et al*. (2013) noted that the performance of a vacuum tube collector was better than for a flat plate collector and was independent of climatic conditions. Reflectors may be used to enhance the efficiency of a solar collector. Maiti *et al*. (2011), while investigating an indirect solar dryer utilised for drying wet papads, showed that use of reflectors enhanced collector efficiency from 40 % to 58.5 %.

A flat plate collector was applied in this research due to the relatively low temperature requirement of 60 °C and also the abundance of solar energy in the region of the research. For such a collector, solar collector area A_c may be determined from eq. (2.1), used by Dabra *et al*. (2013) and Aduewa *et al*. (2014).

$$A_C = \frac{m_a c_{pa}(\dot{T}_o - T_a)}{I_c \eta} \tag{2.1}$$

In the equation, $\dot{m}_a$ and c_{pa} represented mass flow rate and specific heat capacity of air respectively, while I_c and η stood for maximum insolation on collector surface and solar collector efficiency, also respectively. T_o and T_a were used to represent optimum dryer temperature and inlet temperature at ambient.

2.1.2 Types of solar dryers

Drying systems may be classified into two broad categories: fossil or conventional dryers and solar dryers. Fossil dryers utilize fossil fuels as their source of energy. Their disadvantages are those associated with application of fossil fuels as a source of energy. For example, fossil fuel deposits are exhaustible, leading to high prices. Their use also leads to greenhouse gases as well as other pollutant gases (Weiss and Buchinger, 2012). In the tropics, application of solar energy is preferred to that of

other sources of energy since it is abundant, inexhaustible and non-polluting. This makes the use of solar dryers a more attractive option in crop drying (Akinona *et al*., 2006).

Drying using solar energy may be carried out by simply placing the crop in the open where it is exposed to radiation from the sun, in a process called Open Sun drying (OSD). Traditionally, grains have always been dried by OSD (Sodha *et al.*, 1985). In OSD, however, there is considerable loss of the grain due to rodents, birds, insects and micro-organisms. Unexpected rain may result in increasing the moisture in the grain. Other problems encountered in OSD are discolouration due to ultra-violet radiation, as well as contamination by dust, dirt, insects and micro-organisms. There may also be over drying or insufficient drying (Tiwari, 2002).

Solar dryers may be classified into two broad categories namely passive solar dryers and active solar dryers. Passive solar dryers (Fig. 2.1), also called natural convection or natural circulation dryers, depend entirely on solar energy for their operation. Solar heated air is circulated through the crop by buoyancy forces or a result of wind pressure, acting either singularly or in combination (Weiss and Buchinger, 2012; Gregoire, 2009). According to Mumba (1996), passive solar dryers have one major limitation, being inadequate air flow leading to low drying rates and crop rotting. As air passes through the wet crop, it becomes nearly saturated so that its temperature is lowered to nearly ambient temperature. Since air temperature is then not substantially different from that of the ambient air, the resulting buoyancy forces (which are proportional to the temperature difference) are very small and produce very low air flow rates. Afriyie *et al*. (2009) found that a solar chimney may be used to increase air flow rate. However, this is only for low ambient relative humidity.

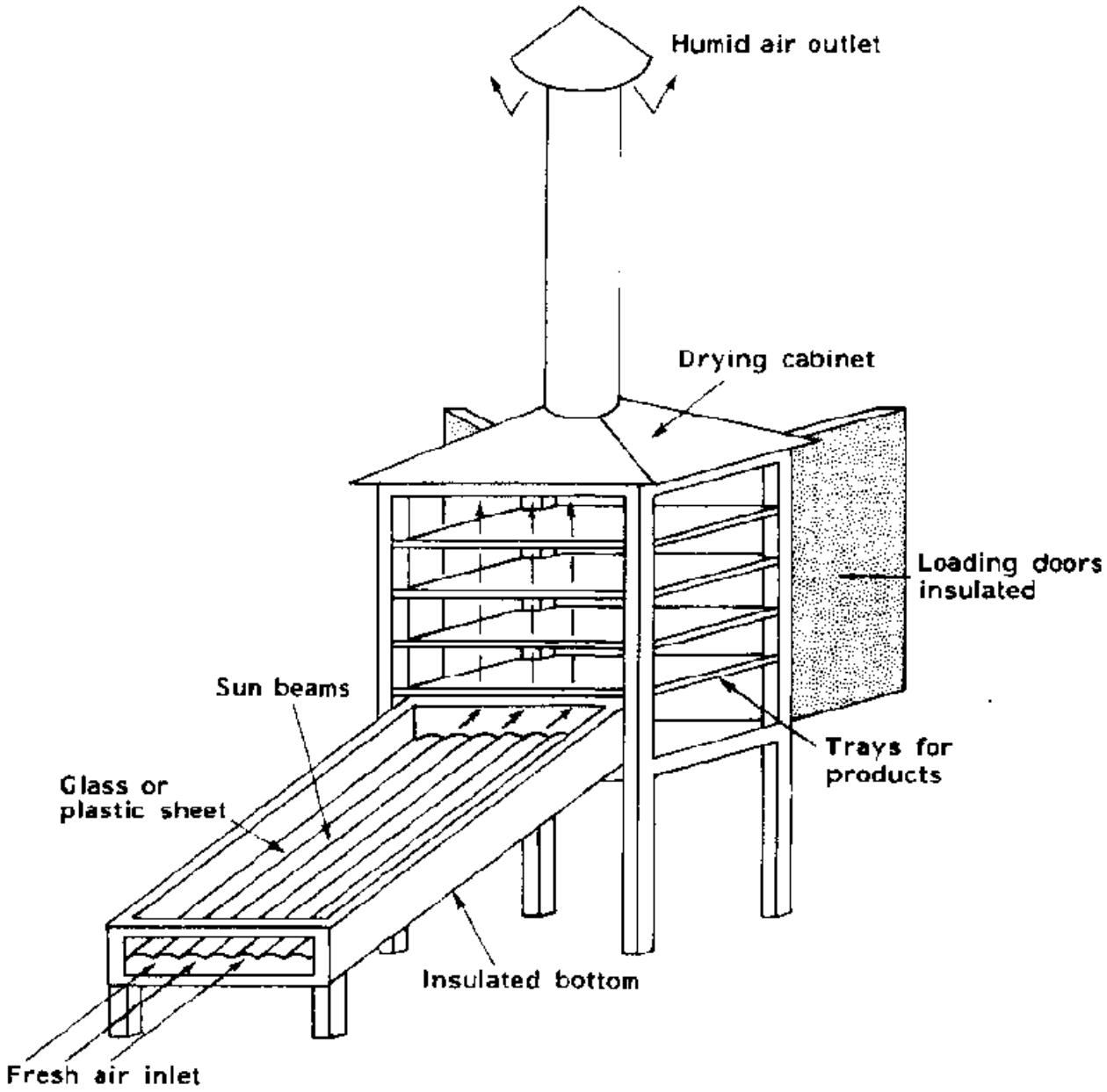

Figure 2. 1: Natural Convection Solar Drier

Source: Tiwari (2016)

Active solar dryers (Fig.2.2), also called forced convection or hybrid solar dryers, use a fan to enhance circulation of the solar heated air. Optimum air flow can therefore be provided throughout the drying process to control temperature and moisture content of the air. The bulk depth is therefore less restricted and the capacity and reliability of the dryer is therefore increased considerably. In such dryers, the larger the ratio of food surface area to volume, the quicker the

evaporation of moisture. Sallam *et al*. (2013) compared drying of mint in two identical prototype solar dryers used under natural and forced convection modes. For the forced convection mode, a 0.75 kW fan was used and air entered the dryer at an inlet velocity of 4.2 m/s. This air velocity was rather high, in the light of findings by Sevik *et al*. (2013) who suggested that drying rate would not be influenced by air velocities above 4.2 m/s. They, however, reported that drying rates were higher for forced convection than for natural convection drying, findings similar to those of Jangai *et al*. (2009) and Ikejiofor (2010).

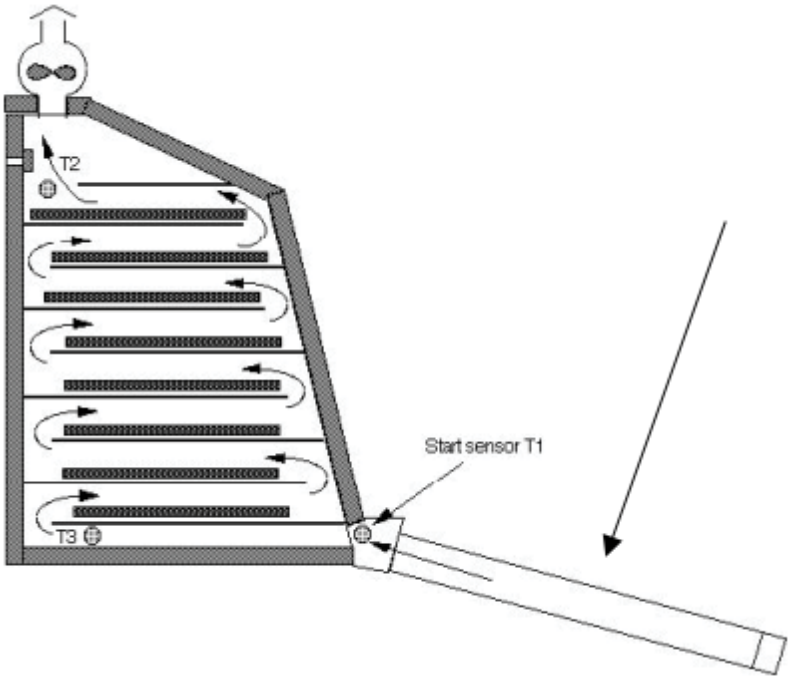

Figure 2. 2: Active Solar Drier 1

Source: Tiwari (2016)

Three distinct subclasses of passive or active solar drying systems can be identified, depending on the design arrangement of the system components and the mode of utilization of solar heat. These are: Integral or direct solar dryers, distributed or indirect solar dryers and mixed mode solar dryers (Weiss and Buchinger, 2012; Gregoire, 2009).

An integral or Direct Solar Dryer (DSD), shown in Fig. 2.3, consists of an insulated drying chamber covered with a transparent material such as glass. A small fraction

of the incident solar radiation is reflected back into the atmosphere by the glass cover, while the rest is transmitted through the glass onto the crop. The crop temperature is raised by the radiation incident on it, and it starts emitting long wavelength radiation, which unlike for OSD, is prevented from escaping into the atmosphere by the glass cover. As a result, the temperature in the chamber above the crop rises. The glass cover also prevents heat loss to the ambient by convection, thereby further increasing the temperature of the crop and chamber. As for OSD, the crop loses water by evaporation. Air entering into the chamber from below and exiting at the top takes away the moisture by natural convection as in passive dryers, or by forced convection, in the case of active dryers. Limitations of direct solar dryers include:

a) Small capacity limiting it to small scale applications
b) Discoloration of the crop due to direct exposure to solar radiation
c) Moisture condensation inside the glass cover reducing its transitivity
d) Insufficient rise in crop temperature affecting moisture removal (Tiwari, 2002).

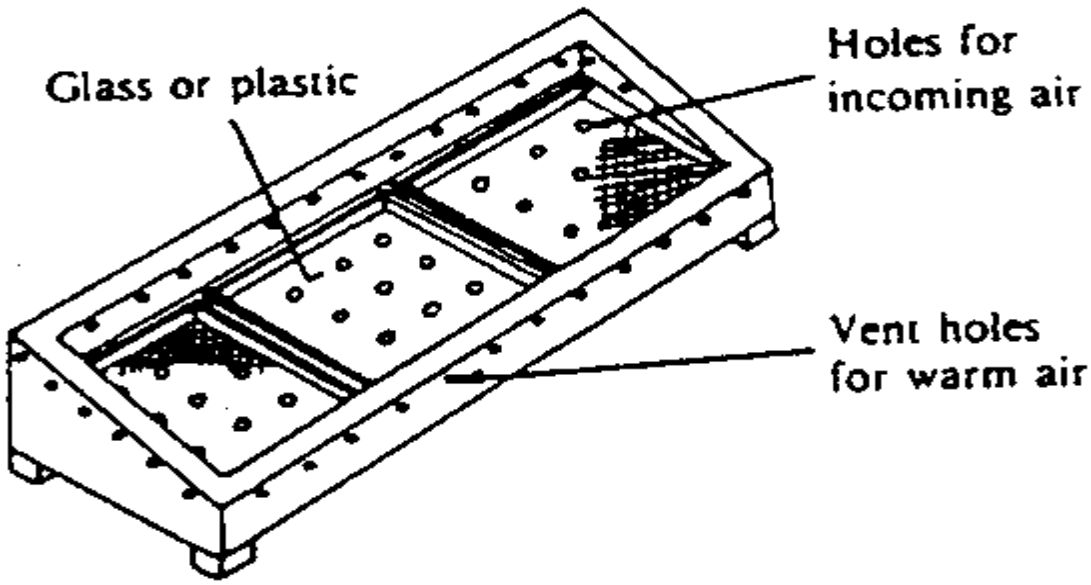

Figure 2. 3: Direct Solar Dryer

Source: Tiwari (2016)

In distributed or indirect solar dryers (ISD), the crop is not directly exposed to solar radiation in order to minimize discoloration and cracking of the crop surface.

Instead, heated air from a separate solar collector is passed through the crop, placed in a separate chamber. Evaporation of moisture from the crop is obtained as in OSD and DSD (Tiwari, 2002).

In a mixed mode solar dryer, heated air from a separate solar collector is passed through a grain bed and at the same time the drying cabinet absorbs solar energy directly through a transparent wall and roof (Bolaji and Olalusi, 2008). Because solar dryers are not functional at night or during rainy or cloudy conditions, studies have been carried out to integrate them with back up heaters or heat storage systems. Kaaya and Kyamuhangire (2010) as well as Rigit *et al*. (2013) showed that use of biomass back up burners not only reduces drying time, but also improves quality of product.

This research adopted an indirect mode of forced convection solar drying. This was to ensure cracking and discoloration of grain, common in the direct mode was prevented. Application of a fan also made it possible to vary air flow rate to investigate how this affected the drying process.

2.1.3 Drying theory

The drying of grain occurs as water at the surface evaporates and water in the inner part migrates to the surface to also get evaporated. If left for long enough, a moist grain will give up water to the surrounding air until the grain reaches its equilibrium moisture content. Much of the moisture present in the crop is ‘free water’, loosely held in the cell pores and is therefore quickly lost after harvest. The remaining water (usually 30-40%) is bound to the cell walls by hydrogen bonds, and is therefore harder to remove. Unsaturated air passing over the grain takes up water from it by evaporation, the heat to evaporate the water being derived from the air and the crop (Twidell and Weir, 2006; Bolaji and Olalusi, 2008).

When a kernel of grain dries, two processes occur simultaneously: transfer of heat from the air to the kernel to evaporate water and transfer of mass as internal liquid and vapour move from kernel to air. Several theories have been advanced to explain movement of moisture within the kernel. All may occur simultaneously, but one may be predominant at any one time. Also, different ones may be predominant at

different times. The diffusion theory relies on Fick's law [eq. (2.2)] to explain liquid diffusion within the kernel. In this equation, P is the rate of permeation while k, A and $\frac{\partial C}{\partial x}$ represent diffusion constant, cross sectional area and concentration gradient respectively.

$$P = -kA[\frac{\partial C}{\partial x}] \quad (2.2)$$

According to the capillary flow theory, the liquid flows through the pores due to molecular attraction between solid and liquid, the rate of flow depending upon size of the pores and their distribution within the material. The gravity theory attributes moisture movement to vertical gravitational pull of the water towards the bottom of the solid. The porous flow theory, however, postulates that moisture flow is due to the combined effect of capillarity suction, external pressure and gravity, and assumes that rate of flow is proportional to moisture density gradient. The vapourisation-condensation theory postulates that temperature differences cause pressure gradients within the solid, which result in evaporation of the liquid and subsequent condensation in the cooler surface. Thus, when the solid is heated at the bottom, vapour diffuses upwards, repeatedly being condensed and evaporated, eventually escaping as vapour in the air. The convection theory says that moisture movement is due to the temperature gradient, and is in the direction of decreasing temperature (Jerger, 1951). Some of these theories were considered relevant to this research while others were not. The diffusion theory, for example was considered relevant since concentration gradient of moisture is affected by layer thickness. For a given amount of moisture, a thinner layer would result in a higher concentration gradient. The porous flow theory would be relevant since greater air velocity is a result of greater external pressure, thus increasing moisture flow. This would also apply to the vapourisation-condensation theory, since increased temperature changes would influence pressure gradients in the grain layer resulting in greater moisture movement rates. However, the gravity theory was considered to be inapplicable since air flow and moisture movement were upwards against gravitational forces. Similarly, capillary flow theory could not account for differences in moisture flow

because one product was investigated, in which pore sizes and distribution could be assumed to be similar.

Kamenan *et al*. (2009), while analysing drying rate curve for cassava and plantain banana, showed the existence of two distinct phases: a constant drying rate phase and a falling drying rate phase. The constant drying rate phase, which is short and not available for all products, involves rise in temperature of the product up to attaining the wet bulb temperature characteristic of the drying environment. It is not taken into account during the analysis of the drying rate curve but describes a rapid movement of free water by capillarity from inside the product to the surface. In this phase, drying does not depend on the nature of the product. It only depends on the drying conditions, the moisture content tending towards the critical moisture content development.

The falling drying rate phase is further subdivided into two: the falling drying rapid rate phase and the falling drying slow rate phase. Once the moisture content is below the critical moisture level, capillary forces are not sufficient to transport moisture to the surface of the product. At the beginning of the falling drying rate phase, drying rate reduces rapidly. The zone of evaporation is now inside the product and there exist two sections with different modes of transport. Upstream in the centre of the product, there is still migration of water by capillarity. Downstream, migration is due to the diffusion phenomenon, in the case of vapour, and diffusion sorption, in the case of tied water. The moisture content now tends towards its level at hygroscopic equilibrium. The falling drying slow rate phase begins once the product is in the hygroscopic domain. During this phase, a resistance to vapour diffusion appears and if the temperature continues to rise, the first fissures in the product may appear (Kamenan *et al*., 2009).

2.2 Airflow Simulation and Sizing of Dryer

Simulation is the imitation of the operation of a real world process or system over time. It is the act of putting models to work (Frangopoulos and Sciubba, 2002). Sizing of the dryer involved determining fan power, number of drying trays as well as determining dimensions of the solar air collector and drying cabinet. In this

research, airflow through the dryer was simulated in order to ensure it would be well distributed within the drying chamber for uniform drying of the grain. . Also, the air must be able to penetrate the grain layers for drying to occur. This can be effected by ensuring the grain layers are not too thick, and that the number of grain layers is not too many for the air to penetrate. A fan that is able to overcome the static resistance to air flow also needs to be selected. According to Misha *et al*. (2013), uneven drying is the consequence of poor air flow distribution in the drying chamber. Product closer to the air inlet is better dried than that further, due to reduced temperature and air velocity. Actual measurement of air flow parameters is not only expensive and time consuming, but is also difficult since sensors have to be installed in many different positions. Simulation is a better option to apply in the investigation of air flow in a dryer. Simulating air flow within the drying cabinet can be used to ensure the design enhances air distribution. This would reduce or eliminate non-uniformity in drying, thereby increasing dryer efficiency. It may also be applied for predicting the pressure drop within the drying chamber, and use it to size the fan.

Misha *et al*. (2015) simulated the air flow distribution in a drying chamber using Computational Fluid Dynamics (CFD) and found that there was good agreement between simulated and experimental data. Onisimi *et al*. (2016) used ANSYS FLUENT, a CFD software to analyse temperature distribution, pressure, air flow and kinetic turbulence at various temperatures between 40 and 60 °C. The average temperature distribution in the system was determined to range between 33.2 and 52.7 °C while the average air velocity in the system was 1.965 m/s, the exit air velocity being constant at 48.74 m/s. The maximum pressure in the system was found to be 6453.32 Pa. Khaldi and Korti (2018) used CFD in investigating effect of air inlet size and packed bed thickness on dynamic and thermal behavior of the dryer. They reported that increasing air inlet size from 0.04 m to 0.10 m increased extraction of air by 13 %, at the same time reducing crop temperature by 14 %. Increasing the packed bed thickness by 0.15 m extended the drying time by 23 %. In the current study, simulation was used to determine fan power requirements for the dryer.

2.2.1 Simulation

Simulation deals with two systems. The first is the physical system, whose performance is to be studied, or whose design is to be optimized. The physical system may be a real system that is actually in operation, or it may only be on paper, and still at the design stage. The second system involved in simulation is a model of the system to be studied. The model may itself be another physical system, or it may be a mathematical model. Usually, simulation involves first, creation of a mathematical model of the system to be studied. This is followed, whenever possible, by manipulation of the model to obtain desired information. A computer is then used as another system to simulate the mathematical model. Then starting from the model, a second physical system is created (Frangopoulos and Sciubba, 2002). This process is summarized in Figure 2.4. Solar drying is, according to Garg and Prakash (2005), a complex phenomenon, depending on several parameters. Simulation models are greatly useful in predicting and studying inter-relationships between various parameters that affect the solar drying process.

Simulation soft wares come in different forms. Analysis Systems (ANSYS) software is a general purpose finite element modeling package for numerically solving a wide range of mechanical problems in areas such as heat transfer, fluid mechanics, static and dynamic structural analysis. It allows the construction of computer models of structures, components or systems, application of operating loads and other design criteria and study of parameters such as temperature distributions, air velocity and pressure. It permits an evaluation of a design without having multiple prototypes in testing (Nakasone *et al.,* 2006).

A finite element solution may be broken into three stages. The first of these stages is preprocessing which involves defining the problem. The major steps included here are definition of the key points, definition of element type and material/ geometric properties; and meshing of lines, areas and volumes. Second is the solution stage, involving specifying of loads and constraints after which the set of resulting equations are solved. Third is the post processing stage, in which one may wish to see lists of nodal displacements, element forces and moments, deflection plots as well as contour diagrams and temperature maps. There are two methods of using

ANSYS. First is by means of the Graphical User Interface (GUI), which uses conventions of popular Windows and X-Windows based programs. The second method uses command files (Nakasone *et al*., 2006). Li *et al*. (2015) used ANSYS to simulate air flow in a mixed flow grain dryer in order to determine how air velocity was influenced by air duct size. They found that smaller air ducts yielded higher air velocities.

Transient Systems (TRNSYS) uses a graphically based software environment to simulate the behavior of transient systems. It is made up of two parts. The first part is the engine, called the kernel. It reads and processes the input files, iteratively solves the system, determines convergence and plots the system variables. The second part is an extensive library of components, each of which models the performance of one part of the system. Models in the library include pumps, wind turbines and basic HVAC equipment, among approximately 150 other models in a standard library (University of Wisconsin, 2013). Habtamu (2008) used TRNSYS to simulate a cereal solar dryer and was able to predict useful energy and collector output temperatures for given incident flux, ambient air temperature and solar collector parameters. However, these predictions were not verified experimentally.

ComsolMultiphysics software is a general purpose software platform based on advanced numerical methods and is used for modeling and simulating Physics based problems. It is suitable for electrical, mechanical, fluid flow and chemical applications, among others. In addition, the user is able to include own equations that may describe a material property, boundary, source or even a unique set of partial differential equations. The user can then create new physics interphases from the equations entered (Comsol, 2012).

2.2.2 Pressure drop and fan sizing

a) Pressure drop

Jia *et al*. (2009) explain that air flow through packed material may be described using the Ergun equation (eq. 2.3). According to this equation, pressure drop (ΔP), for fluid velocity(u_0) depends on particle diameter (d_p), length of bed (L_p), fluid

viscosity (μ), void space (ε) and fluid density (ρ). The effect of cross sectional area (due to container diameter) is ignored in this equation.

$$\frac{\Delta P}{L_p} = \frac{150\,\mu(1-\varepsilon)^2 u_0}{\varepsilon^3 d_p^2} + \frac{1.75\,(1-\varepsilon)\rho\,\mu^2}{\varepsilon^3\ d_p} \qquad (2.3)$$

Although there are many channels through packed material, fluid will normally only flow through a few of them, a phenomenon called channeling. This leads to lack of distribution of fluid flow. Another limitation is that of formation of hot spots, which leads to damage to the bed and packing materials (Sachdeva *et al*., 2012). The pressure drop in the drying chamber limits the number of trays that may be used. Due to high resistance to air flow through drying product, only a few drying shelves can be used without significantly affecting air movement (Aissa *et al*., 2014).

Jia *et al*. (2009) used glass beads and copper coated metal balls and air velocities ranging between 1 m/s – 4 m/s to study pressure drops through packed material and found that experimental data were within 20 % of the values predicted using Ergun equation. This equation was used in this research to simulate airflow up the dryer with grain as the packed material in an attempt to predict the pressure drop. Although the packed material was not grain, the air velocities used in the current research were within the range investigated by Jia *et al.* (2009).

b) Fan sizing

According to Wilcke and Morey (2015), different crops have different airflow requirements for drying, necessitating selection of a fan that will deliver airflows within the recommended range. Greater airflows will require larger fans, leading to increased costs, while smaller ones may result in unacceptable crop quality. Also, the fan must develop sufficient pressure to overcome resistance to airflow. Airflow resistance of a crop (and hence the fan pressure required to overcome it), depends on how fast the air is moving, and on how long and narrow the air paths are. These factors are a function of the particular crop (size and shape of its seeds), crop depth and the required airflow rate.

Typical air flow rates range from 0.25-0.51 $m^3/s.m^2$ of perforated screen area, these flow rates creating relatively low static pressures of 0.249-1.25 kPa in cross flow and mixed-flow dryers. The fan to be used for such a dryer must be of sufficient capacity to overcome this static pressure, being the resistive force the fan works against while trying to push the air through the grain column (Maier and Bakker-Arkema, 2002).

Fan power (P_f) may be obtained either from manufacturers' charts or from eqs. (2.4) and (2.5), as suggested by Wilcke and Morey (2015) and Maier and Bakker-Arkema (2002).

$$P_f = \frac{(\dot{V} x\, P_s)}{63.56\, \eta_{fp}} \tag{2.4}$$

$$P_f = \frac{(\dot{V} x\, P_s)}{3814} \tag{2.5}$$

($\dot{V}$ is air volume flow rate while P_s represents static pressure)

The equations are similar, although for eq. (2.5), an impeller efficiency of 60% has been assumed and incorporated. According to Weiss and Buchinger (2012), fan efficiency ranges between 30 % and 70 %, hence the assumption is reasonable to cater for most fans if cost of fan and that of power is the major consideration. In the current study, eq. 2.5 was adopted to cater for a general situation where efficiency of fan does not have to be used every time.

The fan may either be an axial-flow one, in which air is moved by rotating blades parallel to the shaft, or a centrifugal fan, where air enters parallel to the shaft, is moved radially through the blades, before being discharged tangentially from the scroll housing. Axial fans yield higher airflow rates up to 0.996 kPa and above static pressure, while centrifugal fans are preferred above 1.49 kPa static pressure (Maier and Bakker-Arkema, 2002).

2.3 Effect of Various Factors on Dryer Performance

Various researchers have evaluated the performance of solar dryers on the basis of different criteria. Mohanraj and Chandrasekar (2009) use dryer thermal efficiency, drying rate and specific moisture extraction rate as their basis, while Kassem *et al.* (2011) base their evaluation solely on dryer efficiency. Uniformity of drying in different trays, and even within the same tray, is also important in evaluating dryer performance. Drying time within a permissible maximum temperature so as not to cause loss in flavour, colour, aroma and vitamins is another measure (Murthy, 2009).

This research focused on drying rate and efficiency of dryer as performance criteria, these being factors that would interest the user.

Drying rate $\frac{dM}{dt}$ is given by eq. (2.6) [Twidell and Weir, 2006], M_i and M_f being initial and final moisture fractions, respectively during a drying time t.

$$\frac{dM}{dt} = \frac{M_i - M_f}{t} x\ 100 \tag{2.6}$$

However, drying rate varies every instant and would not be beneficial to the user, in planning drying schedules, for example. This research therefore adopted moisture removal rate (ratio of mass of moisture removed to mass of wet grain per hour) as this would then be used to predict the total drying time for some given quantity of product with certain moisture content.

Factors affecting drying rate include air temperature, air velocity, porosity of product, layer thickness and moisture content of product. Other factors are humidity of the surrounding air, method of drying, moisture diffusivity and drying kiln structure (Twidell and Weir, 2006; Bolaji and Olalusi, 2008; Sevik, 2013). The total energy required to dry a given quantity of material may be estimated using eq. (2.7), the basic energy balance equation for the evaporation of water (Twidell and Weir, 2006; Bolaji and Olalusi, 2008).

$$m_w H_v = m_a c_{pa} (T_1 - T_2) \tag{2.7}$$

In this equation, m_a and m_w represent mass of air through dryer and of water vapour evaporated, respectively. H_v and c_{pa} are the latent heat of vapourisation for water and specific heat capacity of air, while T_1 and T_2 represent initial and final air temperatures, also respectively

Different researchers have used different criteria and equations to determine efficiency of dryers. Average dryer thermal efficiency η_{dr}, applied by Aduewa *et al*. (2014) using eq. (2.8) was determined to be 31.45% at 60°C.

$$\eta_{dr} = \frac{(m_f c_{pf} + m_w c_{pw})(T_2 - T_1) + m_v L_v}{A_c I \alpha \tau} \tag{2.8}$$

Here $m_{f,}, m_w, m_v$ represented masses of dried food, water in the food and water vapour lost, where-as specific heat capacities of food, and of the water, both at constant temperature were represented by c_{pf} and c_{pw}. On the other hand T_2, T_1, and L_v represented final and initial temperatures as well as latent heat of vapourisation of water, while α and τ were the absorptivity of collector plate and transmitivity of the collector glazing, respectively. This equation was not applied in this research since the focus of the study was the utilization of energy available in the hot air entering the drying cabinet in in moisture removal, and not the energy absorbed by the solar collector. Also the equation required mass of dried food, which was not determined in this study.

Aissa *et al*. (2014), however, determined overall system drying efficiency η_d, being the ratio of energy required to evaporate moisture to that supplied to solar dryer (including that consumed by blower), was obtained from eq. (2.9).

$$\eta_d = \frac{m_g H_v}{IAt + Q_b} \tag{2.9}$$

In this equation, m_g, H_v and I represented mass of water removed, latent heat of vapourisation of water and insolation, while A stood for dryer area and Q_b blower energy supplied to dryer in time t. Again, this was not applied in this research due to involvement of solar collector energy, which was not the focus of this research. The

indicator of efficiency adopted in the current research was drying efficiency (ratio of energy used in removing moisture to sum of energy lost by drying air and that used for running fan).

Researchers have investigated products such as longan, bananas, yam, beans, maize, mango and cassava using forced convection dryers. Drying air temperature in most of these studies ranged between 40 °C and 60 °C (Mumba, 1996; Lahsasni *et al*. 2004; Agbossou *et al.*, 2016). Aissa *et al*. (2014) used a wider temperature range of 35.2 °C – 69.8 °C. In the current study, a lower limit of 40 °C was used to ensure drying air temperature was always greater than the ambient, while an upper limit of 60 °C was used to avoid cracking and discoloration of the grain. Air velocities in most studies ranged from 0.22 m/s to 2 m/s (Jangai *et al*. 2009; Kamenan *et al.* 2009; Afriyie *et al*. 2009; Ikejiofor, 2010; Gatea, 2011; Rahmatinejad *et al*., 2016). In this research, the air velocity range applied was 0.21 m/s – 0.41 m/s. Very low air velocities would have resulted in very high drying air temperatures, while high velocities would lead to low air temperatures. Also Sevik (2013) reported that air velocities above 0.42 m/s have no influence on drying rates.

2.3.1 Effect of air velocity

A forced convection solar grain dryer requires adequate air flow in order for the drying process to occur effectively. This requires the use of an appropriate fan, one that will overcome the static pressure developed in the drying cabinet, and also ensure air flow at the appropriate velocity. Murthy (2009) reported that optimum air flow rate is essential for achieving satisfactory dryer performance. Slower air flow rate may increase drying air temperature while higher air flow rate may decrease moisture removed.

a) Drying rate

Studies on dry basil leaves, banana, orange peels and carrots showed that drying rate was directly proportional to drying air velocity (Ikejiofor, 2010; Romdhane and Combarnous, 2011; Lamnatou *et al*., 2012; Sevik, 2013; Rahmatinejad *et al*., 2016; Lingayat *et al.*, 2017). Aissa *et al*. (2014) is in agreement and attributes this to interaction of a large volume of air with the drying product. However, air flow rates

above 6000kg/m^2hr had no influence on drying rate (Sevik, 2013; Tzepelinkos *et al.*, 2014). This is equivalent to an air velocity of 0.42 m/s and influenced the decision on the highest air velocity used in this research. Hedge *et al*. (2015), however, after investigations of banana, reported that 1 m/s drying air velocity resulted in best quality in terms of colour, taste and shape in comparison to 0.5 and 2 m/s. Mghazli *et al*. (2017) dried Moroccan Rosemary leaves at 50 °C, 60 °C, 70 °C and 80 °C at 150 m^3/h and 300 m^3/h and reported that although drying rate increased with increased air flow rate, this was important at low temperature but became insignificant at high temperature. Samira *et al*. (2016) reported that drying air temperature was the parameter that affects drying rate most. They added that air velocity is more effective at lower temperatures.

b) Drying Efficiency

Aissa *et al*. (2014) found overall system drying efficiency (ratio of energy required to evaporate moisture to that supplied to solar dryer, including that consumed by blower) varied from 1.85 % to 18.6 % and was higher for increased air flow rate. Using five different mass flow rates between 0.014 kg/s and 0.036 kg/s in thin layer drying of mulberry, Akubulut and Durmus (2010), found that Energy Utilization Ratio (EUR), increased with increasing drying air mass flow rate. EUR was defined as ratio of energy utilization to energy given from solar collector. The air velocities ranged between 0.046 m/s - 0.118 m/s and were therefore much lower than for the current research. Mumba (1996), found that at a drying air temperature upper limit of 60 °C, a 90 kg batch of freshly harvested maize grain was dried from a moisture content of 33.3% (wet basis) to 25% in 1.4 hours. The mean thermal efficiency of the dryer was found to be 58%. Mohanraj and Chandrasekar (2009) used an indirect forced convection solar dryer with a gravel heat storage for drying chili at 0.25 kg/s mass flow rate. The average dryer efficiency was found to be 21 %, with a specific moisture extraction rate (energy required for removal of one kg of water) of 0.87 kg/kWh. Balbine *et al*. (2015) dried mango at 40 °C, 50 ° and 60 °C using an electric dryer at 0.6 m/s air velocity. The dryer efficiency decreased with increase in drying temperature, and was determined to be 17, 18 and 22% respectively at 40, 50 and 60 °C.

However, Gatea (2011) reported that drying efficiency decreased with increased air flow rate, with a maximum value of 18.41 % at 0.405 kg/s and a minimum of 16.27 % at 0.0675 kg/s flow rate. This finding contradicts those by other researchers and therefore requires further investigation.

2.3.2 Effect of grain layer thickness

The grain layer thickness should not be too big to prevent penetration by the hot air, nor should it be too small to prevent efficient utilization of the available thermal energy. Sarker (2012) carried out experiments to analyse drying behavior of potato at a constant air velocity of 0.6 m/s, temperatures of 40, 45 and 60 °C, and product thicknesses of 3 mm, 5 mm and 7 mm. It was found that drying time increased with increase in thickness, thus implying that drying rate was greater for thinner layers. Romdhane and Combarnous (2011) as well as Delgado and Lima (2014) reported similar results after studies on orange peels. With respect to drying efficiency, Kumar and Shobhana (2011) reported a decrease with size of food product, an equivalent of layer thickness. In this research, effect of grain layer thickness on moisture removal rate and efficiency of dryer was investigated.

2.3.3 Effect of number of trays

The product being dried is generally placed in trays during the application of a solar dryer. This, however, results in uneven drying due to poor air flow distribution. Misha *et al*. (2013) used Computer Fluid Dynamics Simulation and experiments to investigate air flow distribution in the drying chamber. They found that there was good agreement between simulated and experimental data that air velocity decreased with distance from the air inlet. They also found that decreased air velocity resulted in reduced drying rate. Thus, the moisture content differed from one tray to another, the lowest being in the tray closest to the air inlet. The current study, however sought to determine whether use of more than one tray significantly affects the performance of a dryer. Sallam *et al.* (2013) found that when many trays are used, drying rate decreases as distance from the air inlet increases. Aissa *et al*. (2014), found that drying air temperature in the drying cabinet decreased with height, resulting in lowest air temperature and highest moisture content at the top-most parts of the shelf.

2.3.4 Effect of drying air temperature

Using an indirect forced convection solar dryer to study thin layer drying of prickly pear peels, Lahsasni *et al*. (2004) carried out experiments at 50 - 60 ℃ drying air temperature and 0.0277-0.0833 m^3/s drying air flow rate. The main factor controlling drying rate was found to be drying air temperature. Samira *et al*. (2016) reported similar results after drying experiments on potato slices using a tunnel dryer. Experiments were carried out at 45 -70 °C temperatures and 1.60 – 1.81 m/s air velocities. Delgado and Lima (2014) concurred. Though not mentioning effect of other factors, they stated that air temperature affects drying rate more than air flow rate. Researchers such as Romdhane and Combarnous (2011), Sarker (2012), El-sebaii and Shalaby (2013), Tzepelinkos *et al*. (2014) as well as Rahmatinejad *et al*. (2016), among others, showed that drying rate is proportional to drying air temperature. These conclusions emanated from investigations involving products such as thymus and mint.

Drying air temperature also affects the efficiency of the dryer. According to Balbine *et al*. (2015), dryer efficiency decreases with increase in drying air temperature. This appears to be confirmed according to results by Aissa *et al*. (2014), who reported that dryer efficiency increased with increase in air flow rate, a phenomenon that results in reduced drying air temperature.

2.4 Theoretical Framework

2.4.1 Optimisation of dryer performance

One is often faced with a problem for which the solution may follow several different routes. For example, a designer may want to determine the optimal distribution of material in a component to satisfy certain requirements such as minimising mass or maximizing strength. This may be done through the process of optimisation. This is the process of determining the best design based on certain criteria (Parkinson *et al*., 2013). The process of optimisation (Olason and Tidman, 2011), enables finding of the best possible solution under given circumstances. The objective is often some form of maximization or minimization, of a certain performance characteristic (Fang, 2007; Olason and Tidman, 2011). Different optimisation techniques are available for solving such problems. One technique

suggested by Parkinson *et al*. (2013) is to use a combination of judgment, experience, modeling and opinions of others to make design decisions. However, adding that this may not yield an optimal design (especially where many variables with conflicting objectives and/or constraints are involved) they suggest application of computer based approach to multi-objective design optimisation.

Taguchi approach, structural optimisation, genetic algorithm, artificial neural networks and simulated annealing, to mention a few, are examples of the many optimisation techniques that are available for application. In this research, the Taguchi approach was adopted for use, since it is based on experimental data. The other optimisation techniques, discussed in part (b) of this, apply a computer based approach.

a) Taguchi approach

In order to produce a high quality product at a low cost, it is necessary to design experiments to investigate how different parameters affect the process performance characteristics. This may be done using the Taguchi Approach, which allows collection of necessary data to determine which factors affect a product quality most. By studying the effect of individual factors, this approach may be used to enable determination of the best combination of factors. The approach is a powerful and efficient method of optimisation. It does this with a minimum amount of experimentation, thus resulting in savings on time and resources (Fraley *et al*., 2007; Kamaruddin *et al*., 2010; Karna *et al*., 2012).

The first step in the Taguchi method is to define a target value of the performance measure. This measure may, for example, be the efficiency or drying rate. Alternatively, the aim may be to maximize or minimize the performance measure. Secondly, the design parameters that affect the performance measure are identified. These may be variables such as temperature, pressure or air velocity, among others. The number of levels at which each parameter is to be varied is also specified. The third step is to create orthogonal arrays for the parameter design, indicating the number and conditions for each experiment. These Taguchi arrays, which may be derived or found online, depend on the number of factors (parameters) and number

of levels. Next is to conduct the experiments as indicated in the arrays. This is done to collect data on the effect of the parameters on the performance measure. Finally, data analysis is done to determine the effect of the different parameters on the performance measure. A confirmation experiment is then carried out to verify the optimal process parameters obtained, unless the optimal combination coincidentally matches with one the experiments in the orthogonal array (Kamaruddin *et al*., 2010; Fraley *et al*., 2007).

The analysis of data to determine the effect of each variable on the output involves calculation of the Signal to Noise ratio, called the SN number, using eqs. (2.10) - (2.12). The term 'signal' refers to the product quality i.e. the desirable effect, while 'noise' entails the uncontrollable factors i.e. the undesirable effect. Usually, there are three categories of quality of characteristics in the analysis of SN ratio: the-lower-the-better, the-higher-the-better and the-nominal-the-better. Regardless of the category, greater SN ratio corresponds to better quality characteristics, hence the optimal level of the parameter is the level with greatest SN ratio.

$$SN_i = 10log\frac{\bar{y}_i^2}{s_i^2} \tag{2.10}$$

Where: $\bar{y}_i = \frac{1}{N_i}\sum_{u=1}^{N_i} y_{i,u}$ and $s_i^2 = \frac{1}{N_i - 1}\sum_{u=1}^{N_i}(y_{i,u} - \bar{y}_i)$

Also, i is experiment number, u the trial number, N_i the number of trials for experiment, y_i the mean value and $s_i$the variance.

For minimizing the performance characteristic, the SN number is determined using eq. (2.11).

$$SN_i = -10\log\left(\sum_{u=1}^{N_i}\frac{y_u^2}{N_i}\right) \tag{2.11}$$

For maximizing the performance characteristic, eq. (2.12) yields the SN number.

$$SN_i = -10\log\left[\frac{1}{N_i}\sum_{u=1}^{N_i}\frac{1}{y_u^2}\right] \tag{2.12}$$

After calculating the SN number for each experiment, the average SN value is found for each parameter and level, and the larger the mean of SN value for the parameter, the larger its effect on the performance characteristic. Analysis of Variance (ANOVA) on the collected data from Taguchi design experiments may be used to select new parameter values to optimize the performance characteristic. The data from the arrays may also be analysed by plotting and performing visual analysis, and Chi-square test (Kamaruddin *et al*., 2010; Fraley *et al*., 2007).

The Taguchi approach has been applied by different researchers in the optimisation process. For example, Kamaruddin *et al.* (2010) used the optimisation technique and found that a combination of 240 °C melting temperature, 110 bar injection pressure, 96 bar holding pressure, 5 second holding and 10 second cooling time resulted in optimum minimum shrinkage of 0.1645 cm. Muguthu *et al.* (2013) applied the technique to optimize machining parameters that influence the machinability of AI2124SiCp (45 % wt) metal matrix composite. They found that the optimal combination of parameters for lowest specific power were 40 m/min cutting speed, 0.15 mm/rev feed rate, 0.20 mm depth of cut and polychrystalline diamond (PCD) tool. After similar experiments, Singaravel and Selvaraj (2016) determined the optimum combination of cutting speed, feed rate and depth of cut for minimum tool vibration to be 215 m/min, 0.07 mm/rev and 0.5 mm, respectively. It is evident that this technique has, in most cases, been applied in manufacturing sector. However, it was adopted in this research due to its suitability for optimisation that relies on experimental data.

b) Other optimisation techniques

The purpose of Structural Optimisation is to find an optimal material distribution according to the demands of a given structure. The optimisation is done manually and follows three iterative – intuitive steps. First, a design is suggested, after which the design is evaluated by Finite Element Analysis. Finally, the process is finished unless the requirements are not met, in which case modifications are made and the cycle repeated. Because intuition, and sometimes trial and error is used, this optimisation technique is time consuming and at times results in sub-optimal designs. Structural optimisation may take various forms such as sizing optimisation,

shape optimisation and topology optimisation. In sizing optimisation, the shape of the structure is already known, and is optimised by adjusting sizes of the components. In shape optimisation, the topology (number of holes, beams etc.) is known and design variables include, for example, thickness distribution, diameter of holes or radii of fillets (Olason and Tidman, 2011). In topology optimisation, the optimal distribution of material is sought without prior knowledge of the optimal topology. Optimisation soft wares such as Solver Optistract may be used (Bracket *et al*., 2011; Olason and Tidman, 2011). Structural optimisation was not applied in this research, since performance was to be optimized, rather structure.

Genetic Algorithms (GAs) are optimisation techniques inspired from evolution, and which are therefore based on the 'survival for the fittest strategy'. GAs use search operators (selection, mutation and cross over) to determine the optimal solution (Fang, 2007). A GA search begins with a random set of solutions, coded in binary string structures, every solution being assigned a fitness related to the optimisation problem. The population of solutions is then modified into a new one by application of the search operators, through an iterative process that ends when a termination criteria is satisfied (Deb, 2004). In a project aimed at determining optimal design for a hydraulic brake model Fang (2007), applied GAs to determine the combination of inputs (supply pressure and area curves) that resulted in an efficient (largest possible velocity change due to deceleration) and comfortable (predetermined maximum jerk) brake system. This technique was not used in this research because of its computer based approach, as opposed to the experimental method used in this research.

Another optimisation technique is the Neural Networks (NN), also called Artificial Neural Networks (ANN). Mahajan (2013) describes ANN as a computational model consisting of a number of elements (neurons). A neuron is a processing unit that receives input from outside the network and/ or from other neurons, applying a local transformation to the input, thereafter providing a single output, which is then passed on to other neurons or to the outside of the network. The main elements of an ANN are the computing element (artificial neuron), the connection pattern (structure or architecture) and the process used to train the ANN (learning algorithm). Training

of the ANN, according to Berke *et al*. (1993), utilises available useful information from several optimum designs. The trained ANN, as an expert designer, can then be used to predict an optimum design from a new situation. Somasiri *et al.* (2004) applied ANN for optimising the design of a multilayer patch antenna to minimise patch sizes and maximise resonance band width. This technique was also not used in this research because of its computer based approach.

2.4.2 Drying Models, their Selection and Verification

a) The solar drying model

According to Kamenan *et al.* (2009), modeling of solar drying curves is generally to elaborate a function verifying eq. (2.13).

$$X_r = f(t) \tag{2.13}$$

In this case, X_r is moisture ratio, given by eq. (2.14). X is the moisture content, X_{cr} and X_{eq} being the critical and equilibrium moisture contents, respectively.

$$X_r = \frac{X - X_{eq}}{X_{cr} - X_{eq}} \tag{2.14}$$

Lahsasni *et al.* (2004) used eq. (2.15) for the determination of moisture ratio, with X_0 being the initial moisture content.

$$X_r = \frac{X - X_{eq}}{X_0 - X_{eq}} \tag{2.15}$$

According to Osman *et al*. (2001), moisture ratio may be simplified to eq. (2.16) since relative humidity of the drying air continually fluctuates during solar drying. Balmine (2015) states that X_{eq} may be neglected since the values are small compared to those of X.

$$X_r = X/X_0 \tag{2.16}$$

Eq. (2.16) was adopted since relative humidity, which affects equilibrium moisture content, was not controlled in this research. As such, the latter would vary in the

course of the experiments, thus interfering with the results. This is in conformity with assertions by Osman *et al*. (2001).

b) Model selection and verification

Several drying models have been developed to predict variation of moisture ratio with drying time for various products. Table 2.1 is a presentation of some models that have been developed to describe the drying curves for selected products. Various statistical methods are suggested by Eterkin and Firat (2015) for selecting the most suitable model for describing the drying behavior of a product under specific conditions. They are used as a means of comparing experimental data for the drying behavior of the product to those predicted by the drying model. They provide various criteria for determining the goodness of fit, hence enabling selection of the best among different models.

Table 2. 1: Mathematical Models for Drying Curves

S/ No	Model Name	Model Equation	Source	Crop
1	Page	$X_r = \exp(-kt^n)$	Page(1949)	Shelled corn
2	Wang &Singh	$X_r = 1 + at + bt^2$	Wang& Singh(1978)	Rough rice
3	Two Term	$X_r = a\ exp(-k_0 t) + \ bexp(-k_1 t)$	Yi *et al*. (1980)	Corn
4	Modified Page	$X_r = \exp(-(\mathrm{k}\,t)^n)$	White *et al*. (1981)	Pop corn
5	Verma *et al.*	$X_r = a\exp(-kt) + \ (1-a)\exp(gt)$	Verma *et al.* (1985)	Rice
6	Diffusion approach	$X_r = \mathrm{a}\exp -(kt) + (1-a)\exp(-kbt)$	Kassem (1998)	Wheat
7	Midilli *et al.*	$X_r = a\exp(-kt^n) + bt$	Midilli *et al*. (2002)	Mushoom
8	Modified Handerson and Pabis	$X_r = a\exp(-kt) + b\exp(-gt) + c\exp(-ht)$	Ademiluyi *et al*. (2011)	Popcorn

Source: Lahsasni *et al*. (2004); Ertekin and Firat (2015)

One of these statistical tools is the Coefficient of Determination (R^2), which varies between 0 and 1, and is obtained from eq. (2.17) or eq. (2.18). The closer the R^2 value is to 1, the closer the relationship between the experimental and model predicted values (Devore and Farnum, 2005; Hossain *et al*., 2007; Sen, 2008; Eterkin and Firat, 2015). Modelling Efficiency (EF) is another tool [eq. (2.19)], its value tending towards 1 for a good fit. Root Mean Square Error (RMSE) or Root Mean Square Deviation (RMSD) is yet another tool, obtained from eq. (2.20), and for which values should tend to 0 for the best fit Reduced chi-square (χ^2), shown in eq. (2.21), is the mean square of deviations between experimental and predicted values. The lower its value, the better the goodness of fit (Lahsasni *et al*., 2004; Eterkin and Firat, 2015).

$$R^2 = \frac{(\sum MR_{exp} MR_{pre})^2}{\sum MR_{exp}^2 \sum MR_{pre}^2} \quad (2.17)$$

$$R^2 = 1 - \frac{SS_{Res}}{SS_{TO}} \quad (2.18)$$

(Where SS_{Res}= Residual sum of Squares, SS_{To}= Total sum of squares,

$SS_{Res} = \sum(y_i - \hat{y}_i)^2$, $SS_{To} = \sum(y_i - \bar{y})^2$, $\hat{y}$ = predicted value and $\bar{y}$ the mean value)

$$EF = \frac{\sum_{i=1}^{N}(MR_{i,exp} - MR_{i,exp_{mean}})^2 - \sum_{i=1}^{N}(MR_{i,pre} - MR_{i,exp})^2}{\sum_{i=1}^{N}(MR_{i,exp} - MR_{i,exp_{mean}})^2} \quad (2.19)$$

$$RMSE = \{\frac{1}{N} \sum_{i=1}^{N}(MR_{exp,i} - MR_{pre,i})^2 \}^{1/2} \quad (2.20)$$

$$\chi^2 = \frac{\sum_{i=1}^{N}(MR_{exp,1} - MR_{pre,i})^2}{N-n} \quad (2.21)$$

(N and n represent the number of observations and constants respectively, while $MR_{exp,i}$ is the experimental moisture ratio and $MR_{pre,i}$ the predicted moisture ratio)

Oliveira *et al.* (2014) determined relative average error P using eq. (2.22), in which Y, $\hat{Y}$ and N represented the experimental value, model predicted value and number of observations, respectively. Standard error Estimate (SEE) was determined from

eq. (2.23), where $MR_{exp,i}$ and $MR_{pre,i}$ are the *i*th experimental and predicted moisture ratios respectively, and d_f the number of degrees of freedom of the regression model. Coefficient of correlation (r) is the square root of R^2, and is a measure of correlation (linear dependence) between two variables. Its value, obtained from eq. (2.24) varies between +1 and -1 (Aregbesola *et al*., 2015; Eterkin and Firat, 2015).

$$P = \frac{100}{N} \sum \frac{|\boldsymbol{Y} - \hat{\boldsymbol{Y}}|}{\boldsymbol{Y}} \tag{2.22}$$

$$SEE = \frac{\sum_{i=1}^{n} (MR_{exp,i} - MR_{pre,i})^2}{MR_{exp,}} \tag{2.23}$$

$$r = \frac{\sum_{i=1}^{N} (MR_{exp,i} - MR_{exp,ave})(MR_{pre,i} - MR_{pre,ave})}{\sqrt{\{\sum_{i-1}^{N} (MR_{exp} - MR_{exp,ave})^2 \sum_{i=1}^{N} (MR_{pre} - MR_{pre} - MR_{pre,ave})^2}} \tag{2.24}$$

In this research R^2, RMSE and χ^2 , being the most widely used were applied to enable comparison.

2.5 Past studies on selection of drying models

Agbossou *et al*. (2016) used a forced convection solar dryer for drying maize and found that moisture ratio and drying time have exponential and polynomial correlations. Among 14 mathematical models fitted to the experimental drying data using RMSE, R^2 and χ^2, the one by Midilli *et al.* (2002) was shown to give the best fit. They further determined drying constants for maize in the various models (Table 2.2).

Table 2. 2: Drying Models with Model Constants for Maize

S/ No	Model Name	Model Equation	Model Constants for maize
1	Page	$X_r = \exp(-kt^n)$	k= 0.1248 n = 1.0440
2	Wang &Singh	$X_r = 1 + at + bt^2$	a = 0.09199 b = 0.00210
3	Two Term	$X_r = a\ exp(-k_0 t) + \ bexp(-k_1 t)$	k_o= 0.1171 k_1= 0.1239 a=-1.989 b=3.002
4	Modified Page	$X_r = \exp(-(\mathrm{k}\,t)^n)$	k=0.0515 n=1.0932
5	Verma *et al.*	$X_r = a\exp(-kt) + \ (1-a)\exp(gt)$	a=2.089 k=0.1324 g=0.1281
6	Diffusion approach	$X_r = \mathrm{a}\exp -(kt) + (1-a)\exp(-kbt)$	a=7.436 b=0.9879 k=0.1267
7	Midilli *et al.*	$X_r = a\exp(-kt^n) + bt$	k=0.106 n=1.137 a=0.988 b=0.001084

Source: Agbossou *et al*. (2016)

Tahmasebi *et al*. (2011) carried out drying experiments on quercus fruits at temperatures of 50, 60 and 70 °C and air velocities of 0.5 and 1 m/s. It was found that the experimental drying curve best fitted the Page model, out of the five models investigated. The best fit was based on R^2, χ^2 and RMSE values. The model constants were found to depend on the variables studied. Silva *et al*. (2014), however, used R^2 and χ^2 to fit selected drying models to the drying curve for banana

fruit and once again found that the Page model gave the best fit. Moisture ratio was determined using eq. (2.16). Meisami-asl and Rafiee (2009) used three statistical parameters RMSE, χ^2 and modelling efficiency (EF) for selecting the best fitting drying model for thin layer apple drying. Experiments were carried out at temperature ranges of 40 to 80 °C, air velocities 0.5, 1 and 2 m/s as well as slice thicknesses of 2, 4 and 6 mm. The Midilli model gave the best fit.

Akpinar (2008) carried out experiments to select the best fitting drying model for white mulberry. After application of R^2, χ^2 and RMSE to determine the goodness of fit for various existing models, the Logarithmic model, given in eq. (2.25) was selected for forced convection drying while Verma model (Table 2.2) gave a better fit for natural convection drying.

$$X_r = a.\exp(-kt) + c \qquad (2.25)$$

(X_r is moisture ratio while a, c and k and model constants)

Yadollahinia *et al*. (2008) fitted experimental drying curves for rice paddy to eight thin layer drying models using R^2, χ^2 and RMSE and identified the two term model (Table 2.2) as the best fitting one. Experiments were carried out at five temperatures ranging from 30 to 70 °C and air velocities of 0.25, 0.50, 0.75 and 1.0 m/s. Results for other products fitted to various drying models are summarized in Table 2.3.

Table 2. 3: Fitting Different Products to Various Drying Models

Product	Drying Mode	Drying Conditions	Statistical Indicator	Best Fitting Model	Source
Soy bean Grains	Oven (Forced Convection)	40, 55, 70, 85 & 100 °C	R^2 & P	Page	Oliveira *et al*. (2014)
Dika Kernels	Oven (Forced Convection)	50, 60, 70 & 80 °C	R^2 & SEE	Modified Handerson-Pabis	Aregbesola *et al*. (2015)
Dika Nuts	Oven (Forced Convection)	50, 60, 70 & 80 °C	R^2 & SEE	Two term	Aregbesola *et al*. (2015)
Wheat	Forced Convection Dryer	35, 45, 50, 60 & 70 °C 0.3 m/s	r & χ^2	Page	Rafiee *et al*. (2006)
Potato	Forced Convective Tunnel dryer	45- 70 °C 1.6-1.81 m/s	R^2, χ^2 & RMSE	Midilli *et al.*	Samira *et al.* (2016)
Orange slices	Forced Convective Microwave	100, 150 & 200 °C	R^2, SEE & RSS	Midilli -Kucuk	Karaaslan & Erdem (2014)
Red Chilli Pepper	Vacuum Oven	50- 75 °C 0.05, 7 & 13 kPa	R^2	Modified Handerson- Pabis	Alibas (2012)

2.6 Observations from Literature Review

Having reviewed various sources of literature, the following observations were made.

- It was noted that simulation of air flow may be used to improve the design of a dryer so that uneven drying may be reduced. Use of actual measurement to facilitate such design is not only difficult, but it would also be expensive and time consuming. However, few studies have been carried out in this area.

- Studies have been carried out using Taguchi Approach to optimize mechanical processes, but none on solar dryers. It is therefore necessary to carry out research to determine the best combination of factors that would result in the optimum performance of such dryers.

- Many studies have been carried out to select from existing drying models the one that best fits drying curves for different products. It was observed that that the best model not only depended on the product and type of dryer, but also on drying conditions such as drying air temperature and velocity. It is thus necessary to select and verify a drying model for maize under Kenyan conditions in a forced convection dryer.

CHAPTER THREE: MATERIALS AND METHODS

This chapter deals with the methodology applied in this study. First, the research site is described after which the process of developing the experimental dryer is outlined. This is followed by a description of the procedure for testing and optimisation of the experimental dryer. Finally, there is a description of the procedure for selection and verification of an appropriate model for the drying process, as well as development of a computer simulation model to predict drying time for a given moisture ratio.

3.1 Research Site

The study was carried out in Njoro, Nakuru County, Kenya. Njoro is located 18 km South West of Nakuru town. It lies at an altitude of 1800 m above sea level, and experiences temperature ranges between 17-22 ºC. The average rainfall is 1200 mm, distributed trimodally, with peaks in April, August and December. Nakuru County is a moderate to high solar energy potential area. The amount of available solar energy is season dependent, with the December-February season receiving the highest amount of insolation of 678 kWh/m^2. The September-November season receives the least insolation of 602.6 kWh/m^2. Harvesting is normally carried out between August and December, depending on the type of grain (Omwando, 2012; Walubengo, 2007; Maloba *et al.*, 2007).

3.2 Simulation and Sizing of Experimental Dryer

3.2.1 Simulation to estimate grain layer thickness and number of trays

This section of the study sought to carry out simulation in order to determine the optimal grain layer thickness that would be penetrated by the drying air. This was determined by observing the velocity profile for simulated air flow up different layer thicknesses, with the expectation that air velocity would gradually increase up the layer. According to Ergun's equation [eq. (2.3)], the governing equation in the simulation process, fluid velocity increases as pressure drop increases. The latter increases as fluid moves up the grain layer, hence fluid velocity is expected to vary in a similar manner. Simulation was first carried out of hot air flowing through a single grain layer of 0.1 m thickness, at an air velocity of 1 m/s. A parametric sweep was then carried out in order to simulate air flow through various grain layer

thicknesses ranging between 0.1 m – 0.3 m for air velocities ranging between 1 m/s - 5 m/s. A parametric sweep enables simulation within the specified range of parameter values in one process, without having to do it for discrete values. The purpose of the parametric sweep was to determine the maximum grain layer thickness that would allow the fan to overcome static resistance to airflow.

Once the maximum allowable layer thickness was determined, simulation of air flow up increasing number of grain layers was carried out in order to determine the number of layers the air was able to penetrate. In this case, variation of pressure up the drying cabinet with different grain layer numbers was observed. It was expected that pressure would decrease gradually up the drying cabinet. Any behavior to the contrary would suggest air was not able to penetrate.

The simulation process was carried out in two major stages: creation of the model and simulation of the model. Before simulating air flow up the drying cabinet, a 2-D model of it had to be developed using the software SolidWorks. Once created, the model was imported into the COMSOL MULTI-PHYSICS simulation software and the process of simulation carried out. The simulation process was also in two major stages: pre-processing and post-processing. Figure 3.1 summarises the model creation process while Figure 3.2 summarises the preprocessing stage of simulation.

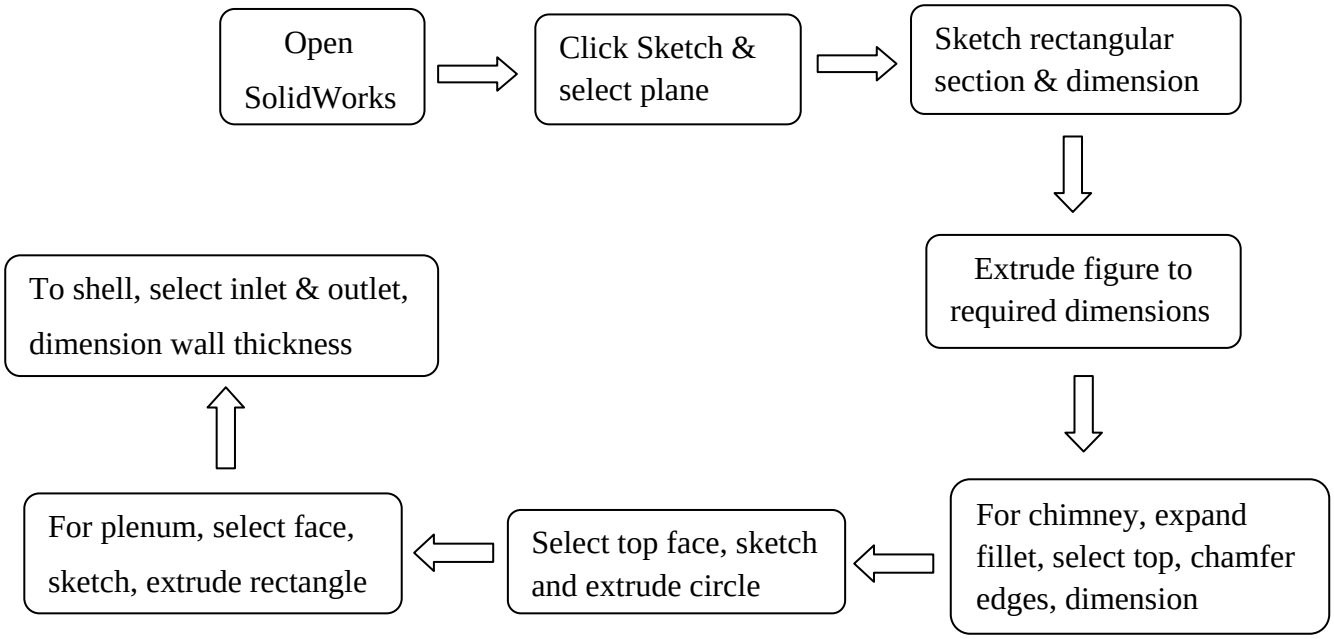

Figure 3. 1: Model creation

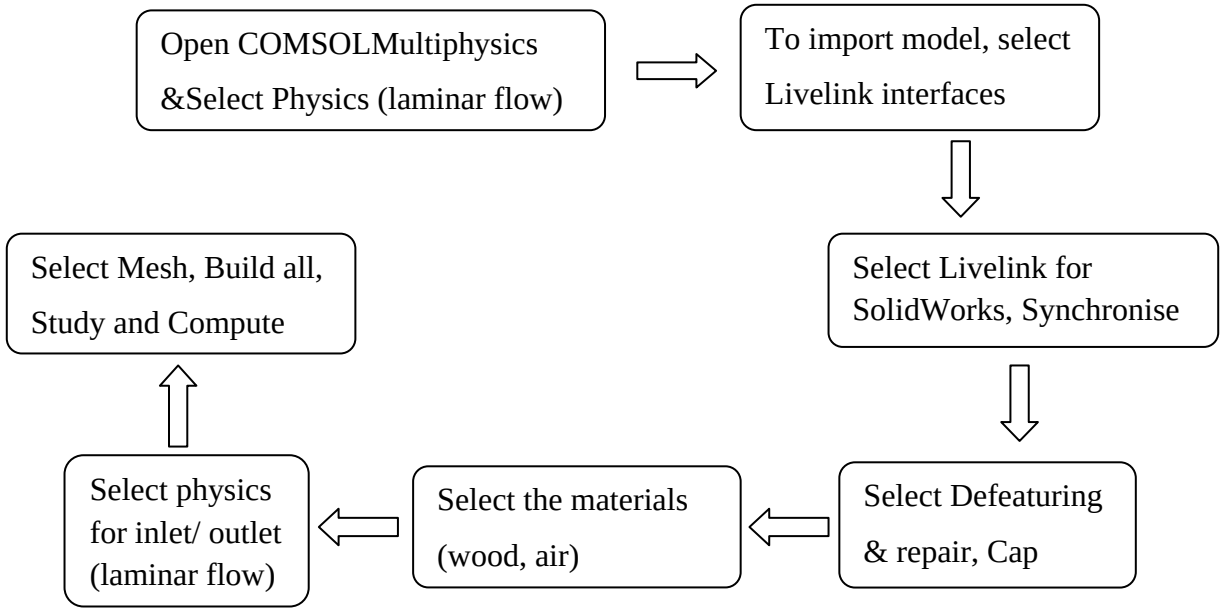

Figure 3. 2: Flow chart of preprocessing stage of simulation

Once simulation was complete, post-processing, summarized in Figure 3.3, was carried out to extract the results in various forms as required.

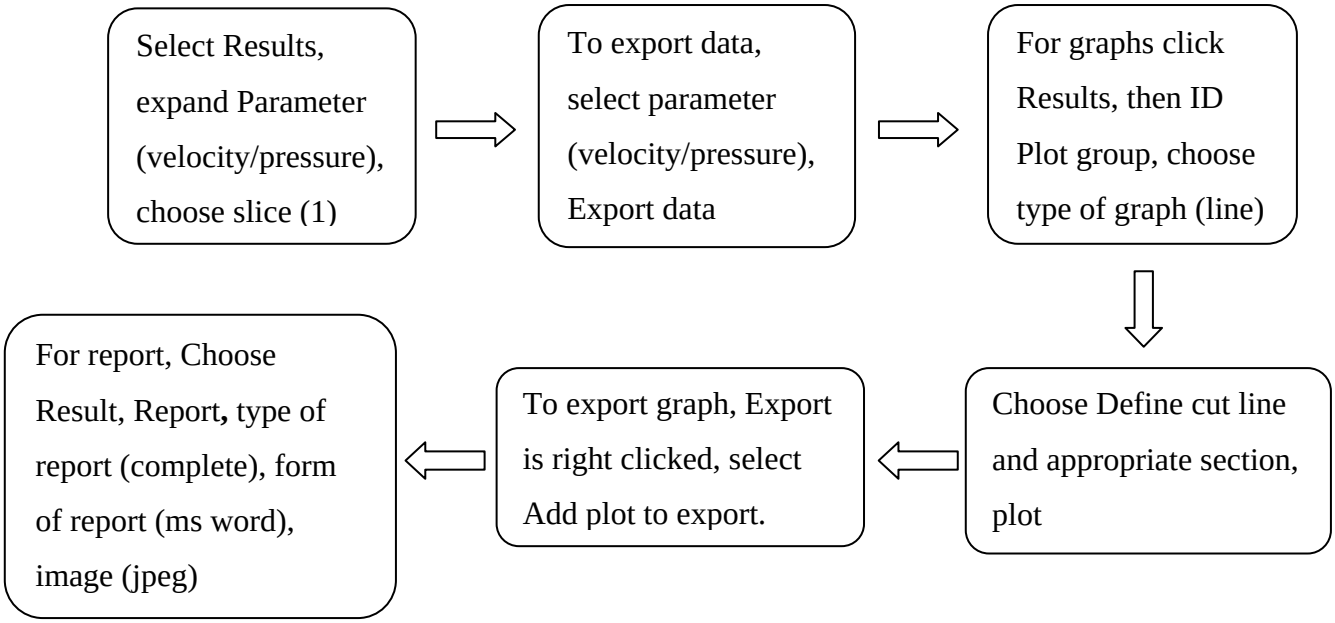

Figure 3. 3: Post-processing stage of simulation

3.2.2 Sizing of solar dryer

a) Fan power determination

Having found the maximum grain layer thickness to allow penetration by the air to be 0.1 m (section 3.2.1), the simulated pressure drop for this layer thickness was taken as being equivalent to the static pressure to be overcome by the suction fan. This static pressure (P_S) as well as the corresponding air flow rate ($\dot{V}$) was applied in eq. (2.5) to determine the power of the appropriate fan. The results are shown in section 4.1.2.

b) Drying cabinet and solar collector

i. Drying cabinet

To determine the cross sectional area of the drying cabinet, a capacity of 18 kg per tray (a mass that an average family would dry for milling, and also that can be carried comfortably when loading) was assumed. The volume (V_{gr}), of grain per tray was determined using eq. (3.1), the grain density for maize being 0.76 g/cc. The cross sectional area of the drying cabinet A_{cb} was then determined from eq. (3.2), the value of t_{gr} (maximum grain layer thickness) having been determined as 0.1 m from section 3.2.

$$V_{gr} = \frac{m_{gr}}{\rho_{gr}} \quad (3.1)$$

$$A_{cb} = \frac{V_{gr}}{t_{gr}} \quad (3.2)$$

(m_{gr} and ρ_{gr} represent mass and density grain respectively)

The height of the drying cabinet was sized to carry two trays, each holding a grain layer thickness equal to t_{gr}. The void space between the trays, having a height equal to that of the grain layer, and a plenum chamber, as well as space above the second tray to accommodate the suction fan were also catered for. The results are shown in section 4.1.2 and Appendix 1C.

ii. Solar collector

The solar collector area (A_c) was determined using eq. (2.1). To find the air mass flow rate ($\dot{m}_a$) eqs. (3.3) and (3.4) were used. Air velocity was measured at dryer exit, which had a diameter of 0.1 m, using a thermo-anemometer, cabinet cross sectional area having been found as shown above.

$$Q = Av \quad (3.3)$$

$$\dot{m} = Q\rho_a \quad (3.4)$$

(Q = flow rate in m^3/s, A= cross sectional area in m^2, v = air velocity in m/s, $\dot{m}$ = mass flow rate in kg/s and ρ_a= density of air in kg/m^3)

T_i was taken to be 23°C (the ambient temperature measured in research area during drying period) and T_o as 58°C (the maximum temperature to maintain grain quality). A value of 1200 W/m^2 was used as Insolation I_c (estimated from measurements in the research area), while a solar collector efficiency (η) value of 83.28 % was used. This solar collector efficiency was similar to that reported by Aduewa *et al*. (2014) at insolation of 1199.46 W/m^2.

3.3 Effect of Selected Parameters on Dryer Performance

The experimental solar grain dryer (Figs.3.4 & 3.5; Plates 3.1 & 3.2), was fabricated and tested in Njoro Sub-County, Nakuru County, in order to evaluate its

performance. Engineering drawings of the dryer are shown in Appendix V. It consisted of a flat plate solar collector (air heater) and a drying cabinet with a centrifugal fan to force the air into the dryer. Although after application of Eq. (2.1) the solar collector area was expected to be 3.25 m^2 (section 4.1.2), the largest single piece of glass sheet available was 2.16 m^2. Hence a collector area of 1.2 m x 1.8 m was adopted to avoid having joints on the glazing, which could have been a possible source of air leakage. The air vent was of height 0.1 m, as used by Aduewa *et al*. (2014) for a similar dryer. The absorber plate comprised of black painted corrugated iron sheet. The glass cover was of 5 mm thick glass, the air heater sides and back plate being made of 5 mm thick ply wood.

The drying chamber was of dimensions 0.5 m x 0.5 m x 1 m, with a 1.25 mm MS sheet metal casing. Its sides consisted of double plates, 40 mm apart with polystyrene in between for lagging. A centrifugal fan was fixed at the upper section of one side. The plenum chamber was covered with a perforated plate 0.2 m from the bottom of the drying cabinet. Having determined, by the simulation process, that not more than four drying trays could be penetrated by the drying air, two trays whose sides were of 1.25 mm MS sheet metal, with bottoms of wire mesh, were used. This was in order to determine whether using more than one tray would result in any significant increase in moisture removal rate. The first tray was 0.1 m above the perforated plate, and the second 0.2 m from the bottom of the first.

The performance of the dryer was evaluated based on drying efficiency as well as moisture removal rate. During the experiments, it was placed in an open area in a North-South direction to ensure the air heater was not shaded at certain times of the day. First, the un-loaded dryer was run for a period of 3 ½ hours to observe the variation of temperature as well as solar radiation. Temperature was measured using resistance thermal detectors (PT 100) whose sensors were placed at various sections of the dryer and the results recorded at intervals of 30 minutes using a data logger (Plate 3.2). Solar radiation was also measured at similar intervals using a solar power meter, allowing 10 seconds for stabilization before taking the highest reading. Whenever the dryer was to be loaded, this was done after running it for 30 minutes

to allow for the plenum temperature to rise above ambient. Results are discussed in section 4.2.

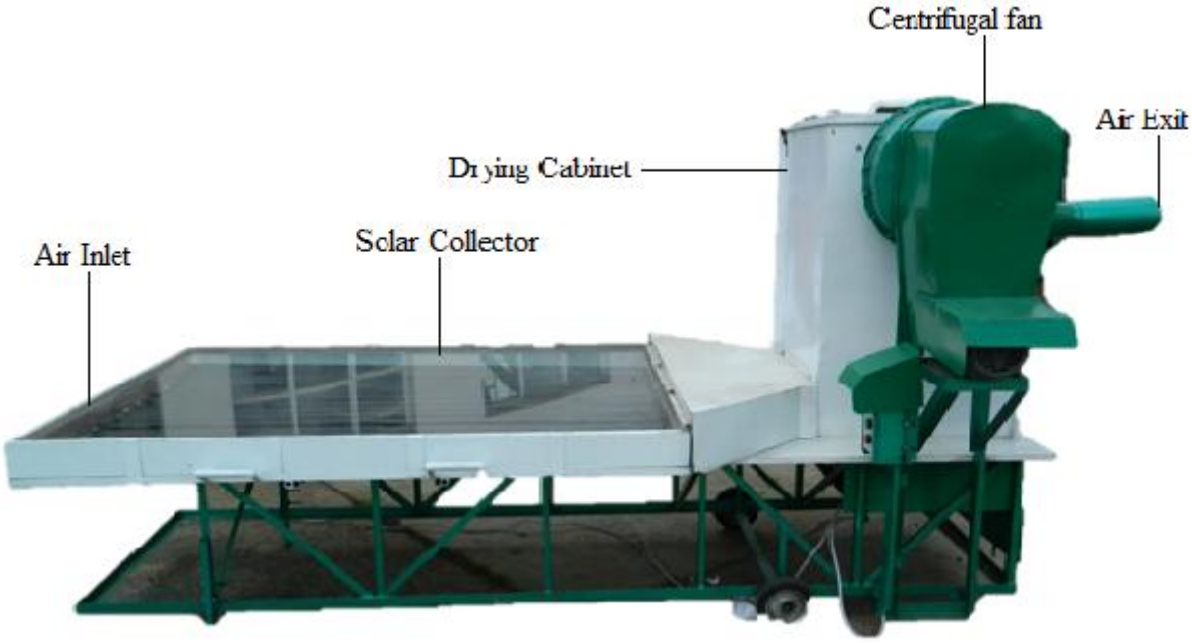

Plate 3. 1: Side View of experimental solar grain dryer

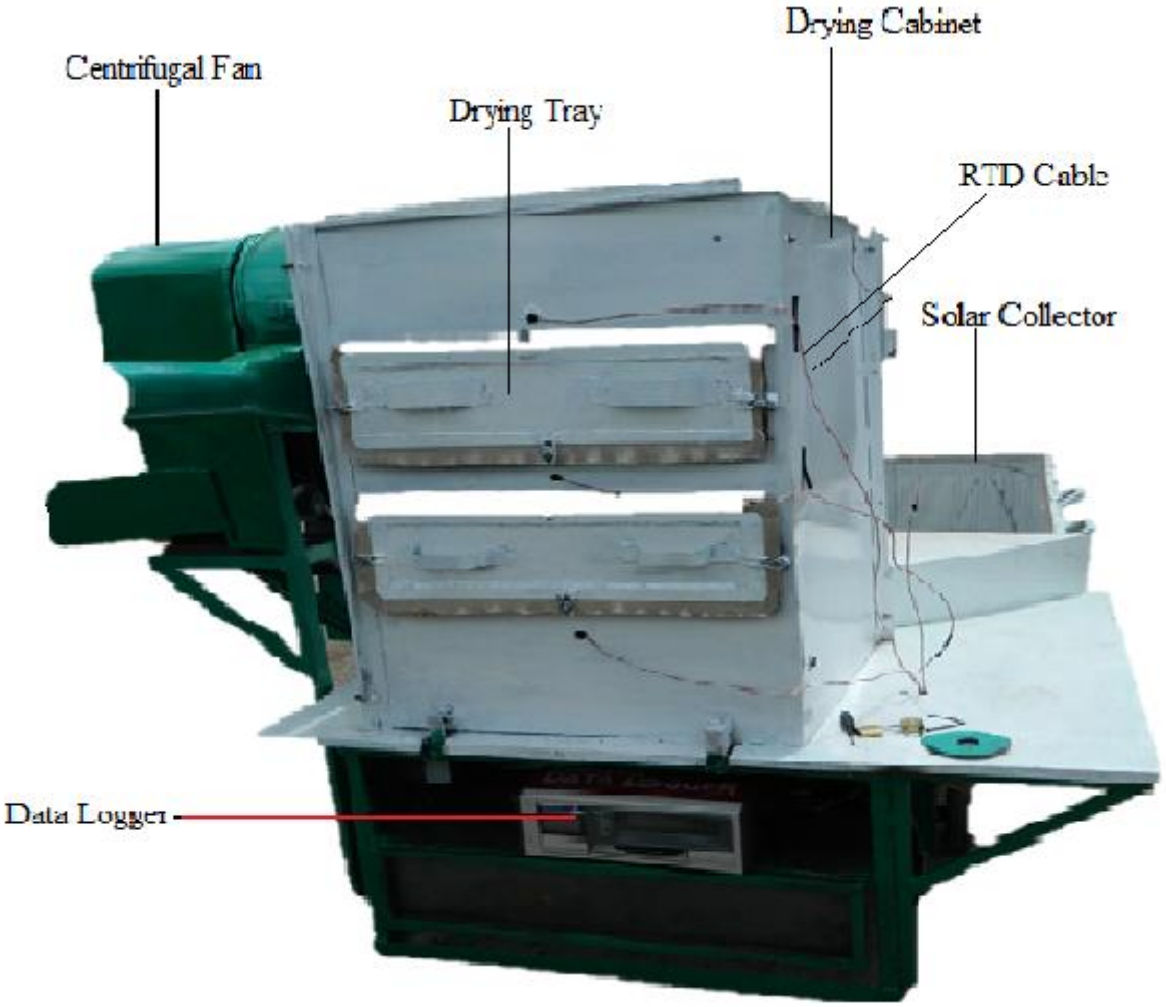

Plate 3. 2: Rear View of experimental solar grain dryer

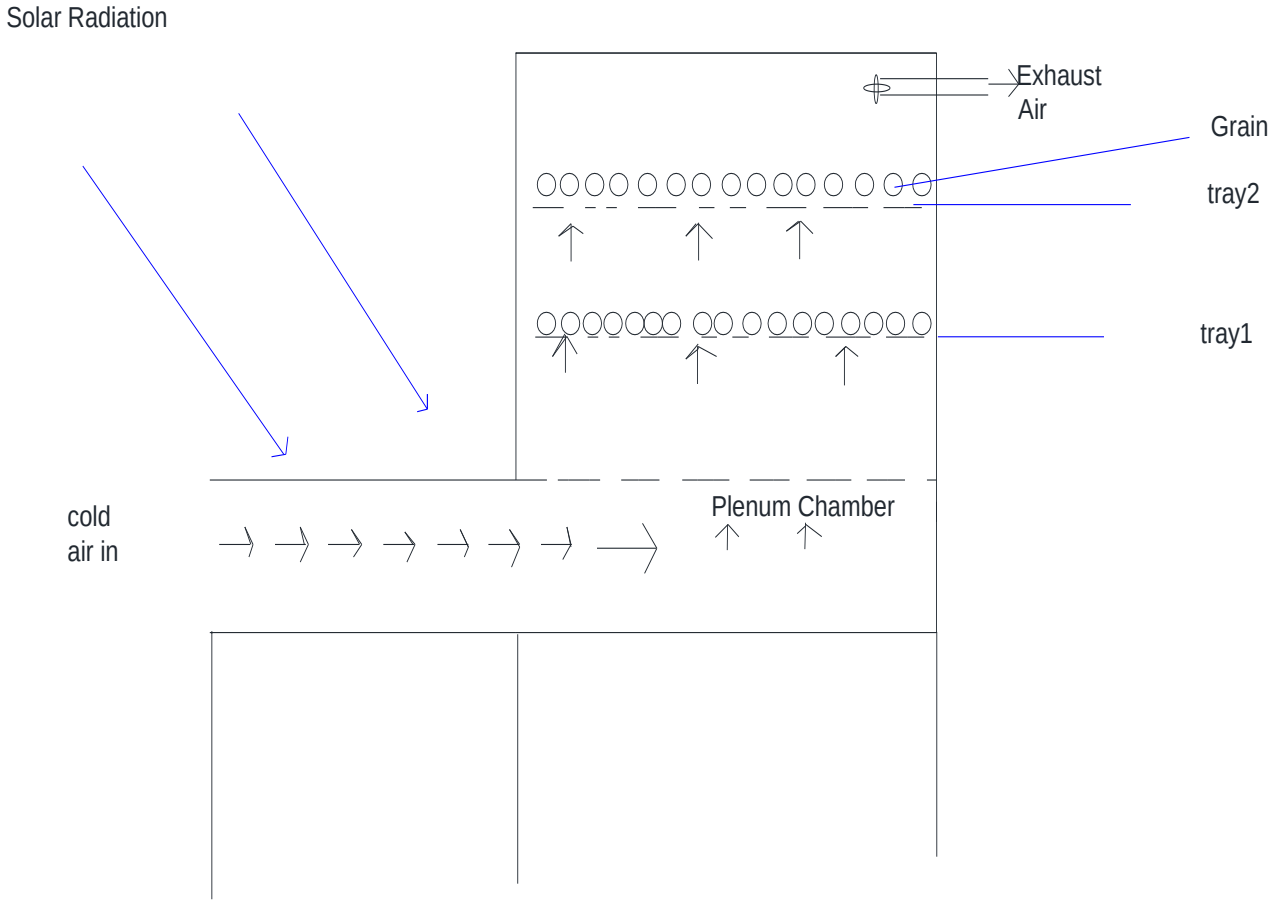

Figure 3. 4: Schematic Diagram of solar grain dryer

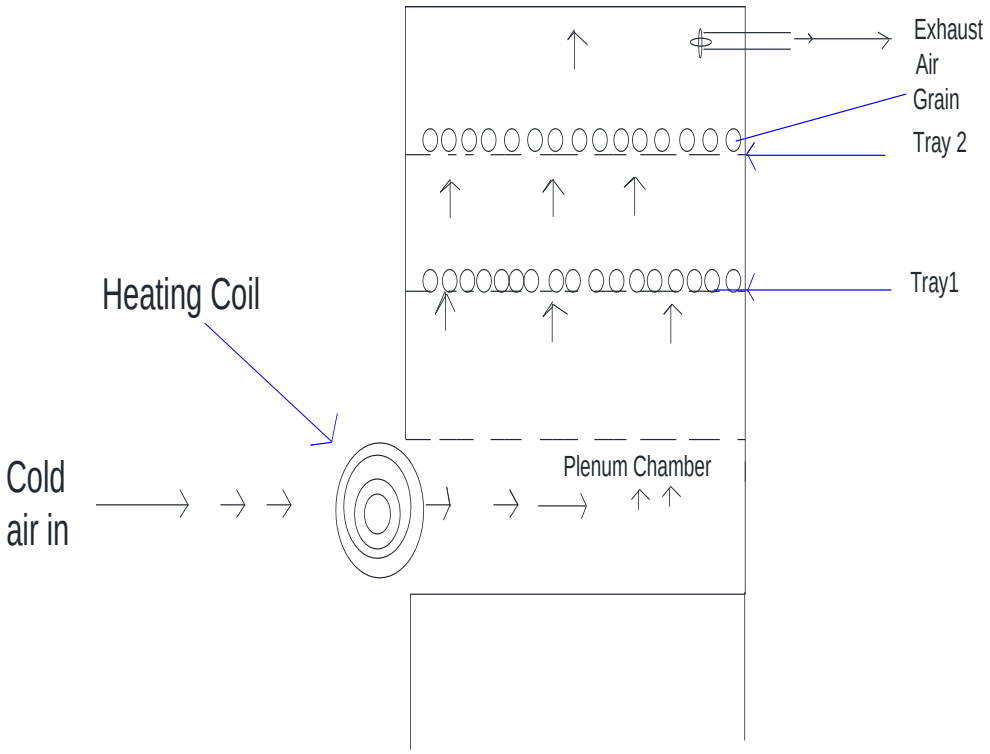

Figure 3. 5: Schematic Diagram of electrically heated grain dryer

3.3.1 Efficiency, moisture content and removal rate

a) Drying efficiency determination

In order to determine the drying efficiency, the energy (E_w) required to remove the moisture from the grain was determined using eq. (3.5), in which m_w and H_v represented mass of water vapour evaporated and latent heat of vapourisation respectively.

$$E_w = m_w H_v \quad (3.5)$$

The energy (E_a) supplied by the hot air to the grain was given by eq. (3.6). In this equation, mass flow rate of air used for drying for a duration of time t_s, and specific heat capacity of air are represented by $\dot{m}_a$ and c_{pa}. ΔT_i represents the temperature drop as the hot air passes through the grain.

$$E_a = \dot{m}_a c_{pa} t_s \Delta T_i \quad (3.6)$$

The energy (E_f) consumed by the fan was given by eq. (3.7), in which t represents the total drying time while P_f is the power consumed by the fan.

$$E_f = P_f t \quad (3.7)$$

P_f was determined from eq. (3.8), with V and I being the voltage and current consumed by the suction fan.

$$P_f = VI \quad (3.8)$$

Drying efficiency (η_{drg}) was then determined for each drying experiments using eq. (3.9), ΔT_m being the mean temperature drop as air passes through the grain.

$$\eta_{drg} = \frac{m_w H_v}{\dot{m}_a c_{pa} t \Delta T_m + P_f t} \quad (3.9)$$

During each experiment, mass of moisture lost (m_w) was determined by weighing the grain at the beginning and at the end of the using a digital balance. Air velocity, measured at the dryer exit, was used to calculate volume flow rate Q for the exit radius of 0.05 m, by applying eq. (3.3). It was then possible to calculate air velocity through the drying cabinet using the same equation. Mass flow rate $\dot{m}_a$ was subsequently obtained from eq. (3.4). Latent heat of vapourisation of water at air exit temperature (H_v) and specific heat capacity of air (c_{pa}) were obtained from Engineering Thermodynamics Properties tables. As suggested by Murthy (2010), H_v was be increased by 15% since bound water was to be removed. Fan power, P_f was obtained from eq. (3.8), the current I being measured using a multimeter, and taking

the voltage V to be 240 V. ΔT_i was determined from temperature readings every 30 minutes and used to fi nd ΔT_m.

b) Determination of moisture content

Moisture content for the grain was determined using the oven drying method, according to the Association of Agricultural Engineers (ASAE) standard S352.2 (ASAE, 1992) for unground grain and seeds. The oven was well insulated to maintain uniform heating inside. 15g of grain, sampled from three different positions at the surface of the grain layer in the dryer, was placed in an aluminium dish and dried in an oven for a period of 24 hours, followed by drying at 1 hour intervals till constant mass was achieved. Weighing was done using a digital balance with accuracy of 0.001g. Moisture content X_w, (wet basis), was obtained from eq. (3.10). Three replications were done in each case.

$$X_w = \frac{m_w}{m_{wg}} \text{ X } 100 \qquad (3.10)$$

(m_w refers to mass of water evaporated while m_{wg} is to total weight of wet grain)

c) Determination of moisture removal rate

To determine moisture removal rate (MRR), moisture loss in each drying experiment was calculated from the difference between the mass of grain before and after drying, weighed using a digital balance. MRR was determined using eq. (3.11), and was defined as the mass of moisture m_m, lost during a drying session of time t for every unit mass of wet grain m_w.

$$MRR = \frac{m_m}{m_{wg}t} \qquad (3.11)$$

3.3.2 Air velocity and grain layer thickness

a) Air velocity

To determine effect of air velocity on drying efficiency and moisture removal rate, the dryer was tested at air velocities of 6.8 m/s, 8.6 m/s, 11 m/s and 13 m/s, measured at the dryer exit using a thermo-anemometer. Air velocity was varied by increasing or decreasing resistance to air flow at the drier exit duct. This was done by placing orifice plates of varying orifice diameter. A grain layer thickness of 0.02

m was used in each case, the dryer being ran for 3 ½ hours. Using eq. (3.3), the equivalent air velocities within the drying cabinet were 0.21 m/s, 0.27 m/s, 0.34 m/s and 0.41 m/s respectively. The lower limit was to ensure that the air velocity was not too low as this would result in drying air temperature exceeding 60 °C, which could result in cracking of the grain. The upper limit was to provide the air with adequate time within the grain layer to remove moisture. This procedure was repeated for 0.04 m, 0.06 m and 0.08 m thick layers. Drying efficiency, as well as moisture removal rate, were determined as described in section 3.3.1. Their variation with air velocity at a given layer thickness is presented in Figures 4.7 - 4.9 and discussed in section 4.2.1.

b) Grain layer thickness

Using results from (a), variation of drying efficiency as well as moisture removal rate with grain layer thickness of 0.02 m, 0.04 m, 0.06 m and 0.08 m at air velocities 0.21 m/s, 0.27 m/s, 0.34 m/s and 0.41 m/s was determined, and are presented in Figures 4.10 – 4.12 and discussed in section 4.2.1.

3.3.3 Number of trays

The solar dryer was tested to determine whether its moisture removal rate would be affected by the use of more than one drying tray. First, a 0.04 m thick grain layer was dried in one tray using an air velocity of 0.41 m/s, and the moisture removal rate determined. The experiment was repeated, using two trays each with 0.02 m thick grain layer at the same air velocity, again determining the moisture removal rate, which was compared to the result for a single tray. This procedure was repeated for an air velocity of 0.27 m/s. Analysis of Variance (ANOVA) was used determine whether using two trays resulted in a significantly greater MRR than using one tray. Results are presented in Table 4.1 and discussed in section 4.2.2.

3.3.4 Drying air temperature

To determine the effect of drying air temperature on dryer performance, experiments were done under laboratory conditions, where drying air temperature was controlled. A 1.8 kW electrical heating coil (placed at the drier inlet), connected to a Proportional Integral Derivative (PID) controller was used to heat air and maintain it

at the required temperature. Temperature was measured using T-type (Copper-Nickel) thermocouple placed at the plenum chamber. First, a 0.04 m grain layer thickness was dried at an exit air velocity of 0.41 m/s and 40 °C, determining the moisture removal rate, as well as drying efficiency using the procedure described in section 3.3.1. This was repeated at 45 °C, 50 °C and 55 °C, maintaining the same grain layer thickness and exit air velocity in order to observe the effect of temperature on the respective performance indicators. Variation of drying efficiency as well as moisture removal rate with temperature was analysed using ANOVA and LSD. As a control, the same experiment was repeated for the same grain layer thickness but with natural convection at 40 °C and the performance compared to that of forced convection (0.41 m/s). Results are presented in Tables 4.2 and 4.3 as well as in Figure 4.13 and discussed in section 4.2.3.

3.3.5 Relative Humidity

Although relative humidity (RH) was not controlled during this research, an attempt was made to determine whether its variation in the ambient would have any impact on the drying process, specifically on moisture removal rate. To investigate whether RH had any effect on MRR, the latter was determined at constant air velocity (0.41 m/s), grain layer thickness (0.04 m) and temperature (40, 45 and 50 °C) using the procedure outlined in section 3.3.1c. Mean values RH for the respective days were obtained from the weather station at Egerton University. At this station, RH was determined by measuring dry-bulb and wet-bulb temperatures, and using a conversion table to deduce the RH value. Two way ANOVA without Replication was then used to determine whether change in RH at different temperatures (45 °C and 50 °C) resulted in any significant change in MRR.

3.4 Optimisation and Verification of Selected Drying Model

3.4.1 Optimisation of dryer performance

a) Dryer in open sun

In order to find the optimum combination of air velocity and grain layer thickness resulting in greatest drying efficiency and moisture removal rate, three approaches namely the Taguchi approach, Analysis of Variance (ANOVA) and Least Square Differences (LSD) were used.

The Taguchi approach was used to select the combination of air velocity and grain layer thickness resulting in greatest drying efficiency as well moisture removal rate. The two parameters and their levels are shown in Table 3.1.

Table 3. 1: Parameters affecting dryer performance and their Levels

Factor	Parameter	Units	Level 1	Level 2	Level 3	Level 4
A	Air velocity	m/s	0.21	0.27	0.34	0.41
B	Grain layer thickness	m	0.02	0.04	0.06	0.08

The L'16 orthogonal array involving 16 experiments was used as indicated in the experimental plan in Table 3.2. In each experiment, with the dryer in the open sun, a specific layer thickness of wet grain was dried in the experimental solar dryer using solar heated air at a specified velocity. The grain was weighed using a digital weighing balance at the beginning, and again at the end of the drying session 3 ½ hours later. MRR and drying efficiency were determined as described in section 3.3.1 and used in eq. (2.12) to calculate the S/N ratio. Taguchi optimisation was also done using Minitab 17 statistical software (procedure in Fig. 3.7) and the results obtained were found to be the same.

Table 3. 2: Experimental Plan (L'16 Orthogonal Array)

Experiment	Parameter/Levels		Actual Values of Parameter/ Levels	
	Air Velocity	Grain Layer Thickness	Air Velocity (m/s)	Grain Layer Thickness (m)
1	1	1	0.21	0.02
2	1	2	0.21	0.04
3	1	3	0.21	0.06
4	1	4	0.21	0.08
5	2	1	0.27	0.02
6	2	2	0.27	0.04
7	2	3	0.27	0.06
8	2	4	0.27	0.08
9	3	1	0.34	0.02
10	3	2	0.34	0.04
11	3	3	0.34	0.06
12	3	4	0.34	0.08
13	4	1	0.41	0.02
14	4	2	0.41	0.04
15	4	3	0.41	0.06
16	4	4	0.41	0.08

The mean S/N ratios for each parameter level were also calculated and used to determine the optimal combination of air velocity and grain layer thickness for maximising the performance indicators. The larger the mean S/N ratio for the

parameter level, the better it was for maximizing the performance characteristic in question. The results were in agreement with the main effect plots obtained from Minitab 17.

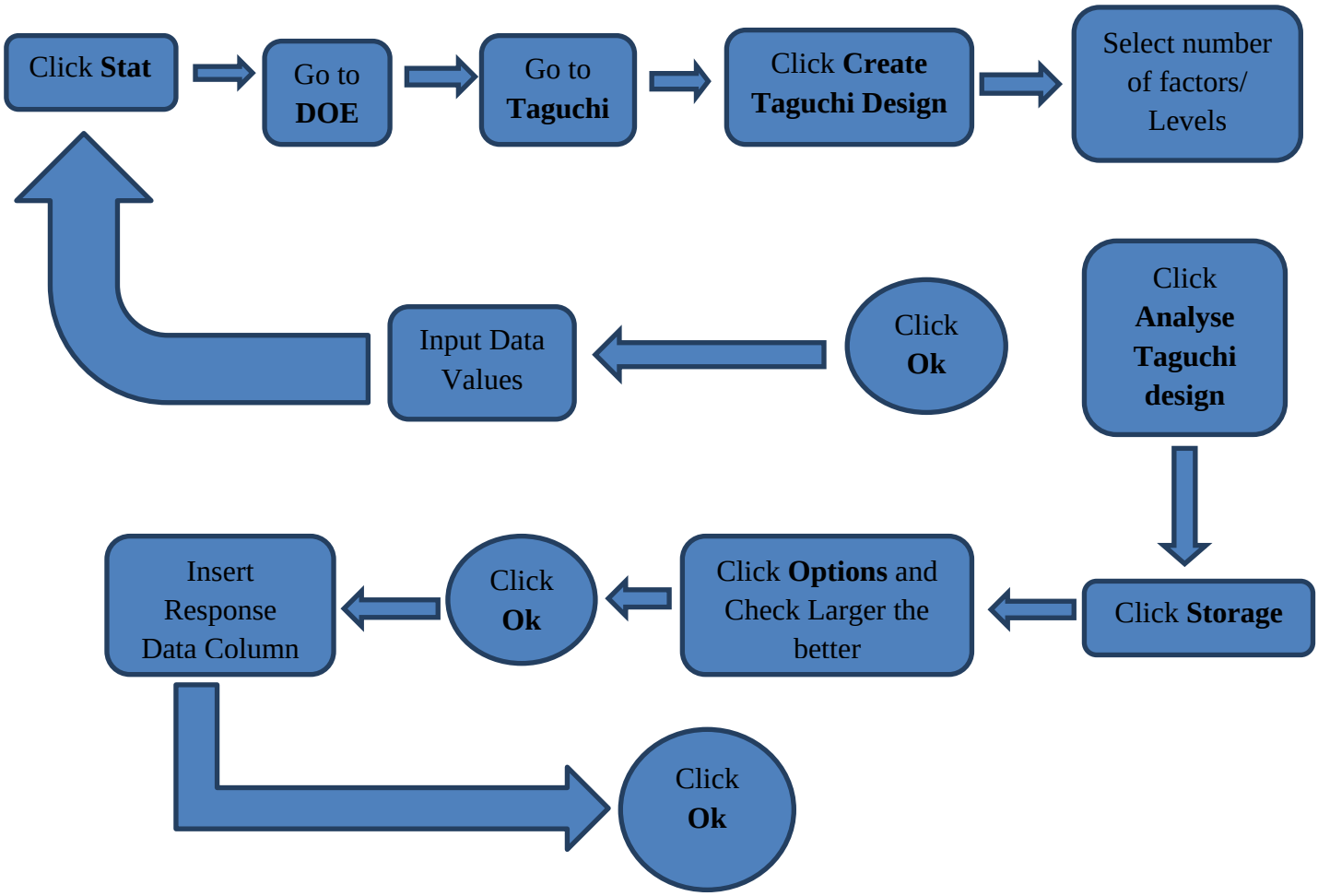

Figure 3. 6: Taguchi optimisation procedure (Minitab 17 Statistical software)

Although the Taguchi approach enabled determination of the optimum combination of air velocity and grain layer thickness for maximizing the dryer performance, it did not show whether the two parameters had any significant effect on the dryer performance characteristics. Two-way Analysis of Variance (ANOVA) was used to test the existence, or otherwise, of significant effects of different air velocities and grain layer thicknesses on dryer performance. When ANOVA gives a significant result, it only indicates that at least one group differs from the other groups. It was thus necessary to do LSD tests to compare pairs of groups for any significant

difference between them. This was done to determine whether the varying air velocity and grain layer thickness levels had any significant effects on dryer performance. Statistical Analysis Systems (SAS) software was used for the analysis. Results are presented and discussed in section 4.3.1.

b) Dryer in Laboratory Conditions

In this section, experiments were carried out in laboratory conditions where in addition to application of different air velocities and grain layer thickness, it was also possible to control drying air temperature. The aim was to determine the combination of these drying parameters resulting in optimal MRR and drying efficiency. The three parameters and their levels are shown in Table 3.3.

Table 3. 3: Parameters Affecting Dryer Performance and their Levels

Factor	Parameter	Units	Level 1	Level 2	Level 3
A	Air velocity	m/s	0.24	0.33	0.41
B	Drying Air Temperature	° C	45	50	55
C	Grain layer thickness	M	0.02	0.04	0.06

Experiments were carried out as in (a) following the experimental plan in Table 3.4 and values of MRR and drying efficiency determined in a similar manner. The results are discussed in section 4.3.1.

Table 3. 4: Experimental Plan (L'9 Orthogonal Array)

Expt.	Parameter/Levels			Actual Values of Parameter/ Levels		
	Air Velocity	Drying Air Temp	Grain Layer Thickness	Air Velocity (m/s)	Drying Air Temp (°C)	Grain Layer Thickness (m)
1	1	1	1	0.24	45	0.02
2	1	2	2	0.24	50	0.04
3	1	3	3	0.24	55	0.06
4	2	1	2	0.33	45	0.04
5	2	2	3	0.33	50	0.06
6	2	3	1	0.33	55	0.02
7	3	1	3	0.41	45	0.06
8	3	2	1	0.41	50	0.02
9	3	3	2	0.41	55	0.04

3.4.2 Testing and verification of drying model

a) Testing of drying model

Solar drying was carried out over a period of 3 hours, retrieving a sample of grain from three positions at the surface of the grain layer every 20 minutes, and using it to determine moisture content as described in section 3.3.1 (b). This was done using 0.04 m grain layer thickness and 0.41 m/s air velocity this being the combination that resulted in greatest drying efficiency. Moisture ratio was thereafter calculated using eq. (2.16). Variation of moisture ratio with time were used to produce a scatter plot (Fig. 4.18). The regression equation for moisture ratio, along with selected drying models, were tested to select the best fit for the experimental drying data. This was done using coefficient of determination (R^2) [eq. (2.18)], χ^2 [eq. (2.21)] and RMSE [eq. (2.20)]. Results are shown in Table 4.9. The model constants used were adopted from Agbossou *et al*. (2010) [Table 2.2], who carried out similar drying experiments for maize under similar climatic conditions. The best fitting model or equation was thus adopted for use in predicting drying time. It was used to

develop a computer simulation model (Fig. 4.21) for predicting drying time for given moisture content or moisture ratio.

The model constants by Agbossou *et al*. (2010), adopted above, were generalized for all conditions. However, Ayadi *et al*. (2014), determined drying constants for spearmint and found that they varied as a function of temperature. It was therefore necessary to determine and verify model constants for 40, 45, 50 and 55 °C before they could be applied in the computer simulation model.

0.04 m thick maize grain was dried for three hours at 40 °C, at an air velocity of 0.41 m/s, determining the moisture content every 20 minutes as in 3.3.1 (b). This was used to determine the variation of moisture ratio [Eq. (2.16], with time during the drying process. The drying curve of Midilli *et al*. (2002), having been selected, was then customized in the software MATLAB R2012B, and the experimental data for variation of moisture ratio at 40 °C fitted to it, using Coefficient of Determination (R^2) and RMSE to determine the best fit. The values of the Midilli coefficients were then determined using the software. The same was repeated for the same grain layer thickness dried at the same air velocity, but at varying temperatures (45 °C, 50 °C and 55 °C). Thus, the drying constants at 40 °C, 45 °C, 50 °C and 55 °C (shown in Table 4.10) were determined for use in the computer simulation model.

b) Verification of drying model

A computer simulation model to predict moisture ratio for a given drying time was developed (Fig. 4.21). The input parameters were drying time, as well as the constants a, b, k and n. The output parameter was moisture ratio, X_r which could then be used to determine moisture content for known initial moisture content. Fig. 3.8 shows a flow chart for the computer simulation model. The best fitting model equation obtained in section 4.3.2 and the model constants determined in the same section were used in the model. The program Visual Studio 2012 was used in the model development, with application of the language C#.

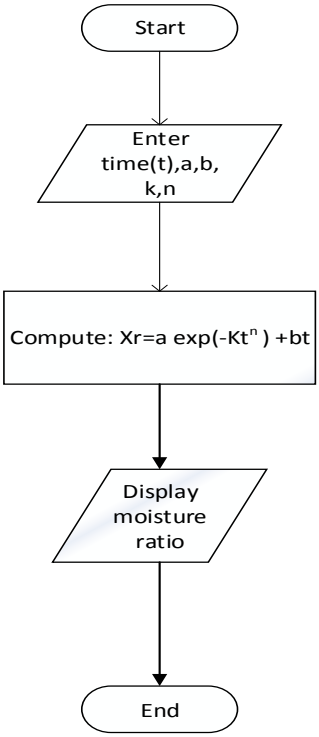

Figure 3. 7: Flow Chart for Computer Simulation Model

To validate the computer simulation model, its results were compared to experimental results. Coefficient of Determination (R^2) and Root Mean Square Error (RMSE) were used to test the reliability of the model. These results are shown in Table 4.11 as well as figures 4.19 and 4.20.

CHAPTER FOUR: RESULTS AND DISCUSSION

This chapter presents and discusses the results obtained in the course of this research. First, it deals with simulation and sizing of the experimental dryer. It then looks at the results obtained after fabricating and testing the experimental solar dryer. It also discusses the results of the optimization process. The selection of an appropriate drying model for the drying curve, as well as determination of the drying constants, are then presented and discussed. Finally, a computer simulation model for predicting drying time is presented.

4.1 Simulation and Sizing of Experimental Dryer

4.1.1 Grain layer thickness and number of trays

In order to select the appropriate grain layer thickness, air flow through different layer thicknesses was simulated. The expectation was that air velocity would increase gradually up the grain layer. Any variation from this expectation would imply an inappropriate layer thickness. Appendix 1A (Figs. A1 – A4) shows velocity profiles for different layer thicknesses. It is evident that for grain layer thickness of 0.1 m, air velocity increased gradually up the entire grain layer, leveling off at the top. This was according to expectations. This implied that 0.1 m would be an appropriate grain layer thickness for this dryer, and that the suction fan would be able to overcome the static pressure i.e. resistance to air flow, in this case. For other layer thicknesses, this was not the case. For example for grain layer thickness of 0.2 m at inlet velocities 1 m/s, velocity increased gradually up to a grain layer height of 0.04 m, before falling sharply. Air velocity was again showed to be increasing sharply at the upper sections of the grain layer. The trend at the section at a height between 0.07 m- 0.18 m did not show, making it difficult to explain what happened. However, because the expectation was for the air velocity to rise steadily up the grain layer, it was concluded that this was not an appropriate grain layer thickness to use.

For the velocity profile up 0.25 m grain layer thickness at 1 m/s, air velocity increased up the grain layer, but only up to a height of 0.03 m before decreasing, showing again that this was not an appropriate grain layer thickness to use. In the case of a 0.3 m grain layer thickness, once again air velocity increased up the grain

layer, but the increase was not sustained. The velocity dropped way before the top of the grain layer, at a height of about 0.2 m. This showed that this was not an appropriate grain layer thickness to use. Thus it was concluded that the maximum grain layer thickness should be 0.1 m.

Pressure profiles for simulated air flow up a drying cabinet with different numbers of grain layers are shown in Appendix 1A (Figs. A5- A9). Beyond four (4) grain layers, the linear trend in pressure drop ceased. It was evident that from five (5) grain layers and above, there were sections where there was little or no change in pressure, suggesting that there was little or no air flow. Sections where the curve remained horizontal indicated no pressure drop. This trend intensified as number of grain layers increased, with the horizontal sections of the curve becoming longer, indicating no pressure drop for greater distances up the grain layers. This continued to the extent that for sixteen (16) grain layers and beyond, the graph was a horizontal line, showing that there was no pressure drop at all, hence suggesting that no air flow through the grain layers occurred. All these are shown in Appendix IB. It was therefore concluded that the grain dryer should be loaded with at most four (4) trays, each with a maximum grain layer thickness of 0.1 m.

4.1.2 Sizing of solar dryer

Fig.4.1 shows variation of pressure for simulated air flow up a single 0.1 m grain layer. It indicates that there was a linear drop in pressure from the lower section of a grain layer upwards.

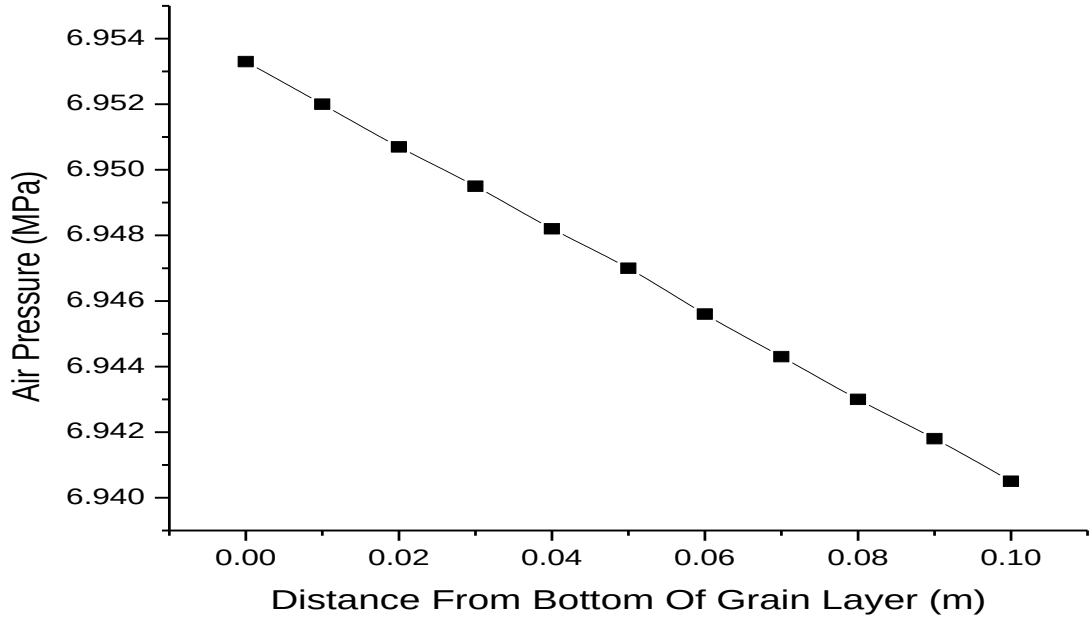

Figure 4. 1: Variation of Pressure for a Single Layer of Thickness 0.1 m

Results of the simulation of air velocity (Fig. 4.1) showed that the total pressure drop for a single 0.1 m thick layer was 1.28 x 10^4 Pa, being the difference between the highest (6.9533 MPa) and the lowest pressure (6.9405 MPa). For two layers or trays, the total pressure drop would therefore be equal to twice this value. This was due to the assumption that pressure drop would be the same for each layer, since they were of equal thickness. As shown in eq. (2.3) pressure drop depends on length of bed and void space which were constant. The other variables, namely particle size, fluid viscosity and density were also assumed to be constant. This yielded a total pressure drop of 2.56 x 10^4 Pa for two (2) grain layers. Selected was a 0.039 kW fan, determined as shown in Appendix 1C.

Although it was found that maximum number of trays should be four, the experimental dryer was designed to carry two trays. Each drying tray with a capacity of 18 kg, was sized to be of square cross section, 0.5 m x 0.5 m. The lowest tray was to be placed 0.3 m from the bottom to allow for the plenum chamber, and the second one 0.2 m above. With each tray having a height of 0.1 m (from simulated maximum layer thickness), and leaving 0.3 m above the upper tray for fitting the fan, this resulted in a total drying cabinet height of 1 m. The required solar collector area was determined to be 3.25 m^2. Detailed calculations are shown in Appendix IC.

4.1.3 Simulation of air flow through experimental dryer

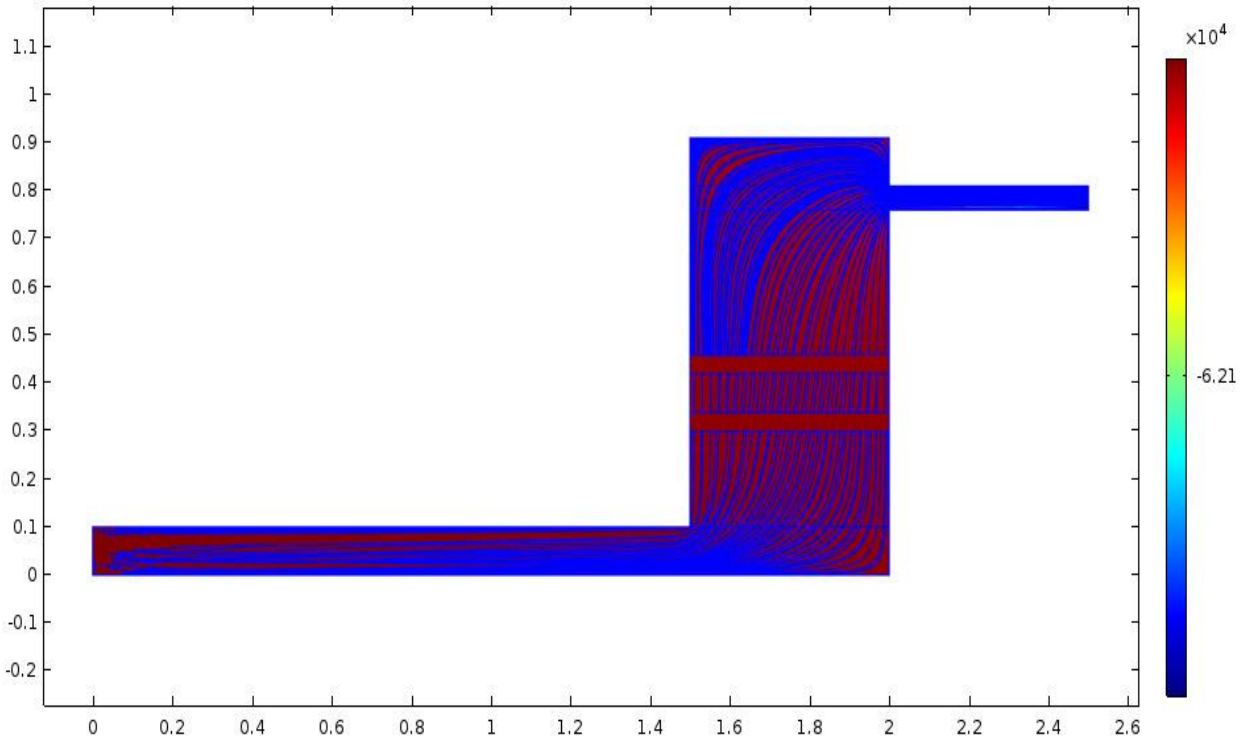

Figure 4. 2: Side view of Solar Dryer

The simulation results (Fig. 4.3), showed that the air, initially flowing at an approximate velocity of 0.33 m/s, maintained the same velocity up the dryer cabinet. However when it reached the first grain layer at the height of 0.3 m, its velocity dropped sharply to almost zero, and remained so all through the grain layer. This was due to the static resistance to its flow within the grain layer. As the air left the grain layer, its velocity rose sharply, but did not reach its initial value, stabilizing at about 0.29 m/s. It had lost some of its kinetic energy as it overcame the resistance to its flow within the grain layer. The velocity remained almost constant within the void space, but sharply declined again to almost zero at the next grain layer at a height of 0.6 m. As before, the air velocity rose sharply at the end of the grain layer, again without attaining its previous magnitude, but rather stabilizing at about 0.26 m/s, a level it sustained until it reached the top of the drying cabinet. Thus, air velocity in a tray further from the air inlet is less than for one closer. This conforms to observations by Misha *et al*. (2013) that air velocity decreases as distance from inlet increases.

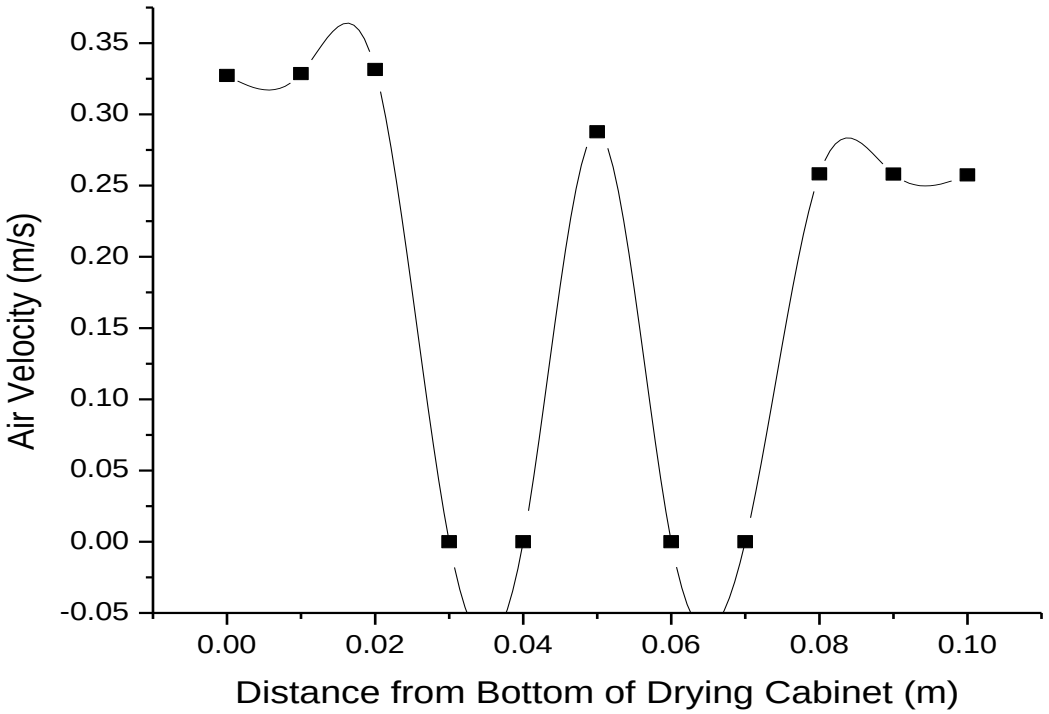

Figure 4. 3: Simulated Air Flow through Drying Cabinet

4.2 Effect of Selected Parameters on Performance of Experimental Dryer

Air was forced up the unloaded dryer in order to observe variation of temperature at various sections of the dryer. Figures 4.4 and 4.5 show the results for an air velocity of 0.21 m/s. It was found that variation of ambient, plenum and tray 1 exit temperatures (Fig. 4.4), followed a similar trend to that of solar radiation (Fig. 4.5), although variation of solar radiation was more intense. It was also noted that plenum and tray 1 exit temperature were, at every instance, very close to each other, although the latter was constantly slightly lower than that at the former. This suggests that there were only slight losses of heat in the drying chamber, between the plenum and the exit, there being no load. These losses may have been due to imperfect insulation. Ambient temperature was constantly below plenum temperature due to the heat absorbed at the solar air heater. Ambient temperature ranged between a low of 23.0 °C and a high of 30.0 °C before a slight reduction, while plenum temperature ranged from 26.8 °C at 10:00 hours to 37.7 °C at 15:00 hours.

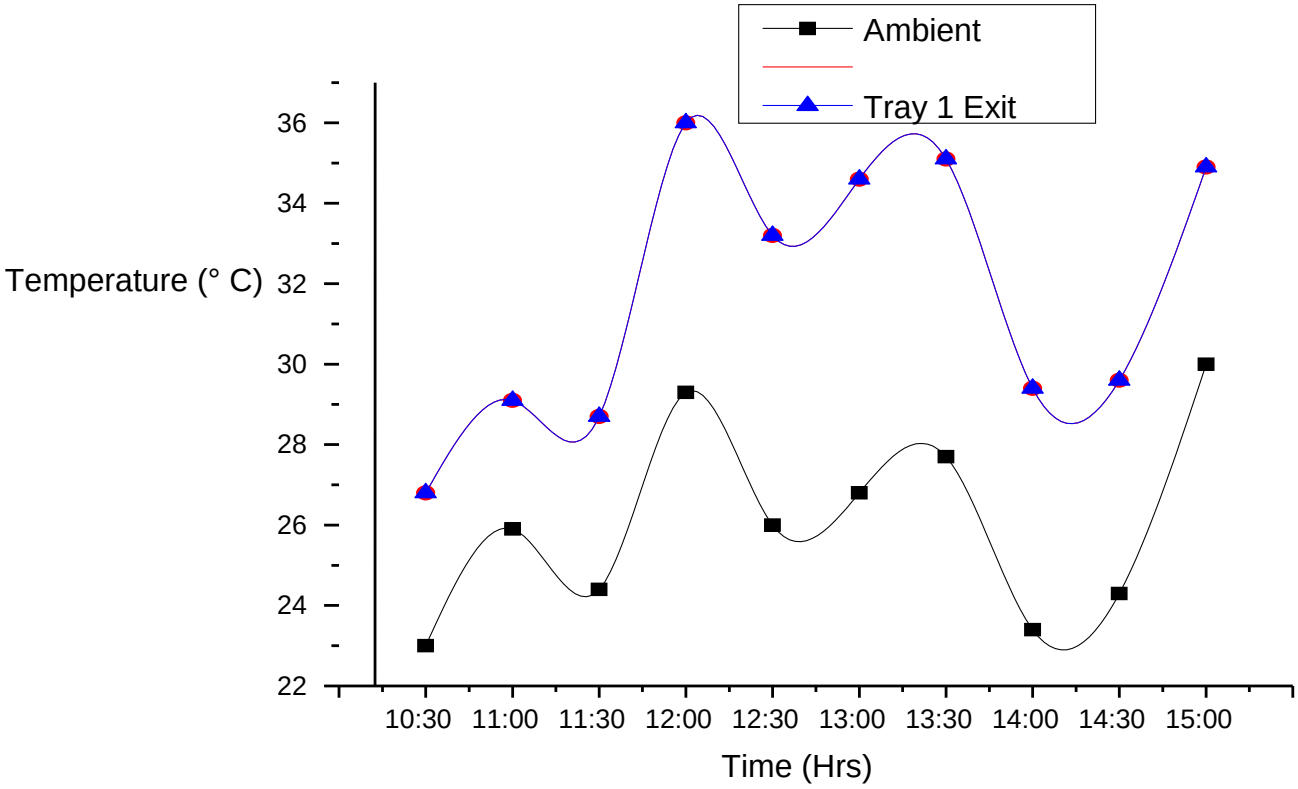

Figure 4. 4: Temperature Variation for Unloaded Dryer

Solar radiation increased and decreased intermittently, the lowest value of 212 W/m^2 being recorded at 13:30 hours, with the highest value of 1202 W/m^2 being observed at 14:30 hours.

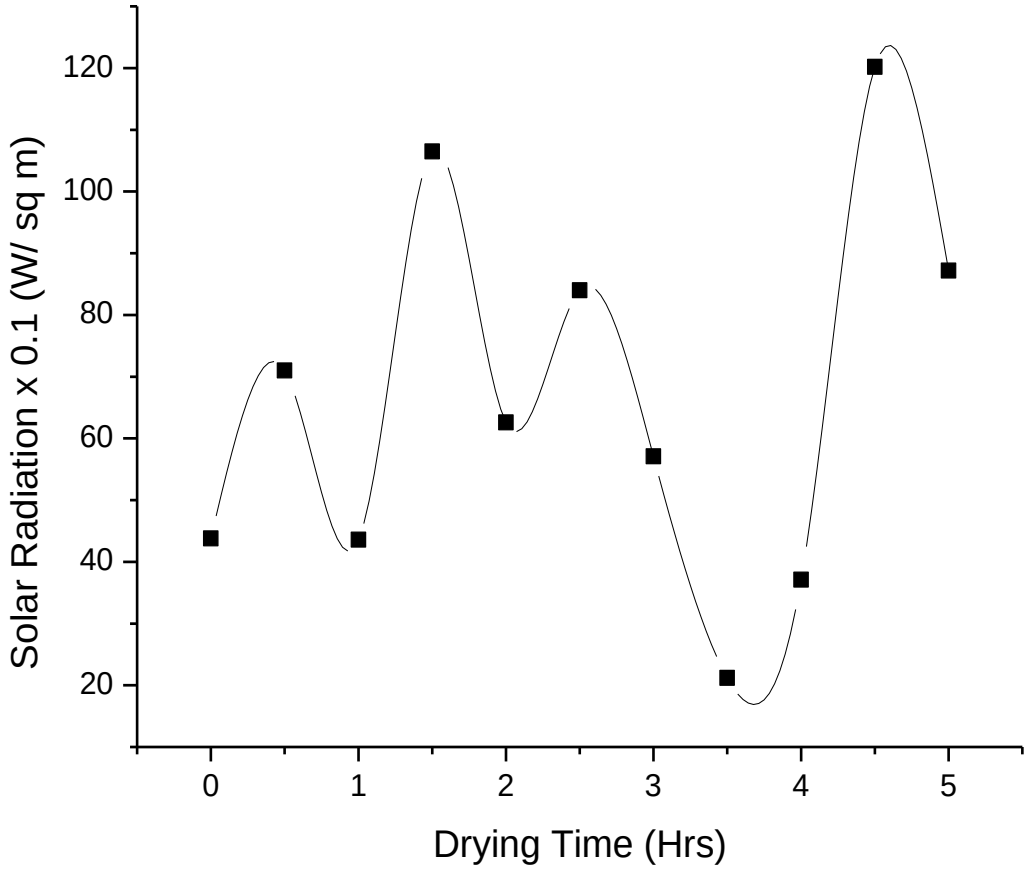

Figure 4. 5: Variation of Solar Radiation with Time for Unloaded Dryer

The dryer was then ran for 3 ½ hours with one tray loaded with 0.1 m thick grain layer. Fig. 4.6 shows variation of temperature during the drying session that began at 09:30 hours. The highest air heater exit temperature was 56.2 °C, towards the end of the drying period. This temperature was found to be appropriate, being just below the 60 °C recommended maximum drying temperature for maize intended to be milled for human consumption. Above this temperature, cracking and discoloration of maize would occur, interfering with its quality (Weiss and Buchinger, 2012; Maier and Bakker-Arkema, 2002). It may be seen that the air heater exit temperature was consistently higher than the ambient, showing the effectiveness of the air heater. The plenum temperature was also consistently lower than the air heater exit temperature, suggesting that the lagging between the air heater exit and the plenum was not perfect, and allowed loss of some heat. There was also a consistent and considerable drop in temperature between the plenum and tray 1 exit, the heat lost being used in the drying process. The difference between ambient and air heater exit

temperatures increased as the drying process continued, suggesting that the solar collector efficiency improved as temperature increased. This is in agreement with results of Aissa *et al*. (2014), which showed that collector efficiency was greater at higher temperatures.

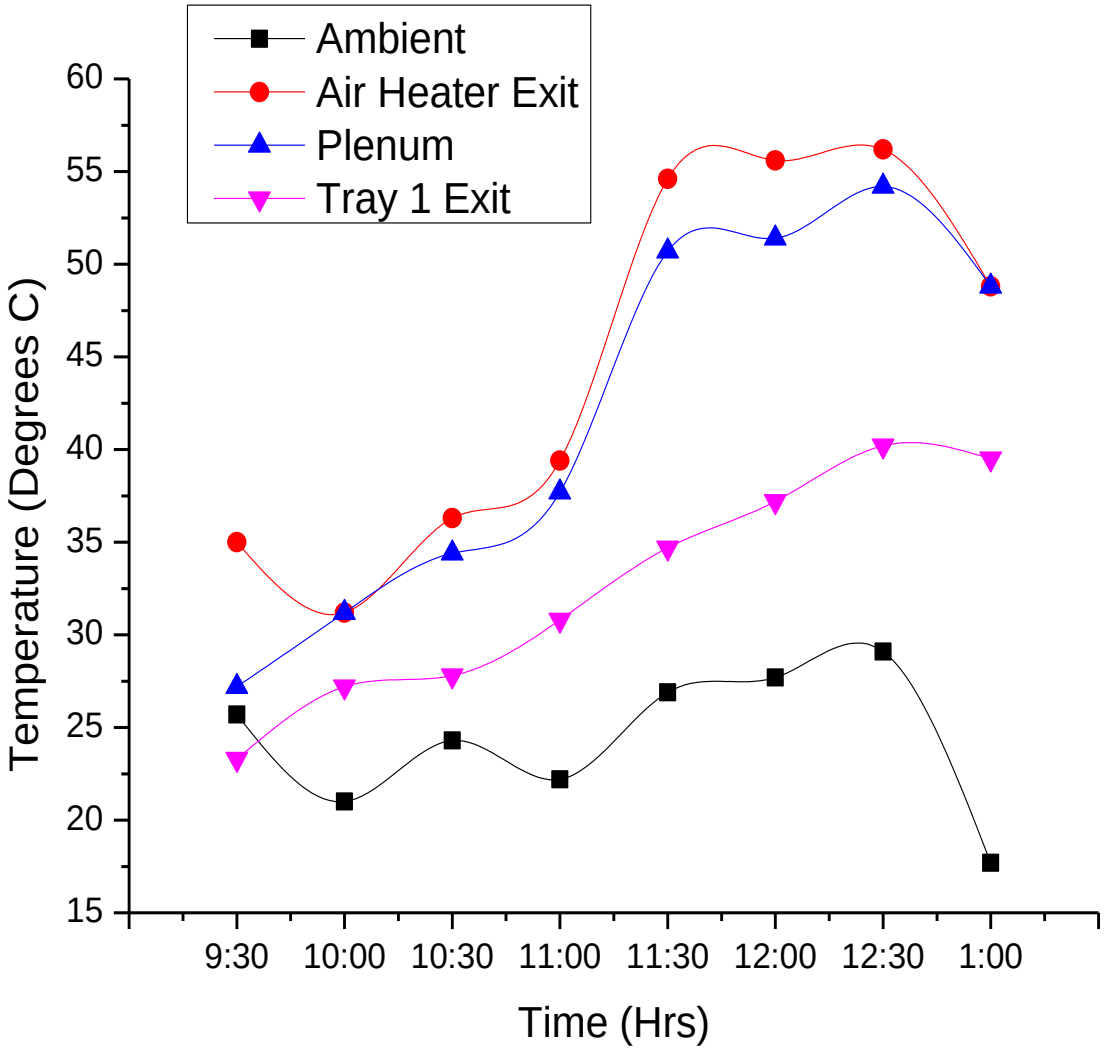

Figure 4. 6: Temperature variation for dryer loaded with grain

Fig. 4.7 shows variation of temperature, including that of the grain during an afternoon drying session between 13:00 hours and 16:30 hours. Solar radiation takes a downward trend, again with intermittent rises and falls. Grain temperature is consistently lower than both plenum and tray 1 exit temperature. Indeed, it is even lower than ambient temperature. Plenum temperature rises slightly before gently

falling to 29.8 °C at 16:30 hours while tray 1 exit, ambient and grain temperatures both fall gently after a slight dip at 13:30 hours.

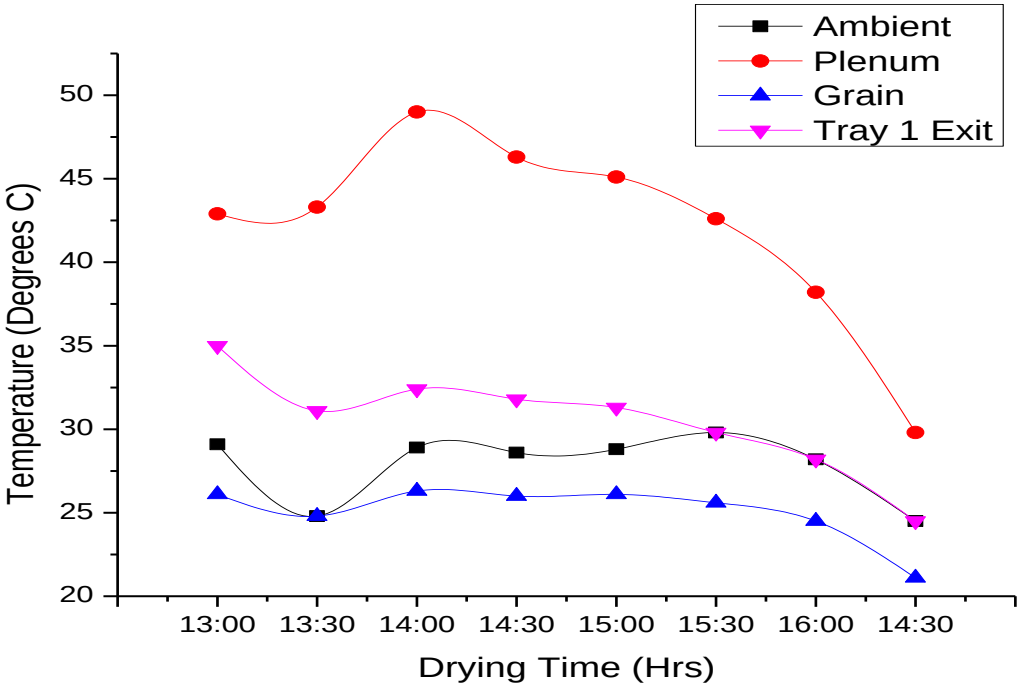

Figure 4. 7: Temperature variation (including grain surface temperature)

4.2.1 Air velocity and grain layer thickness

a) Air velocity

Fig. 4.8 is a clustered bar chart of the variation of drying efficiency with air velocity for different fixed grain layer thicknesses. It was noted that drying efficiency generally increased with air velocity for a given grain layer thickness. This was in agreement with other researchers, such as Akubulut and Durmus (2010) and Aissa *et al*. (2014) who found that higher air velocity resulted in greater drying efficiency. The greatest drying efficiency was observed for a grain layer thickness of 0.04 m, being 13.9 % at an air velocity of 0.41 m/s while the lowest drying efficiency for the same layer thickness was 8.2 % at 0.212 m/s. Increase in drying efficiency with air velocity occurred because the faster moving air was able to carry with it more moisture over a given period of time. This trend was evident for the other layer thicknesses. However, for the 0.08 m grain layer thickness, drying efficiency dropped from 5.4 % at 0.21 m/s air velocity to 4.7% at 0.27 m/s instead of

increasing as was expected. This could be attributed to the drop in mean plenum temperature from 41.9 °C in the former case to 37.6 °C in the latter. It is notable that drying efficiency values were very low. This was due to the considerable amount of energy utilised to drive the fan.

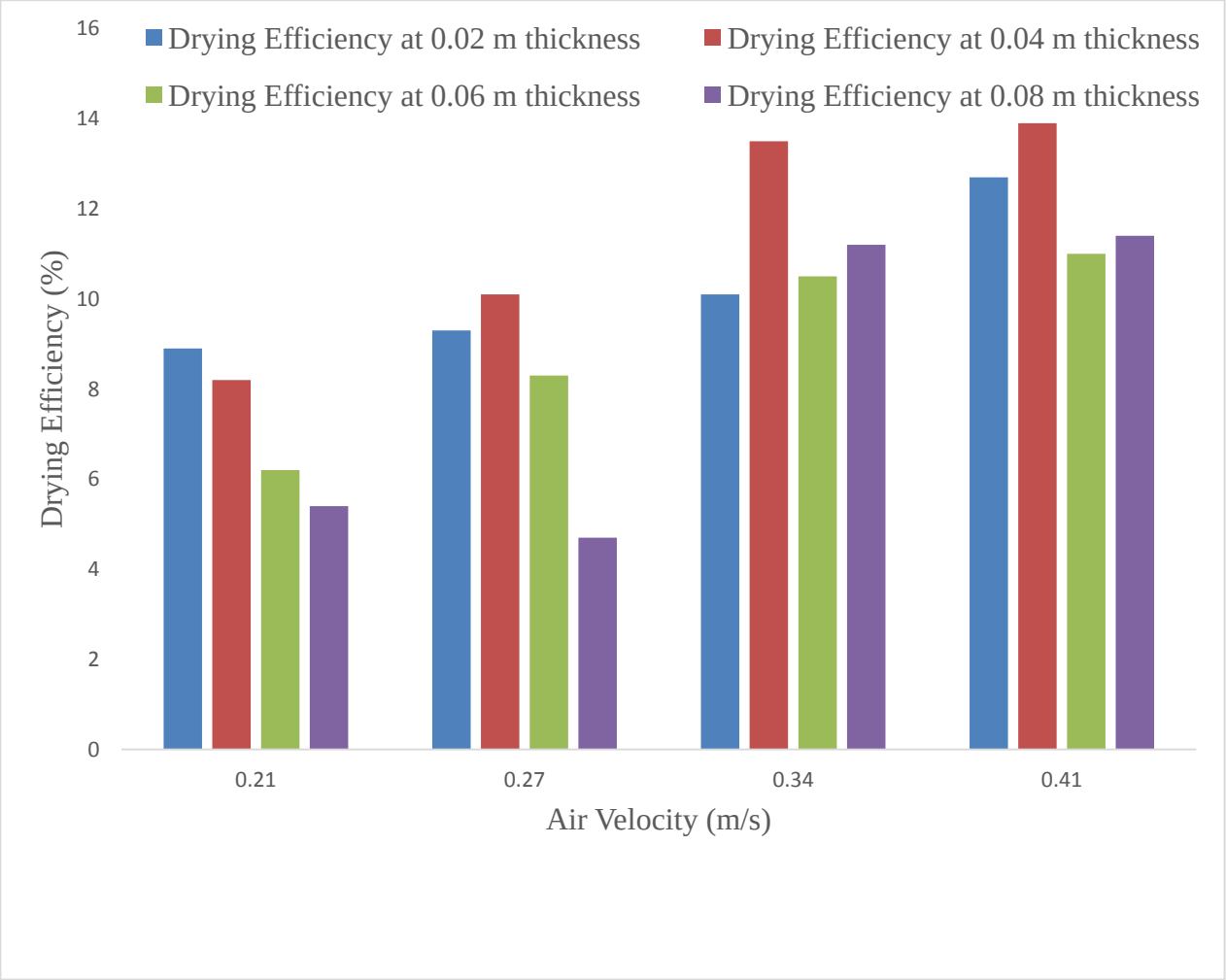

Figure 4. 8: Drying Efficiency vs Air Velocity

Variation of Moisture Removal Rate (MRR) with air velocity for fixed grain layer thicknesses are presented in fig. 4.9. It is notable that for low grain layer thickness, MRR generally increased with increase in air velocity for a given grain layer thickness. This is because at greater velocity, the air was able to carry away more moisture for a given temperature drop. Ikejiofor (2010), Romdhane and Combarnous (2011) as well as Rahmatinejad *et al*. (2016) and Mghazli et al. (2017) reported similar results, although theirs were with respect to drying rate, a criteria similar to

moisture removal rate. The highest MRR was for 0.02 m grain layer thickness, and was 0.061 kg moisture/ (kg wet grain. hour) at 0.41 m/s air velocity, while the lowest was 0.048 kg moisture/ (kg wet grain. hour) at 0.21 m/s. It is, however, evident that for 0.04 m, 0.06 m and 0.08 m grain layer thicknesses, there is a slight decrease in MRR from 0.21 m/s to 0.27 m/s. This could have been due to a decline in temperature, which was not controlled during the experiment due to variation of insolation.

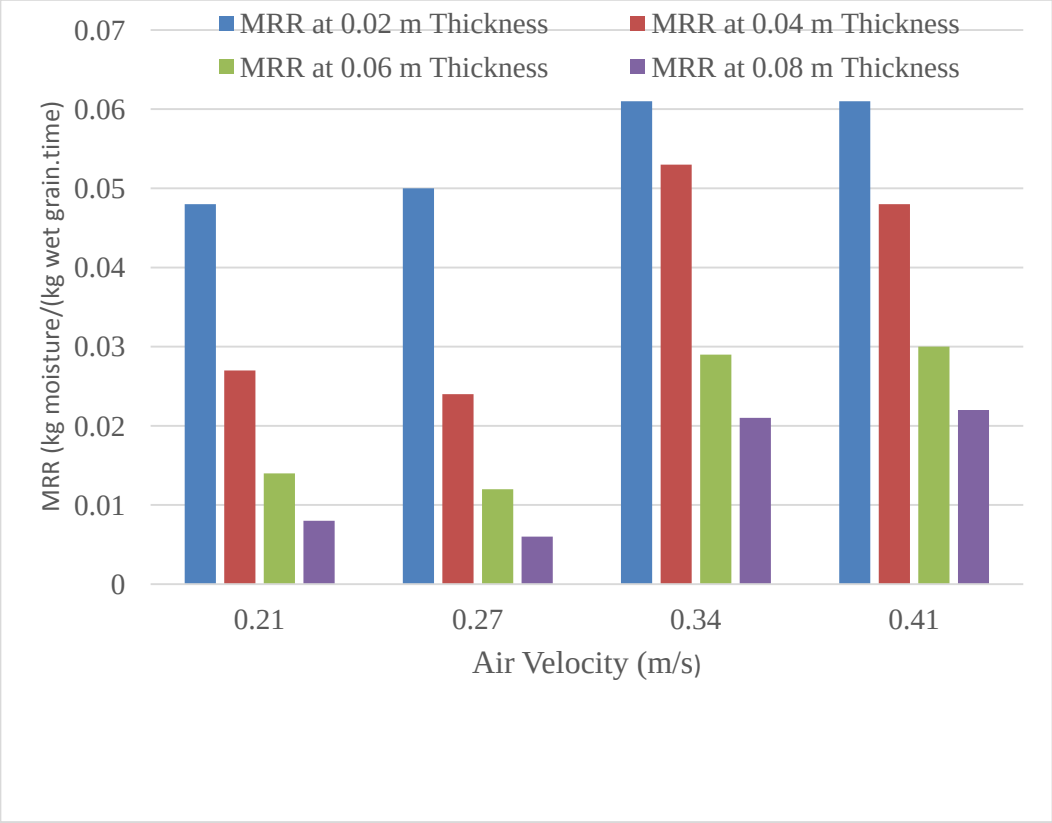

Figure 4. 9: Moisture Removal Rate vs. Air Velocity

Various theories, as proposed by Jerger (1951), may be used to explain the increase in moisture removal rate as drying air velocity increases. The gravity, capillary flow and porous flow theories of drying may be eliminated as possible explanations. This is because the gravity theory accounts for movement of moisture to the bottom, whereas in the case at hand, moisture moved upwards. The capillary flow theory, on the other hand, attributes change of drying rate to the sizes of the pores and their distribution within the material. These were not necessarily altered by the change in air velocity during these experiments, as the same grain was under investigation.

This theory would therefore not be relied upon to explain the change in moisture removal rate. The porous flow theory was a possible explanation although it relies on capillarity suction and gravity, eliminated earlier. However, this theory also attributes moisture removal in a grain to external pressure which increased as air velocity was increased, and could therefore have led to increased moisture removal. Another explanation could have been the diffusion theory. According to Fick's law of diffusion [eq. (2.2)], which is the basis of this theory, a higher concentration gradient increases permeation rate of the moisture. Increased diffusion at higher mass flow rate of air, which in turn increased concentration gradient, could thus be the reason for the increased moisture removal rate observed.

b) Grain layer thickness

Experiments were carried out as described in section 3.3.2. Variation of drying efficiency with grain layer thickness at fixed air velocity is shown in Fig. 4.10. For the lowest air velocity of 0.21 m/s, there was a general decline in drying efficiency as grain layer thickness increased. This was probably because the air became more humid as it rose up the grain layer. In the process, its capacity to absorb more vapour declined as it approached saturation. This effect became more profound as the grain layer became thicker. Thus it was possible for a greater percentage of moisture to be removed from a thinner grain layer by the less humid air. The trend was almost similar for air velocity of 0.27 m/s. For air velocities of 0.34 m/s and 0.41 m/s, the trend was not as clear. For example, at 0.34 m/s air velocity, drying efficiency is considerably higher at a grain layer thickness of 0.04 m than for 0.02 mm. This could be attributed to the slightly greater mean plenum temperature of 38.7°C when the 0.04 m thick grain layer was dried, compared to 37.8°C when the 0.02 m thick layer was dried. Similarly, for the same air velocity, the mean plenum temperature was 39.6°C when the 0.08 m thick layer, compared to 38.3°C when the 0.06 m thick layer was being dried, resulting in a greater drying efficiency for the former.

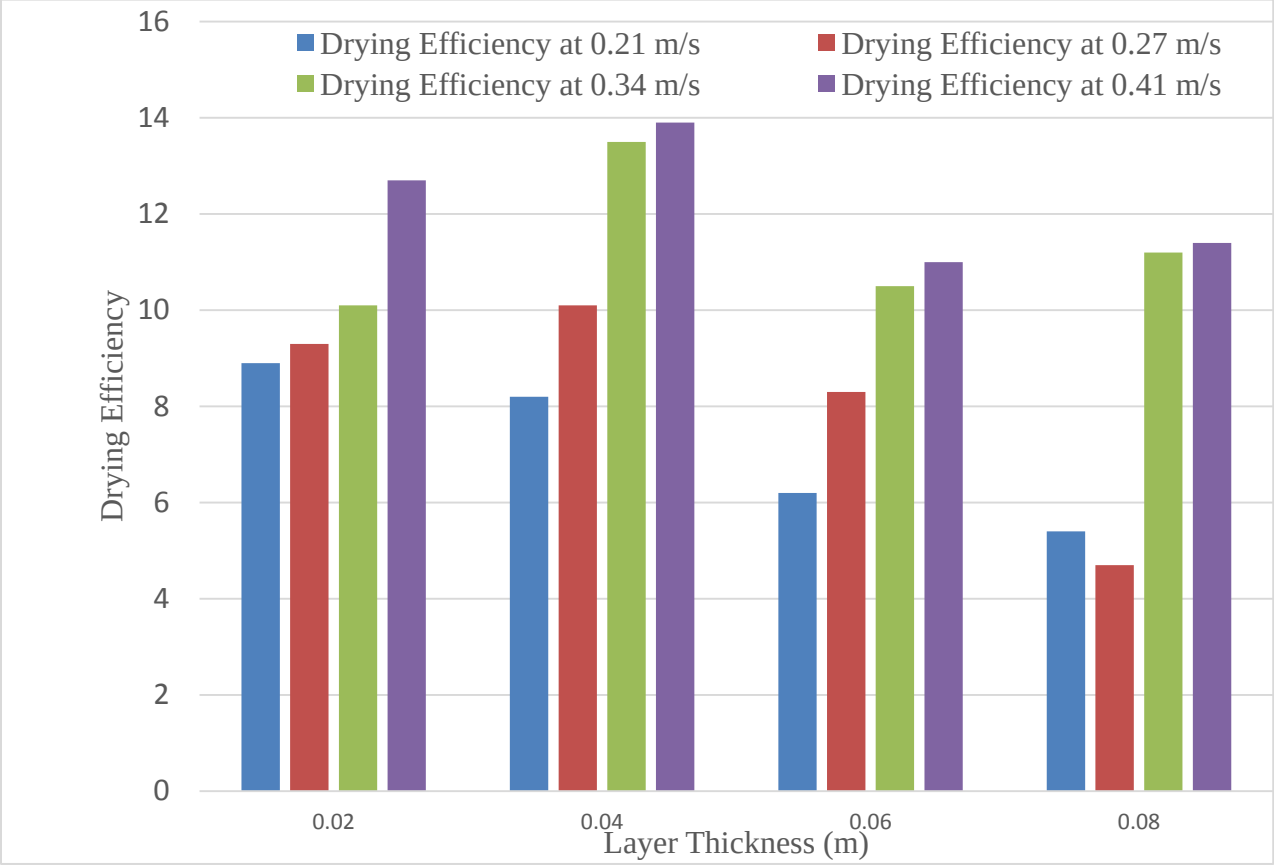

Figure 4. 10: Drying Efficiency vs Grain Layer Thickness

Fig. 4.11 shows how moisture removal rate varied with grain layer thickness at constant air velocity. It may be seen that for any given air velocity, moisture removal rate decreased as the grain layer thickness increased. These results are similar to those of Sarker *et al*. (2012) as well as Delgado and Lima (2014). The possible explanation is that as grain layer thickness increased, the air absorbed more and more moisture as it was rising up. It thus became more humid resulting in a decline in its capacity to remove more moisture as it approached saturation. Also, applying Fick's law, the rate of permeation was lower for a greater layer thickness since the quantity $\left[\frac{\partial C}{\partial x}\right]$ decreased, as the denominator (thickness) increased in spite of the numerator (concentration) remaining unchanged. It was also noted that the moisture removal rates at 0.21 m/s and 0.27 m/s on one hand, and for 0.34 m/s and 0.41 m/s on the other, were very close. This was probably because the intervals for air velocities were not uniform, that between 0.27 m/s and 0.34 m/s, for example being greater than that between 0.21 m/s and 0.27 m/s.

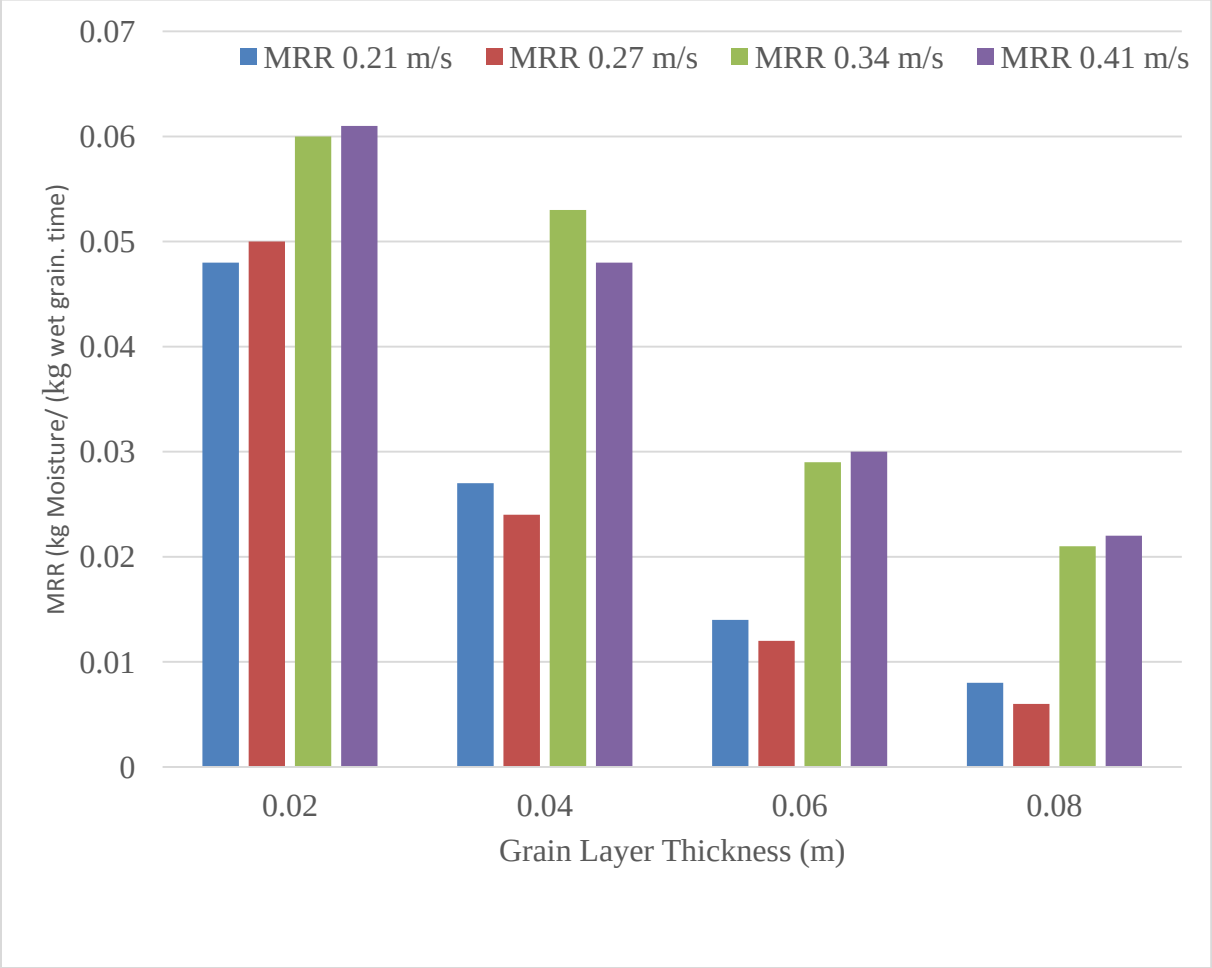

Figure 4. 11: Moisture Removal Rate vs. Grain Layer Thickness

4.2.2 Number of trays

The intention here was to compare moisture removal rate for the dryer when using different numbers of trays. Table 4.1 is a comparison of the MRR of the dryer when 0.04 m grain layer thickness was dried as a single layer in one tray on one hand, and as two single layers of 0.02 m each in two trays, on the other. The mean drying temperatures also changed since the maize was dried on different days.

Table 4. 1: Moisture Removal Rate for One and Two Trays

No of Trays	Air Velocity (m/s)	Mean Plenum Temperature (°C)	Mass of Wet Grain (g)	Moisture Loss (g)			Moisture Removal Rate (kg Moisture.kg^{-1} wet grain Hr^{-1})
				Tray 1	Tray 2	Total	
1	0.41	32.1	6194	1057	-	1057	0.048
1	0.27	24.1	6376	486	-	486	0.022
2	0.41	36.8	7854	747	636	1383	0.050
2	0.27	39.9	7266	823	515	1338	0.053

ANOVA was carried out to determine whether drying 0.04 m grain layer thickness as a single layer in one tray, or in two 0.02 m layers in two trays would have any significant effect on the MRR of the dryer if air velocity was constant. The results for air velocity of 0.41 m/s showed the existence of no significant difference (p>0.05; F_{comp} = 1.008; $F_{Crit.\ 5\%}$ = 19.000) for the effect of changing number of trays on moisture removal rate (Appendix II). This is in spite of air temperature rising from 32.1 °C for a single tray to 36.8 °C for two trays. Thus there would be no significant benefits in using more than one tray in the dryer. This is because the hot air acquires no extra capacity to remove air even if extra trays are used. Indeed, it is evident that where two trays are used, then moisture removal rate is greater in the first tray. This is in agreement with findings reported by Sallam *et al*. (2013) after studies on drying of mint. The situation where an air velocity of 0.27 m/s was used (for one and two trays) was difficult to compare since drying air temperature increased by 15.8 °C, probably explaining the significant increase in MRR from 0.022 kg Moisture.kg^{-1} wet grain Hr^{-1} for one tray, to 0.053 kg Moisture.kg^{-1} wet grain Hr^{-1} for two trays.

4.2.3 Drying air temperature

Fig. 4.12 shows the variation of dryer performance with drying air temperature when drying was carried out using the electrically heated air described in section 3.3.4. It was found that where forced convection was used, drying efficiency generally decreased as temperature increased. This is in agreement with other researchers, such as Balbine *et al*. (2015) and Aissa *et al*. (2014). During the drying of a 0.04 m thick grain layer at an air velocity of 0.41 m/s, the greatest drying efficiency of 23.5% was observed at a temperature of 40 °C, while the lowest was 10.1 % at 55 °C. Drying efficiency decreased with increase in temperature possibly due to the imperfect insulation of the drying cabinet. This is because as the drying temperature increased, heat loss due to conduction through the wall of the drying cabinet increased, since heat flow by conduction is proportional to temperature difference between two surfaces. However, a comparison of drying efficiency for the same temperature showed that forced convectional drying was more efficient than natural convection, their values having been 23.5 % and 13.8 % respectively at 40 °C.

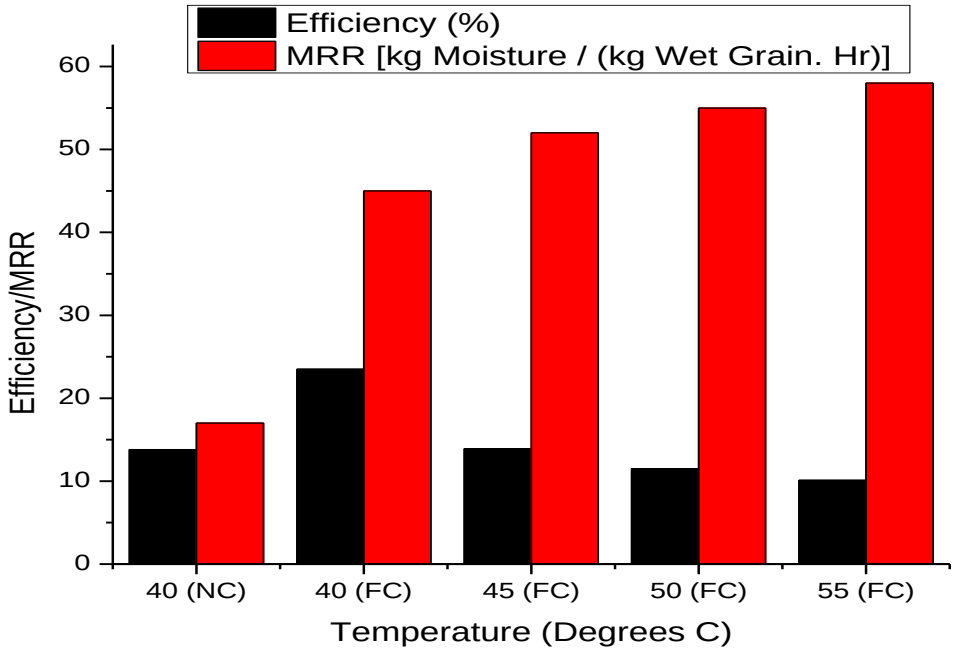

NC= Natural Convection FC= Forced Convection

Figure 4. 12: Effect of Temperature on Dryer Performance

Moisture removal rate, however, increased with drying air temperature, and was also lower for natural convection than forced convection (Fig. 4.12). Romdhane and Combarnous (2011), El-sebaii and Shalaby (2013), Tzepelinkos *et al*. (2014), as well as Rahmatinejad *et al*. (2016), reported similar results, though with respect to drying rate. MRR is a measure of drying rate. The various theories of drying, mentioned earlier, may again be used to explain the increase in moisture removal rate as drying air temperature increases. Once again, and for similar reasons to those outlined for air velocity, the gravity and capillary flow may be eliminated as possible explanations. Also, in this case the porous flow theory was not a plausible explanation as it relies on capillarity suction and gravity, as well as external pressure, which remained the same at the various temperatures. However, applying the diffusion theory, increased diffusion at higher temperature, which in turn increased concentration gradient, could thus be the reason for the increased moisture removal rate observed. Rafiee *et al*. (2006) studied the drying of wheat using a convective dryer and concluded that moisture removal is governed by the diffusion phenomenon. The vapourisation-condensation theory could also account for the increased moisture removal rate. The temperature drop within the grain layer was found to be greater at higher temperature (Fig. 4.13), therefore leading to higher pressure gradients and hence more transfer of vapour to the air.

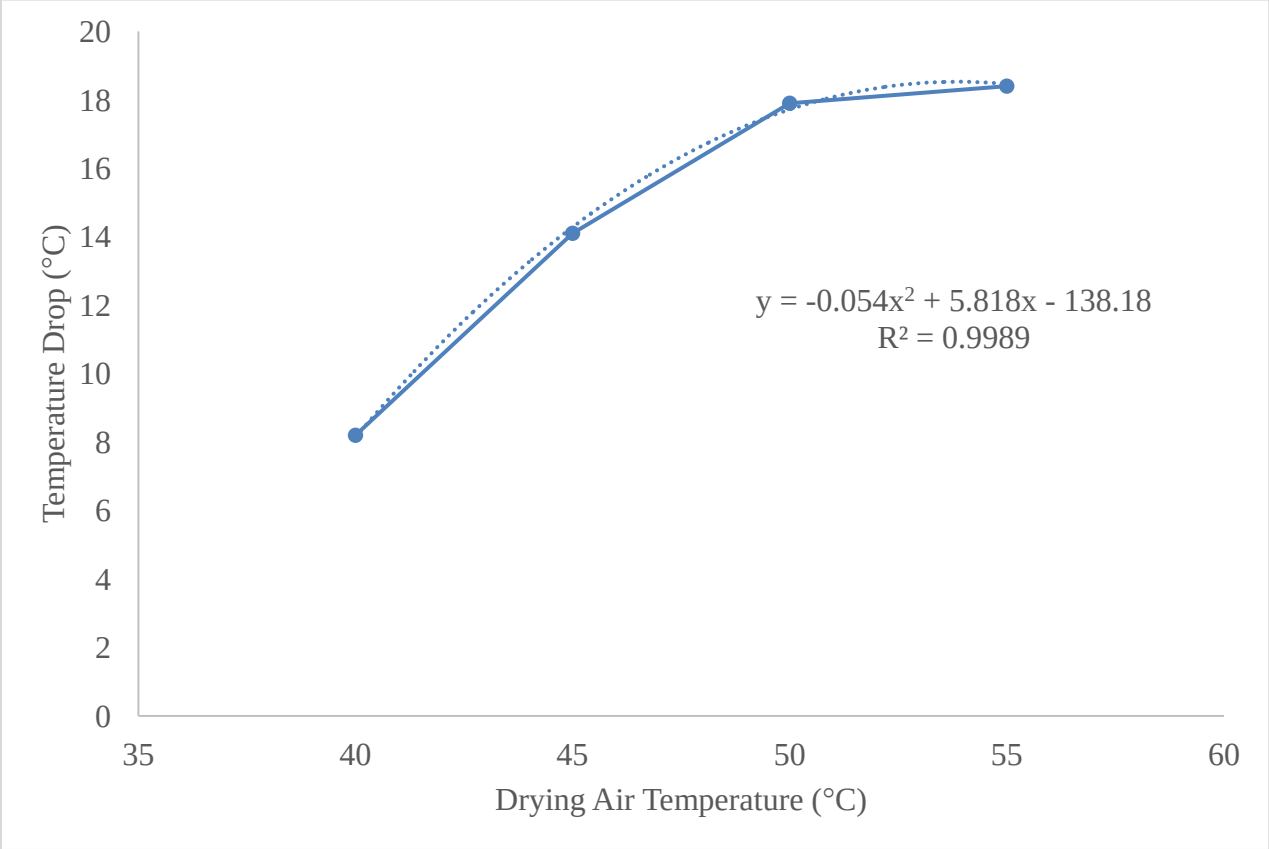

Figure 4. 13: Temperature drop within grain Layer

One way ANOVA was carried out to determine whether the effect of temperature on drying efficiency was significant. Using the Turkey method for information grouping (95 % Confidence Level), it was found that increasing temperature between 40 to 45 ºC, 45 to 50 ºC and 50 to 55 ºC in each case significantly reduced drying efficiency, during forced convection drying. There was also a significant difference in drying efficiency between drying at 40 ºC using natural convection, from when forced convection is applied at the same temperature. This is summarized in Table 4.2.

Table 4. 2: Effect of Temperature on drying efficiency (Turkey Method)

Temperature (ºC)	Mean Dryer Efficiency (%)	Grouping
40 (Natural convection)	13.8	B
40 (Forced convection)	23.5	A
45 (Forced convection)	13.9	B
50 (Forced convection)	11.5	C
55 (Forced convection)	11.1	D

(*Groupings that do not share a letter are significant*)

When similar analysis was applied to determine the effect of temperature on moisture removal rate (Table 4.3), it was found that changing temperature from 40 to 45 ºC caused a significant increase. However, increasing temperature from 45 to 50 ºC, and 50 to 55 ºC, in each instance had no significant effect on moisture removal rate.

Table 4. 3: Effect of Temperature on Moisture Removal Rate (Turkey Method)

Temperature(ºC)	Mean Moisture Removal Rate (H^{-1})	Grouping
55 (Forced convection)	0.058	A
50 (Forced convection)	0.055	A
45 (Forced convection)	0.053	A
40 (Forced convection)	0.045	B
40 (Natural convection)	0.017	C

(*Groupings that do not share a letter are significant*)

4.2.4 Relative humidity

The ANOVA results showed the existence of no significant difference ($P > 0.05$; $F_{comp} = 1.120$, $F_{Crit\ 5\%} = 19.000$) for the effect of relative humidity on MRR (Appendix III). RH was varied between 54 and 62 % first at 40 °C, then 45 °C, keeping air velocity and grain layer thickness constant (0.41 m/s and 0.04 m respectively). This insignificant change of MRR may be because of the air temperatures at which drying was carried out. Ondier *et al*. (2010), reported that lower humidity had greater potential to increase drying rates than higher ones. They found that lowering relative humidity at a temperature of 26 °C had a greater effect

on drying rate as compared to doing the same at 30 and 34 °C. It would otherwise have been expected that drying rate should decrease as relative humidity increases. Experiments by Estrada and Litchfield (1993) showed that increase in humidity reduces drying rate up to a relative humidity of 44%. However, in the current study, humidity within the drying cabinet was not controlled. It is therefore likely that the ambient relative humidity, which is what was measured, could not affect drying rate in the drying chamber.

4.3 Optimum Dryer Performance and Selected Drying Model

4.3.1 Optimum dryer performance

a) Dryer in open sun

Table 4.4 shows experimental results for Moisture Removal Rate (MRR) and drying efficiency obtained using the L16 orthogonal array. The corresponding S/N ratios are also shown.

Table 4. 4: Moisture Removal Rates & S/N Ratios

Test run	Air Velocity (m/s) / Layer Thickness(m)	MRR (kg Moisture kg^{-1}Wet Grain. Hr^{-1})	S/N Ratio (MRR)	Drying Efficiency (%)	S/N Ratio (Drying Efficiency)
1	0.21/0.02	0.048	-26.38	8.9	18.99
2	0.21/0.04	0.027	-31.17	8.2	18.28
3	0.21/0.06	0.014	-37.08	6.2	15.85
4	0.21/0.08	0.008	-41.94	5.4	14.60
5	0.27/0.02	0.050	-26.02	9.3	19.37
6	0.27/0.04	0.024	-32.4	10.1	20.09
7	0.27/0.06	0.012	-38.42	8.3	18.38
8	0.27/0.08	0.007	-43.10	4.7	13.44
9	0.34/0.02	0.061	-24.29	10.1	20.09
10	0.34/0.04	0.053	-25.51	13.5	22.61
11	0.34/0.06	0.029	-30.75	10.5	20.42
12	0.34/0.08	0.021	-33.56	11.2	20.98
13	0.41/0.02	0.061	-24.29	12.7	22.08
14	0.41/0.04	0.048	-26.38	13.9	22.86
15	0.41/0.06	0.030	-30.46	11.0	20.83
16	0.41/0.08	0.022	-33.15	11.4	21.14

Table 4.5 shows the mean SN ratios for each of the levels of air velocity and grain layer thickness. The means were computed after isolating the SN ratios for each level of a given parameter. For example, to find the mean SN ratio for air velocity at 0.21 m/s (air velocity level 1), the SN ratio values for experiments 1-4 were averaged. Similarly, to determine the mean SN ratio for 0.02 m grain layer thickness (grain layer thickness level 1), SN ratio values for experiments 1, 5, 9 and 13 were averaged.

Table 4. 5: Mean SN Ratios for Moisture Removal Rate

Symbol	Parameter/Factors	Mean SN Ratio			
		Level 1	Level 2	Level 3	Level 4
A	Air Velocity	-34.14	-34.99	-28.75	-28.57
B	Grain Layer Thickness	-25.25	-28.87	-34.18	-37.94

It is evident from Table 4.5 that the greatest mean S/N ratio for air velocity (A) is at level 4, while that for grain layer thickness (B) is at level 1. This is confirmed by the Main Effects Plot shown in Fig. 4.14, which displays the mean values of SN ratios for the various levels of factor A (air velocity) and factor B (grain layer thickness). Thus the optimum combination for greatest moisture removal rate is 0.41 m/s air velocity and 0.02 mm grain layer thickness.

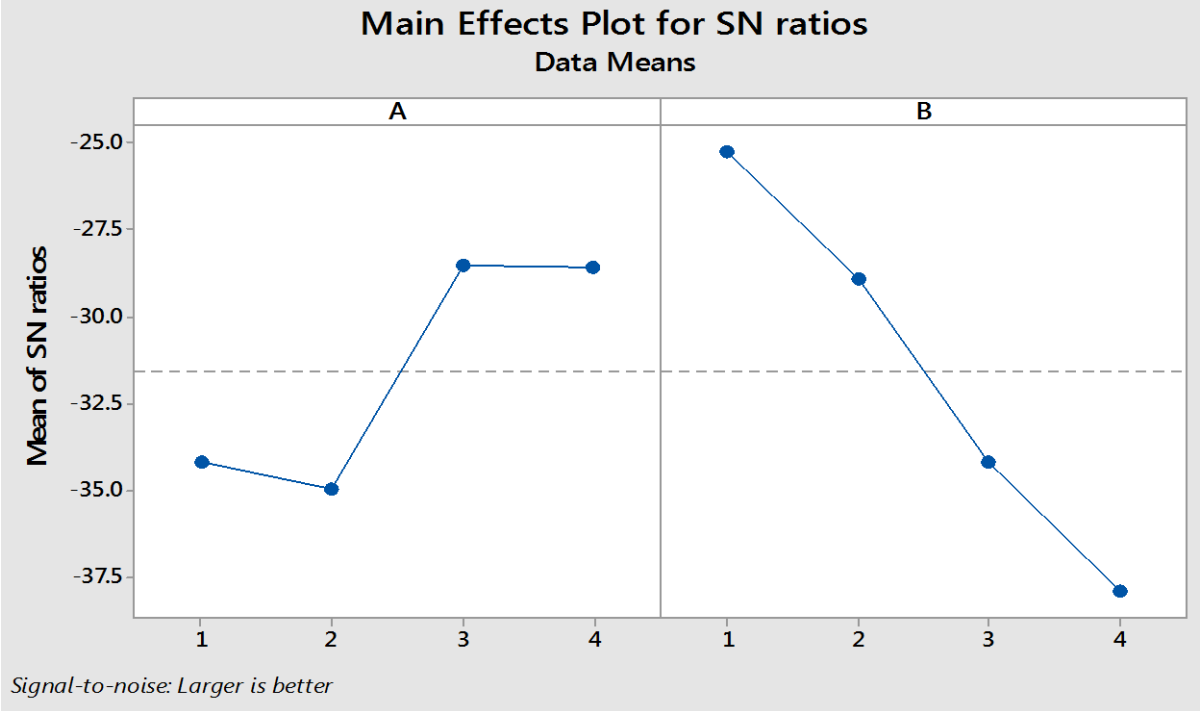

Figure 4. 14: Main effects Plot for MRR during Solar Frying

The mean SN ratios for drying efficiency are shown in table 4.6, and the main effects plot in Fig. 4.15. It is evident that the mean SN ratio value for air velocity (Factor A) is highest at level 4. This implies that air velocity of 0.41 m/s gives the best performance in terms of drying efficiency. In the case of grain layer thickness (Factor B), the highest mean SN ratio is at level 2, suggesting that a grain layer

thickness of 0.04 m provides greatest drying efficiency. This is in spite of the fact that a layer thickness of 0.02 m was expected to yield highest drying efficiency. The discrepancy may be attributable to higher mean plenum temperatures during the drying of the former. Thus, the optimum combination for greatest drying efficiency was air velocity of 0.41 m/s and grain layer thickness of 0.04 m.

Table 4. 6: Mean SN Ratios for Drying Efficiency

Symbol	Parameter/Factors	Mean SN Ratio			
		Level 1	Level 2	Level 3	Level 4
A	Air Velocity	16.93	17.82	21.03	21.73
B	Grain Layer Thickness	20.13	20.96	18.87	17.54

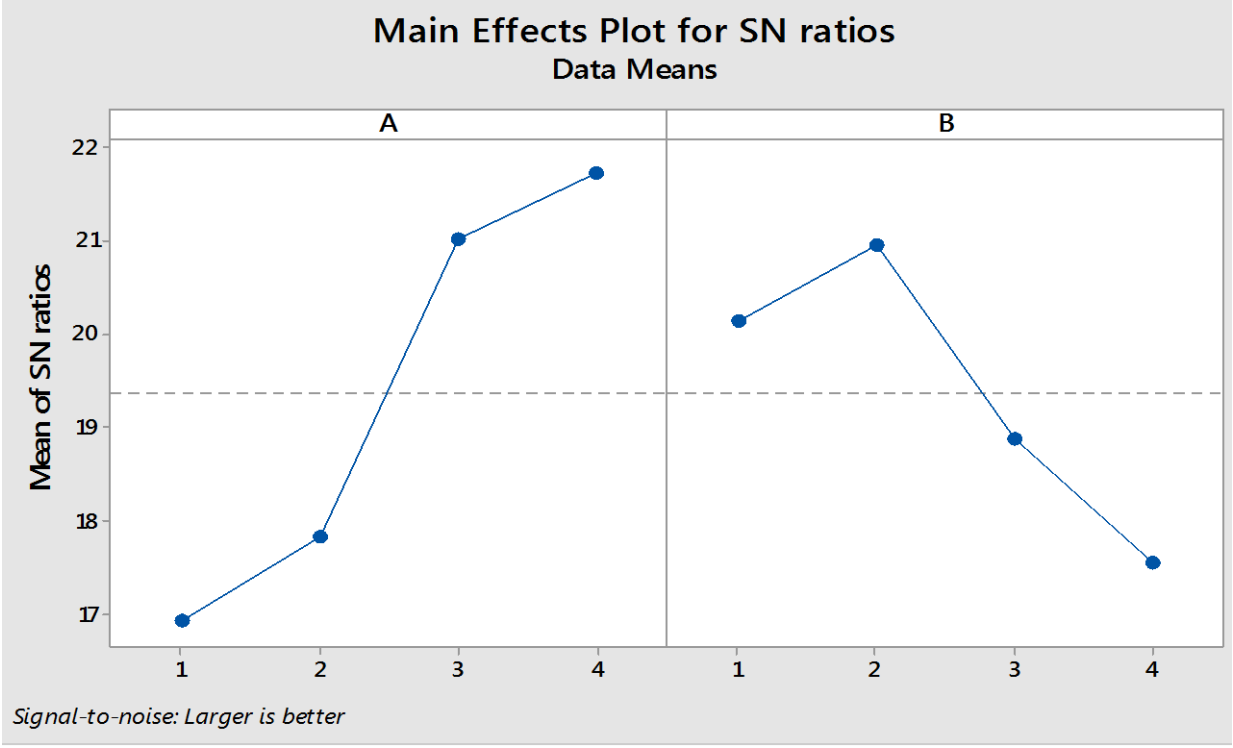

Figure 4. 15: Main Effects Plot for Drying Efficiency during Solar Drying

ANOVA results (Appendix III) showed the existence of a significant difference (p<0.05; F_{comp} = 5.654; $F_{Crit.\ 5\%}$ = 3.863) for the effect of grain layer thickness on drying efficiency. Similarly, change of air velocity had a significant effect on drying efficiency (p < 0.05; F_{comp} = 16.775; $F_{Crit.\ 5\%}$ = 3.863). Also, there existed a

significant difference (p<0.05; F_{comp} = 103.639; $F_{crit.\ 5\%}$ = 3.863) for the effect of grain layer thickness on moisture removal rate and a significant difference (p<0.05; F_{comp} = 30.202; $F_{Crit.\ 5\%}$ = 3.863) for the effect of air velocity on moisture removal rate. These results showed that changing between at least one pair of grain layer thickness levels, and at least one pair of air velocity levels, had a significant effect on drying efficiency and moisture removal rate. However, it was not possible to tell the specific pair of levels that would significantly affect drying efficiency and moisture removal rate. It was therefore necessary to perform least significant difference (LSD) tests, the results of which are shown tables 4.7 and 4.8.

Table 4.7 shows that changing air velocity from 0.21 m/s to 0.27 m/s had no significant effect on neither moisture removal rate nor drying efficiency, since in all cases, the difference between the means were less than $LSD_{\alpha=0.05}$. The same applied to changing from 0.34 m/s to 0.41 m/s. However, changing air velocity from 0.27 m/s to 0.34 m/s had a significant effect on both moisture removal rate and drying efficiency, since in these cases, the difference between the means exceeded $LSD_{\alpha=0.05}$.

Table 4. 7: Effects of Air Velocity on MRR and Drying Efficiency

Velocity (m/s)	Moisture Removal Rate (kg Moisture.kg^{-1} wet grain. Hr^{-1})	Drying Efficiency (%)
0.21	0.024^{b}	7.175^{b}
0.27	0.023^{b}	8.100^{b}
0.34	0.041^{a}	11.325^{a}
0.41	0.040^{a}	12.250^{a}
$LSD_{\alpha=0.05}$	0.006	1.918

(Means with same superscript are not significant)

From table 4.8, it is evident that changing from each of the grain layer levels to the next had a significant effect on MRR. However, while changing from 0.04 m to 0.06 m grain layer thickness had a significant effect on drying efficiency, changing from 0.02 m to 0.04 m, as well as 0.06 m to 0.08 m grain layer thicknesses did not.

Table 4. 8: Effect of Grain Layer Thickness on MRR and Drying Efficiency

Grain Layer Thickness (m)	Moisture removal Rate (kg Moisture.kg^{-1} wet grain. Hr^{-1})	Drying Efficiency (%)
0.02	0.055^{a}	10.250^{a}
0.04	0.038^{b}	11.425^{a}
0.06	0.021^{c}	9.000^{b}
0.08	0.014^{d}	8.175^{b}
$LSD_{\alpha= 0.05}$	0.006	1.918

(Means with same superscript are not significant)

Thus, it would be prudent to use an air velocity of 0.34 m/s since using 0.41 m/s would end up in greater power consumption (for driving fan faster) without any significant advantage as far as drying efficiency and moisture removal rate are concerned. A grain layer thickness of 0.04 m would be preferable if drying efficiency were the major criterion, since using 0.02 m would reduce through-put without necessarily reducing drying efficiency. However, if moisture removal rate was the main consideration, a grain layer thickness of 0.02 would be preferred since it would result in the highest moisture removal rate.

b) Dryer in laboratory conditions

As shown in the main effects plot in Fig. 4.16, the greatest mean SN ratios were found to be at 0.41 m/s (level 3) for air velocity (Factor A), 45 °C (level 1) for drying air temperature (Factor B) and 0.02 m (level 1) for grain layer thickness (Factor C). This would therefore be the best combination resulting in the highest MRR.

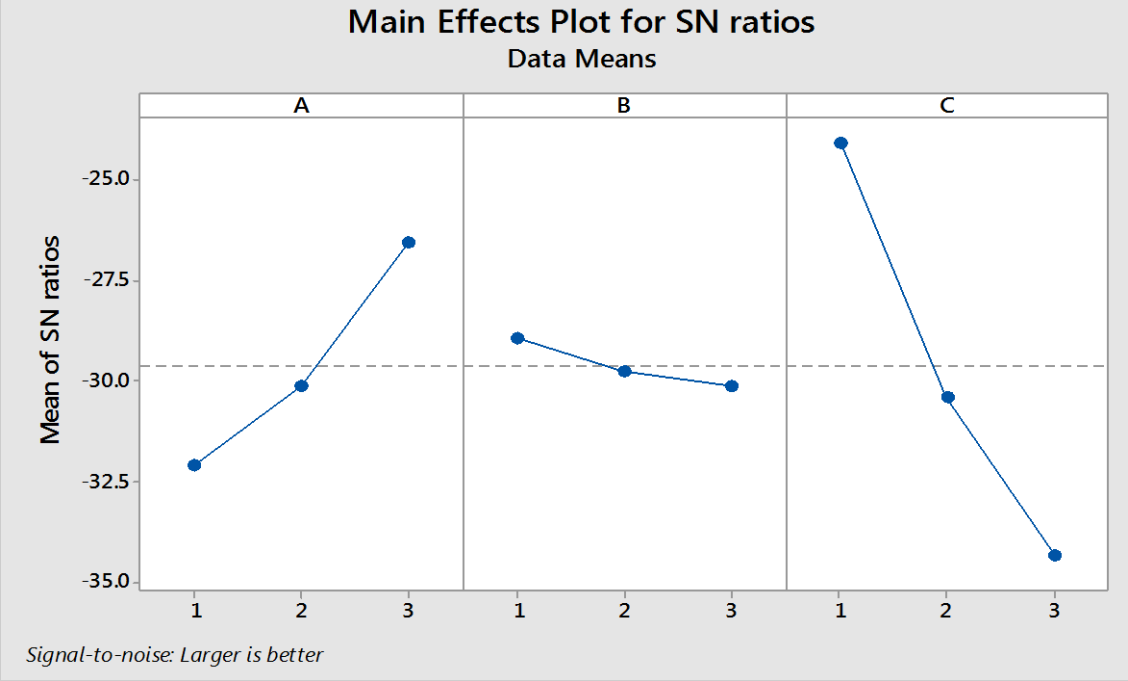

Figure 4. 16: Main Effects Plot for MRR during Laboratory Drying

Fig. 4.17 shows that the highest mean SN ratios are at levels 3 - 1 - 1 for air velocity (Factor A), drying air temperature (Factor B) and grain layer thickness (Factor C) respectively. Thus, the best combination of parameter levels for greatest drying efficiency was found to be 0.41 m/s, 45 °C and 0.2 m/s.

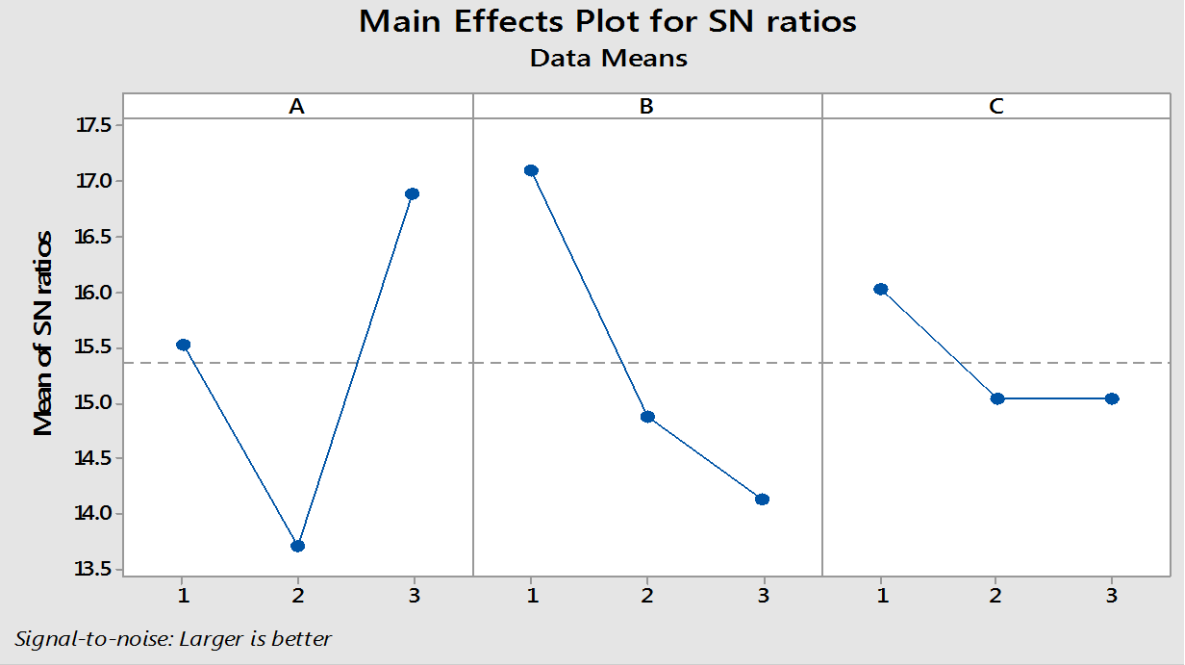

Figure 4. 17: Main Effects Plot for Drying Efficiency during Laboratory Drying

4.3.2 Tested and Verified Drying Model

a) Best fitting model

Figure 4.18 shows variation of moisture ratio with time when dried between 10.40 hrs and 14.40 hrs. Both moisture content (X) and moisture ratio (X_r) were found to be decreasing gradually and followed the same trend. The regression equations for X and X_r are shown in eqs. (4.1) and (4.2). These are polynomials, and were selected due to their high R^2 values of 0.9857 and 0.9855 respectively.

$$X = 0.00009t^2 - 0.1096t + 38.446 \quad (4.1)$$

$$\boldsymbol{X_r = 0.000003t^2 - 0.003t + 1.0245} \quad (4.2)$$

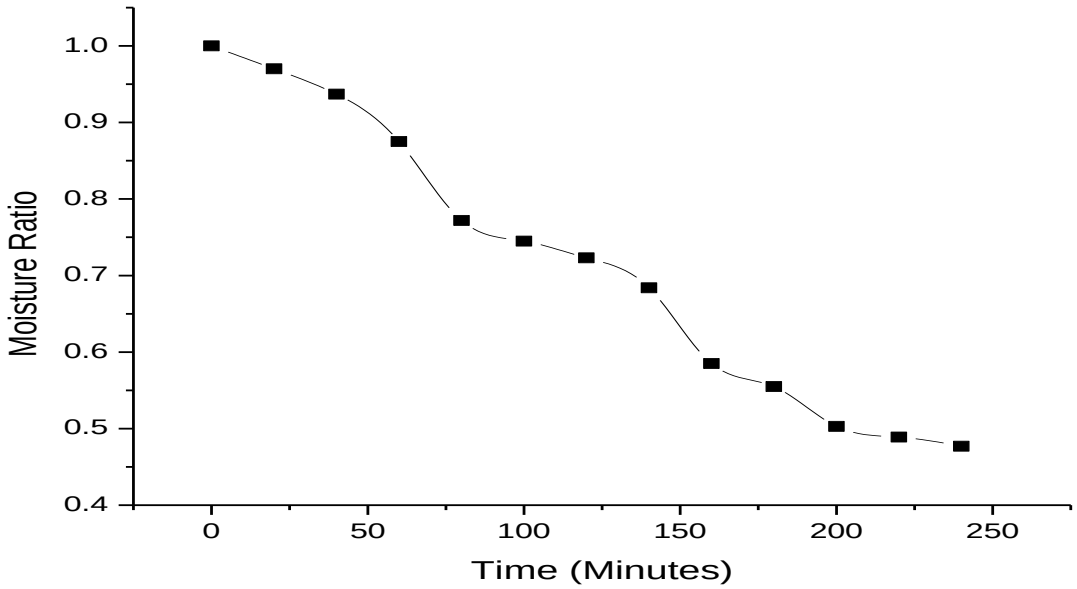

Figure 4. 18: Variation of Moisture Ratio with time

Table 4.9 shows $\boldsymbol{\chi^2}$, R^2 and RMSE values for the various models tested to select the one that would best fit the drying curve for maize in the solar dryer. It was found, based on R^2 values (the higher, the better), that the one by Midilli *et al*. (2002) was best. This was confirmed by the values of χ^2 and RMSE (the lower, the better). This was in agreement with the findings of Agbossou *et al*. (2016). However, it was noted that based on all the three statistical tests, the experimental regression equation would be best in predicting moisture ratio during the drying of maize.

Table 4. 9: χ^2, R^2 & RMSE for Different Models

Model No	Model Name	Equation	χ^2	R^2	RMSE
1	Page	$X_r = \exp(-kt^n)$	0.5981	0.2745	0.2038
2	Two Term	$X_r = a\exp(-k_0 t) + b\exp(-k_1 t)$	0.5980	0.2730	0.2037
3	Modified Page	$X_r = \exp[-(kt)^n]$	0.5193	0.4862	0.1899
4	Midilli *et al.*	$X_r = a\exp(-kt^n) + bt$	0.4278	0.9487	0.1723
5	Regression Equation	$X_r = 0.00009t^2 - 0.109t + 38.446$	0.0008	0.9857	0.0243

Table 4.10 presents the model coefficients for Midilli *et al.* (2002) with 95 % confidence bounds, determined using MATLAB R2012B (Appendix IIID, Figs. A16-A19), as well as the goodness of fit values for R^2 and RMSE. It may be seen that the values changed with temperature. The best fitting coefficients are the ones obtained for 45 °C.

Table 4. 10: Midilli Coefficients and Goodness of Fit Values

Temperature (°C)	Midilli coefficient	R^2 value	RMSE value
40	a =1 b = 0.0064 k = 0.0003 n = 0.8719	0.6159	0.1328
45	a =1 b = 0.0693 k = -0.0010 n = 0.3476	0.9915	0.0233
50	a =1.0090 b = 0.0069 k = 0.0024 n =1.021	0.6237	0.1314
55	a = 0.9812 b = 8.258 k = -0.0022 n = -5.318	-4.824	0.5059

b) Verification of the model

The selected model was verified by comparing the moisture ratios predicted by it to those obtained experimentally. Table 4.11 shows the variation of experimental and predicted moisture ratios with time at different drying air temperatures, when 0.04 m grain layer thickness was dried using air at a flow rate of 0.41 m/s.

Fig. 4.19 is a presentation of predicted and experimental moisture ratios for 40 °C temperature, and shows that there is considerable agreement between the values. They band closely around the linear trend line, with an R^2 value of 0.9909. Similar results were observed for 45 °C, 50 °C and 55 °C.

Table 4. 11: Predicted and Experimental Moisture Ratios at Different Temperatures

Moisture Ratio at 40 (°C)		Moisture Ratio at 45 (°C)		Moisture Ratio at 50 (°C)		Moisture Ratio at 55(°C)	
Predicted	Experimental	Predicted	Experimental	Predicted	Experimental	Predicted	Experimental
1	1	1	1	1	1	1	1
0.8915	0.908	0.7677	0.838	0.8813	0.973	0.9144	0.897
0.8132	0.83	0.6900	0.769	0.7885	0.859	0.8477	0.808
0.7482	0.8	0.6281	0.722	0.7276	0.774	0.7809	0.713
0.6927	0.74	0.5735	0.674	0.6929	0.739	0.7142	0.703
0.6446	0.673	0.5233	0.599	0.6795	0.652	0.6474	0.647
0.6025	0.639	0.4761	0.536	0.6832	0.62	0.5807	0.609

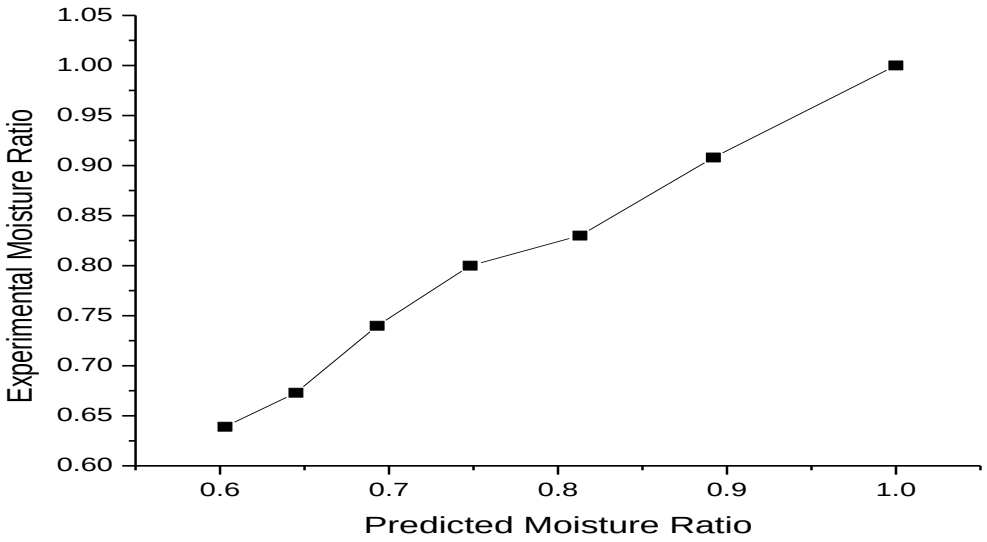

Figure 4. 19: Predicted vs Experimental Moisture Ratios

Fig. 4.20 shows that predicted and experimental moisture ratios vary very closely with time, again confirming that the selected model may be used to predict moisture ratio at different drying times.

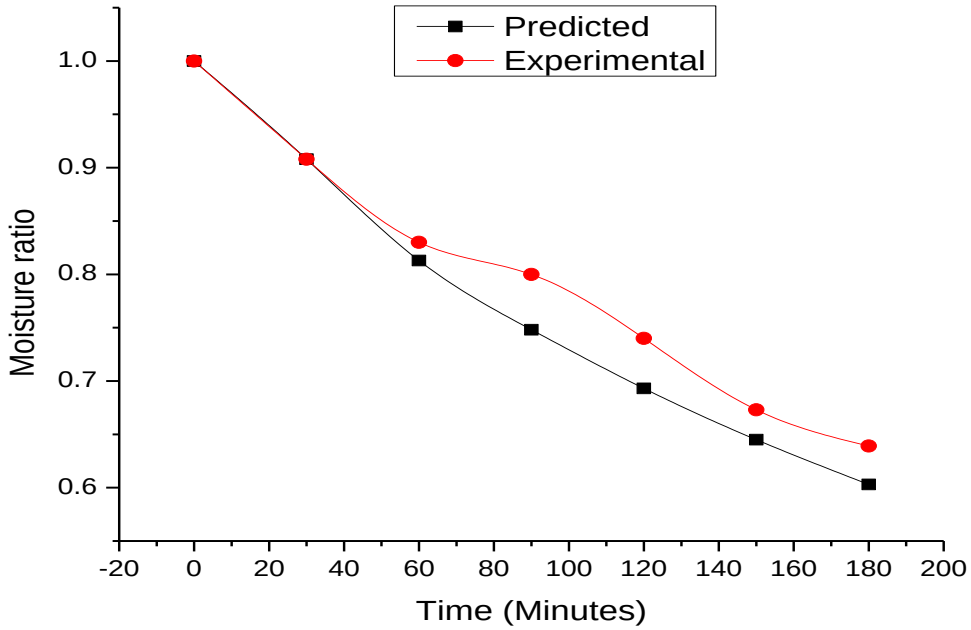

Figure 4. 20: Curves for Predicted and Experimental Moisture Ratio at 40 °C

R^2 and RMSE values (Table 4.12) also showed a good fit between predicted and experimental results. It may therefore be concluded that the selected model can be

used to satisfactorily predict moisture contents and ratios during the drying of maize grain.

Table 4. 12: R^2 and RMSE values for Predicted and Experimental Moisture Ratio Curves

Drying Temperature (°C)	R^2 value	RMSE value
40	0.9225	0.0330
45	0.9609	0.0325
50	0.9757	0.0567
55	0.9378	0.0325

c) Computer simulation model

Fig. 4.21 is an image of the computer simulation model that may be used for determining the moisture ratio at any given time as long as the constants a, b, k and n are known.

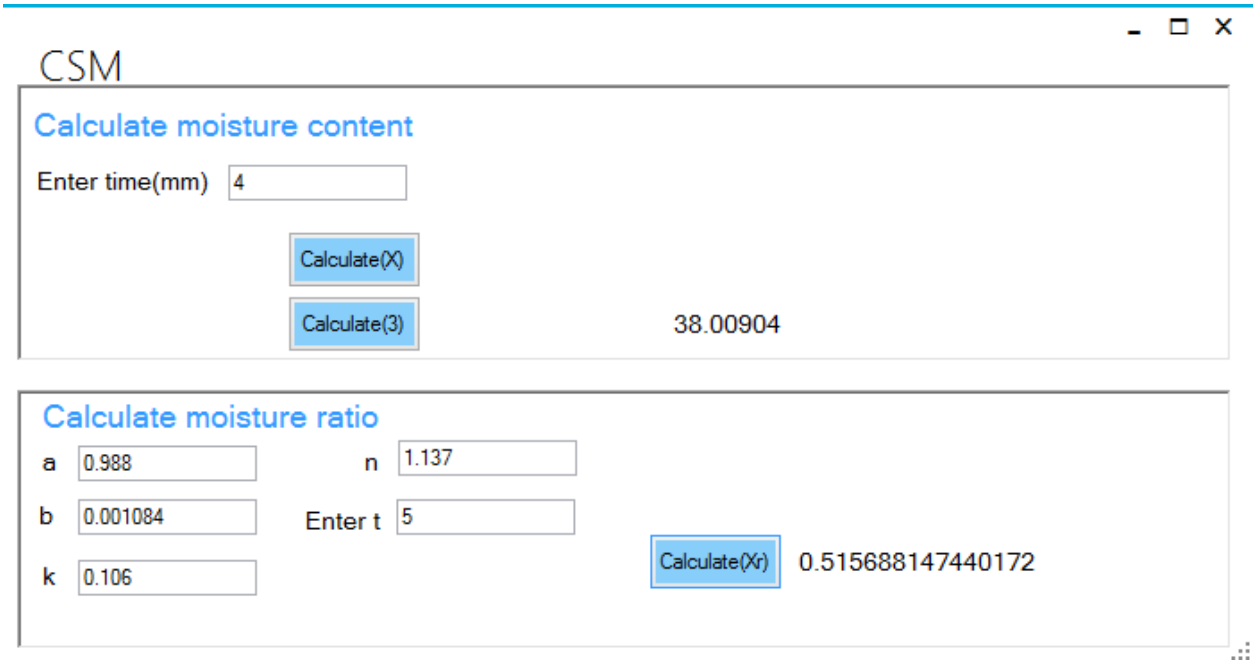

Figure 4. 21: Computer Simulation Model for Moisture Ratio

CHAPTER FIVE: CONCLUSIONS AND RECOMMENDATIONS

5.1 Conclusions

As a result of the simulation process, an experimental grain dryer was sized through simulation and calculation. It had a drying cabinet of dimensions 0.5 m x 0.5 m x 1.0 m, and was equipped with a 0.039 kW centrifugal fan. The solar air heater had a collector area of 2.16 m^2

It was found that Moisture Removal Rate (MRR) increased with air velocity if grain layer thickness was kept constant. For a grain layer thickness of 0.02 m, MRR increased from 0.048 to 0.061 kg moisture / (kg wet grain. hour) when air velocity was increased from 0.21 m/s to 0.41 m/s. MRR, however, decreased with increase in grain layer thickness as long as air velocity was kept constant. For 0.21 m/s air velocity, as grain layer thickness increased from 0.02 to 0.08 m, MRR decreased from 0.050 to 0.006 kg moisture / (kg wet grain. hour). Also, MRR increased with temperature when air velocity and grain layer thickness remained constant. For a grain layer thickness of 0.04 m and an air velocity of 0.41 m/s, MRR increased from 0.045 to 0.058 kg moisture / (kg wet grain. hour) as temperature increased from 40 °C to 55 °C. In the case of drying efficiency, there was increase with air velocity if grain layer thickness was kept constant. At a grain layer thickness of 0.04 m, drying efficiency increased from 8.2 % to 13.9 % as air velocity increased from 0.21 to 0.41 m/s. Drying efficiency decreased with drying air temperature at constant air velocity and grain layer thickness. At 0.04 m layer thickness and 0.41 m/s air velocity, drying efficiency decreased from 23.5 % to 10.1 % as temperature increased from 40 °C to 55 °C. Drying efficiency also tended to decrease with increase in grain layer thickness.

For the solar dryer operating in open sun conditions, the optimal combination of grain layer thickness and air velocity were found to be 0.02 m and 0.41 m/s after application of the Taguchi Approach. For the electrically heated dryer operating under laboratory conditions, it was found that applying air velocity of 0.41 m/s, drying air temperature of 45 °C and grain layer thickness of 0.02 m would result in greatest MRR and drying efficiency. The drying model that best describes the drying

curve was found to be the one by Midilli *et al.* (2002). The model coefficients were found to vary with drying air temperature. Based on R^2 tests (0.9225 - 0.9786) and RMSE tests (0.0325 – 0.0750), the drying model was found to satisfactorily predict moisture ratios at 40, 45, 50 and 55 °C.

5.2 Recommendations

The following are recommended for further study.

1. In view of the fact that this dryer may be used to dry other grain apart from maize, it is recommended that the effect of grain porosity and shape on dryer performance be investigated. This is would enable application of the dryer for drying grains of varying shapes and sizes.

2. It was noted that the exhaust air, though moist, was at a temperature ranging from 31.7 °C for a drying temperature of 40 °C and 36.2 °C for a drying temperature of 55 °C. It is necessary to find ways of putting this warm air to use.

3. The computer simulation model developed as a result of this study should be adopted by users of the dryer to assist in planning their drying schedules.

4. The optimum operating conditions determined from this study should be adopted by users of the dryer to maximize MRR and drying efficiency.

REFERENCES

Adebayo, B.A., Ndunguru, G., Mamiro, P., Alenkhe, B.,Mlingi, N., &Bekunda, M.(2014). Post-harvest Food Losses in a Maize-based Farming System of Semi-arid and Savannah Areas of Tanzania. *Journal of Stored Products and Research* 57: 49-57

Aduewa, T.O., Ogunlowo, A.S. & Ojo, S.T. (2014). Development of Hot Air Supplemented Solar Dryer for White Yam (Dioscorea Rutundata) Slices. *IOSR Journal Of Agricultural And Veterinary Services* 7(12):114-123

Afriyie, J.K., Nazha, M.A.A., Rajakaruna, H. & Forson, F.K. (2009). Experimental Investigations of a Chimney Dependent Solar Crop Dryer. *Renewable Energy* 34: 217-222

Afriyie, J.K., Nazha, M.A.A., Rajakaruna, H. &Forson, F.K. (2011). Simulation and Optimisation of the Ventilation in a Chimney Dependent Solar Crop Dryer. *Solar Energy* 4: 1560-1573

Agbossou, K., Napo K. & Chakraverty, S. (2016). Mathematical Modeling and Solar Drying Tunnel Characterictics of Yellow Maize. *American Journal of Food Science and Technology* 4 (4): 115-124

Aissa, W., El-Sallak, M. & Elhakem, A. (2014). Performance of Solar dryer Chamber used for Convective Drying of Sponge-cotton. *Thermal Science* 18 (2) :451-462

Akinona, O. A., Akinyemi, A.A. & Bolaji, B.O. (2006).Evaluation of Traditional and Solar Fish Drying Systems towards Enhancing Fish Storage and Preservation in Nigeria. *Fish International: Pakistan* 1(3):44-49

Akpinar, E. K. (2008). Mathematical Modelling and Experimental Investigation on Sun and Solar Drying of Mulberry. *Journal of Mechanical Science and Technology* 22: 1544-1553

Akubulut, A. & Durmus,A.(2010). Energy and Exergy Analyses of Thin Layer Drying of Mulberry in a Forced Convection Solar Dryer. *Energy* 35:1754-1763

Alqadhi, A., Misha, S., Rosli, M.A.M & Akop, M.Z. (2017). Design and Simulation of an Optimised Mixed Mode Solar Dryer Integrated with Desiccant

Material. *International Journal of Mechanical and Mechatronic Engineering* 17(6) 65-73

Aregbesola, O. A., Ogunsina, B. S., Sofolahan, A. E. & Chime, N. N. (2015). Mathematical Modelling of Thin Layer Drying Characteristics of Dika (Irvingia gabonensis) Nuts and Kernels. *Nigerian Food Journal* 33(1): 83-89

ASAE (American Society of Agricultural Engineers) (1992). *ASAE Standards for Moisture Measure*. https://engineering .purdue.edu

Ayadi, M., Mabrouk, S. B. Zouari, I. & Bellugi, A. (2014). Kinetic Study of the Convective Drying of Spearmint. *Journal of Saudi Society of Agricultural Science*. 13 (1): 1-7

Balmine, M., Marcel, E., Alexis, K. and Belkacem, Z. (2015). Experimental Evaluation of the Thermal Performance of Dryer Airflow Configuration. *International Journal of Energy Engineering.* 5(4): 80-86

Barawal, P. & Tiwari, G.N. (2008).Grape Drying by Using Photovoltaic Thermal (PV/T) Green House Dryer: An Experimental Study of Solar Energy. *Solar Energy*. 62(12): 1131-1144.

Berke, L., Patnaik, S. N. & Murthy, P. L. N. (1993). Application of Artificial Neural Networks to the Design Optimisation of Aerospace Structural Components. National Aeronotics and Space Administration (NASA) Technical Memorandum, NASA. https://ntrs.nasa.gov/archive/nasa/casi.ntrs.nasa.gov/19930012642.pdf. Retrieved on 10th March 2017

Bett, C. & Nguyo, R. (2007). Post-harvest Storage Practices and Techniques used by Farmers in Semi-arid Eastern and Central Kenya. African Crop Science Conference Proceedings 8: 1023-1222

Bolaji, B.O. & Olalusi, A.P. (2008). Performance Evaluation of a Mixed Mode Solar Dryer. *AU.J.T* 11(4):225-231

Brackett. D., Ashcroft, I. and Hague, R. (2011). *Topology Optimisation for Additive Manufacturing*. Wolfson School of Mechanical and Manufacturing Engineering, Loughborough University, Leiceterture, UK

Comsol. (2012).*ComsolMultiphysics Reference Guide*. http://www.comsol.com/comsol-multiphysics, Retrieved on 14th December 2015

Dabra,V., Yadav, L. & Yadav, A. (2013). The Effect of Tilt Angle on Performance of Evacuated Tube Solar Air Collector: Experimental Analysis. *International Journal of Engineering, Science and Technology 5(4):100-110*

Deb, K. (2004). *Introduction to Genetic algorithms for Engineering Optimisation.* link.springer.com/chapter/10.1007%2F978-3-540-39980-8_2. Retrieved on 10th March 2017

Delgado, J. M. & Barbosa de Lima (2014). *Transport Phenomena and Drying Solids and Particulate Materials*. Springer International Publishing Company: New York

Devore, J. L. & Farnum, N. R. (2005). *Applied Statistics for Engineers and Scientists*. Curt Hinrichs: Belmont, C. A

El-sebaii, A.A. & Shalaby, S.M. (2013). Experimental Investigation of an Indirect-mode Forced Convection Solar Dryer for Drying Thymus and mint. *Energy Conversion and Management* 74: 109-116

Ertekin, C. & Firat, M. Z. (2015). A comprehensive Review of Thin-Layer Drying Model Used in Agricultural Products. *Critical Reviews in food Science and Nutrition* 57(4): 701-717

Estrada, J. A. & Litchfield, J. B. (1993). High Humidity Drying of Corn: Effect on Drying Rate and Product Quality. *Drying technology* 11(1): 65-84

Fang, X. (2007). *Engineering Design using Genetic Algorithms*. Doctor of Philosophy Dissertation. Iowa State University, Iowa, USA

FAO (Food and Agriculture Organization), United Nations (1998). *Maize in Human Nutrition.* Retrieved from http: //www.fao.org/docrep/TO395E00.html

Fraley, S., Oom, M., Terrien, B. & Zelewski, J. (2007). *Design of Experiments via Taguchi Methods:OrthogonalArrays.*https://controls.engin.umich.edu/wiki/index.php/Design_of_experiments_via_taguchi_methods:_orthogonal_arrays.Retrieved on 5th January 2016

Frangopoulos, C.A. & Sciubba, E. (2002). *Energy Systems Analysis and Optimisation* –Vol II Modeling, Simulation and Optimisation in Energy Systems.http:/www.eolss.net/Eolss-sampleAllchapter.aspx.Retriehtttved on 17th September 2014

Garg, H. P. & Prakash, J. (2005). *Solar Energy: Fundamentals and Applications*. Tata McGraw-Hill Publishing Company Ltd: New Delhi

Gatea, A. B. (2011). Design and Construction of a Solar Drying System, a Cylindrical Section and Analysis of the Performance of the Thermal Drying System. *African Journal of Agricultural Research* 6(2): 343-351

Gregoire R.G. (2009).*Understanding Solar Food Dryers*. Volunteers in Technical Assistance (VITA) Virginia

Habtamu, T. E. (2007). Simulation of Solar Cereal Dryer using TRNSYS. MSc Thesis, Addis Ababa University, Addis Ababa

Harun, D., Maulana, M. I., Akhyar, H. & Husaini (2016). 6th Experimental Investigation on Open Sun-drying and Solar Drying of Bilimbi. Paper presented at International Annual Engineering Seminar (InAES), Yogyakarta, Indonesia

Hedge, V. N., Hosur, V. S., Rathod, S. K., Harsoor, P. A. & Narayana, K. B. (2015). Design, Fabrication and Performance Evaluation of Solar dryer for Banana drying. *Energy, Sustainability and Society* 5:23-35

Hodges, R. (2009). *Supplying Cereal Grain Postharvest Losses Information: the Examples of ALPHIS (African Postharvest Loss Information System*. Natural Resources Institute, UK. Retrieved from http:/www.rsis.edu.sg/nts/doc/session%20420Hodgespdf on 13th May 2013

Hossain, M. A., Woods, J. L. & Bala, B. K. (2007). Single Layer Drying Characteristics and Colour Kinetics of Red Chilli. *International Journal of Food Science and Technology* 42(11): 1367-1375

Irungu, J. (2010). *Post Harvest Challenges to Food Security in Kenya*. A paper presented at KCB Leadership Center, Karen, Nairobi

Jangai, S., Lambert, N., Intawee, P., Mahayottee, B., Bala, B.K., Nagle, M. & Muller, J. (2009). Experimental and Simulated Performance of a PV-

Ventilated Solar Green House Dryer for Drying of Peeled Longan and Banana. *Solar Energy* 83:1550-1565

Jerger, E.W. (1951). *Mechanism of Moisture Movement in the Drying of Organic Granular Solids*. PhD Dissertation at Iowa State University (Retrospective Theses and Dissertations, Paper 13871)

Jia, Y., Li, Y. & Hlavka, D. (2009). *Flow through Packed Beds*. http:/ www.me .rochester.edu/courses/ME241/11-sand.pdf.Retrieved on 14th September 2014

Kaaya, A.N. & Kyamuhangire, W. (2010). Drying Maize Using Biomass Heated Natural Convection Dryer increases Grain Quality during Storage. *Journal of Applied Sciences* 10(11) 967 -974

Kamaruddin, S., Khan, Z. A, & Foong, S. H. (2010). Application of Taguchi Method in the Optimisation of Injection Moulding Parameters for Manufacturing Products from Plastic Blend. *International Journal of Engineering and Technology* 2(6): 574-580

Kamenan, B.K., Kassinou, W.F., Gbaha, P. & Toure, S. (2009).Mathematical Modeling of Thin Layer Solar Drying of Banana, Mango and Cassava. *Energy* 34:1594-1602

Kardi, S. & Korti, A. N. (2018). Applying CFD for Studying the Dynamic and Thermal Behaviour of an Indirect Solar Dryer: Parametric Analysis. *Mechanics of Mechanical Engineering* 22(1) 253-272

Karna, S. K., Singh, R. V. & Sahai, R. (2012). Application of Taguchi Method in Process Optimisation. *Proceedings of the National Conference on Trends and Advances in Mechanical Engineering, YMCA University of Science and Technology, Faridabad, Haryana* (pp. 718 – 722)

Kassem, A. S., Al-Sulaiman, M. A., Aboukarima, A. M. & Kassem, S. S. (2011). Predicting Drying Efficiency during Solar Drying Process of Grapes Clusters in a Box Dryer using Artificial Neural Network' *Australian Journal of Basic and Applied Sciences* 5(6): 230-241

Klaus, J., Olindo, I., Amo, H. M. S., Rene, A.C., & Miro, Z. (2014). *Solar Energy: Fundamentals, technology and Systems.* Delft University of Technology. https:/ courses.edxorg.Delft X.ET.3034 Tu/asset/solar Energy-viapdf

Kumar, S. & Shobhana, S. (2011). Performance Evaluation of a Forced Convection Mixed-Mode Solar Dryer: An Experimental Investigation. Conference Paper presented at World Congress on Sustainable Technologies, WSCT

Ikejiofor, M. (2010). *Design, Development and Performance Evaluation of an Active Solar Dryer for Biomaterial Processing*. Masters Thesis, Faculty of Engineering,University of Nigeria, Nsukka, Nigeria

Lahsasni, S., Kouhila, M., Marhouz, M. & Idlimam, A. (2004).Thin Layer Convective Solar Drying and Modeling of Prickly Pear Peel (Opuntiaficusindica). *Energy* 29:211-224

Lamnatou, C., Papanicolaou, E., Belessiotis, V. & Kyriakis, N. (2012). Experimental Investigation and Thermodynamic Performance Analysis of a Solar Dryer using an Evacuated Tube Air Collector. *Applied Energy* 94:232-243

Li, Z., Mei, S., Andrianor, N. & Kong, L. (2015). Simulation of Air Flow in a Mixed-Flow Grain Dryer. *UDC 677*: 258 -265

Lingayat, A., Chandramohan, V.P. & Raju, V.R.K. (2017). Design, Development and Performance of Indirect Solar Dryer for Banana Drying. *Energy Procedia* 109: 409-416

Mahajan, R. & Kaur, G. (2013). Neural Networks using Genetic algorithms. *International Journal of Computer Applications* 77(14): 6-11

Maier, D .E. & Bakker-Arkema, F.W. (2002).*Grain Drying Systems*. Paper presented at Facility Design Conference of Grain Elevator and Processing Society held on July 28-31 in St Charles, Illinois, USA

Maiti, S., Patel, P., Vyas, K., & Ghosh, P.K. (2011). Performance Evaluation of a Small Scale Indirect Solar Dryer with Static Reflectors during Summer Months in the Saurshtra Region of Western India. *Solar Energy* 85(11) 2686-2696

Maloba, H., Shivonga, W., Muchiri, M. & Miller, S.N.(2008). *Use of Benthic Macro-invertebrates as Indicators of Water Quality in Njoro River, Kenya*. Proceedings of TAAL 2007: the 12th World Lake Conference 2161-2168

Meisami-asl, E. & Rafiee, S. (2009). Mathematical Modelling of Kinetics of Thin Layer Drying of Apple. *Agricultural Engineering International : the CIGR Journal* 11: 1185-94

Mercer, D. G. (2012). A Comparison of the Kinetics of Mango Drying in Open-Air, Solar and Forced Air Dryers. *African Journal of Food, Agriculture, Nutrition and Development* 12(7):6835- 6852

Mghazli, S., Ouhammou, M., Hidar, N., Lahnine, L., Idlimam,A & Mahrouz, M. (2017). Drying Characteristics and Kinetics of Solar Drying of Moroccan Rosemary Leaves. *Renewable Energy* 108:303-310

Misha, S., Mat, S., Rosli, M. A. M., Ruslan, M. H., Sopian, K. & Salleh, E. (2013). Simulation of Air Flow in a Tray Dryer by CFD. *Recent Advances in Renewable Energy Sources* 1:29-34

Misha, S., Mat, S., Rosli, M. A. M., Ruslan, M. H., Sopian, K. & Salleh, E. (2015). Simulation of Air Flow in a Tray Dryer by CFD. Conference Paper presented at 9th WSEAS International Conference on Renewable Energy, Kuala Lumpur, Malaysia

Mohanraj, M. & Chandrasekar, P. (2009). Performance of a Forced Convection Solar Dryer Integrated with Gravel as Heat Storage Material for Chili Drying. *Journal of Engineering Science and Technology* 4(3): 305-314

Muguthu, J. N., Dong, G. & Ikua, B. W. (2015). Optimisation of Machining Parameters Influencing Machinability of AI2124SiCp (45 % wt) Metal Matrix Composite. *Journal of Composite Materials* 49 (2): 217-229

Mumba, J. (1996). Design and Development of a Solar Grain Dryer Incorporating Photovoltaic Powered Air Circulation. *Energy Conversion and Management* 37(5): 615-621

Murthy, M.V.R. (2009). A review of new Technologies, Models and Experimental of Solar Dryers. *Renewable and Sustainable Energy Reviews 835*-844

Nakasone, Y., Yoshimoto, S. & Stolarski, T.A. (2006). *Engineering Analysis of ANSYS Software*. Elsevier Butterworth-Heinemann: Amsterdam

Ondier, G. O., Siebenmorgen, T. J. & Mauromoustakos, A. (2010). Low-Temperature, Low-Relative Humidity Drying of Rough Rice. *Journal of Food Engineering.* 100: 545 - 550

Olason, A. & Tidman, D. (2011). *Methodology for Topology and Shape Optimisation in the Design Process*. Masters Thesis. Chalmers University of Technology. Goteborg, Sweden

Oliveira, D.E C., Resende, O., Bessa, J. F. V., Kester, A. N. & Smaniotto, T. A. S. (2014). Mathematical Modelling and Thermodynamic Properties for Drying Soybean Grains. *African Journal of Agricultural Research* 10(1): 31-38

Omwando, L. M. (2012).*Assessment of Solar Energy Potential for Nakuru, Kenya*. Unpublished Masters Thesis. Jomo Kenyatta University of Agriculture & Technology, Kenya

Onisimi, S. S., Nosike, N.C., Adetoro, V.A., Segun, A. & Chibuzor, I.D. (2016). Optimisation of Developed Multipurpose Food Dryer using ANSYS. *Journal of Scientific and Engineering Research*. 3(5): 72 - 76

Osman, Y., Ertekin, C. & Uzun, H. (2001). Mathematical Modeling of Thin Layer Solar Drying of Sultana Grapes. Energy 26:457-465

Parkinson, A. R., Balling, R. J. & Hedengren, J. D. (2013). *Optimisation Methods for Engineering design: Applications and Theory.* Brigham Young University

Rafiee, S., Keyhani, A. & Jafari, A. (2006). Modelling Effective Moisture Diffusivity of Wheat (Tajan) during Air drying. *International Journal of Food Properties* 11(1): 223-232

Rahmatinejad, B., Hosseinzadeh, H., Sharifi, O. & Rezazadeh, A. (2016). The Effect of Temperature and Speed of Wind on Drying Time of Basil Leaves in the Solar-Photovoltaic Dryer. *International Journal of Biotechnology and research (IJBR)* 7(4): 432-437

Rigit, A. R.H., Jakhrani, A.Q., Kamboh, S.A. & Kie, P.L.T. (2013).Development of an Indirect Solar Dryer with Biomass Back up Burner for Drying Pepper Berries. *World Applied Sciences Journal* 22(9) 1241-1251

Romdhane, B.S. & Combarnous, M. (2009). Study of Orange Peels Drying Kinetics and Development of a Solar Dryer by Forced Convection. *Solar Energy* 85:570-578

Sachdeva, S., Pareek, S., Mahadevan, B. & Deshapande, A. (2012). *Modeling and Simulation of Single Phase Fluid Flow and Heat Transfer in Packed Bed.* Proceedings of 2012 COMSOL Conference, Bangalore

Sallam, Y. I., Aly, M. H., Nassar, A. F. & Mohamed, E. A. (2013). Solar drying of Whole Mint Plant under Natural and Forced Convection. *Journal of Advanced Research* 6: 171-178

Samira N., Etesami, N., Najafabady, A. P. & Falavarjani, M. G. (2016). Mathematical Modelling of Drying of Potato Slices in a Forced Convective Dryer based on Important Parameters. *Food Science and Nutrition* 4(1): 110-118

Sarker, A., Islam, M. N. & Shaheb, M. R. (2012). A Study on the Drying Behaviour of a Local Variety (Lalpakri) of Potato (Solanum tuberosum L.). *Bangladesh J. of Agric. Res*. 37 (3): 505-514

Sen, Z. (2008). *Solar Energy Fundamentals and Modeling Techniques: Atmosphere, Environment, Climate Change and Renewable Energy* Springer: London

Sevik, S. (2013). Design, Experimental Investigation and Analysis of a Solar Dryer System. *Energy Conversion and Management* 68:227-234

Sharma, K. & Wadhawan, N. (2018). Effect of Natural and Forced Convection Solar Dryers on Retention of Proximate Nutrients in Tomato. *International Journal of Current Microbiology and Applied Sciences* 7(7): 1175-1186

Silva, W. P., Silva, M. D., Gama, F. J. A. & Gomes, J. P. (2014). Mathematical Models to Describe Thin-Layer Drying and to Determine Drying Rate of Whole Bananas. *Journal of the Saudi Society of Agricultural Sciences* 13(1): 67-74

Simate, I.N. (2003). Optimisation of Mixed-mode and Indirect-mode Natural Convection Solar Dryers. *Renewable Energy* 28: 435-453

Singaravel, B. & Selvaraj, T. (2016). Application of Taguchi Method for Optimisation of Parameters in Turning Operation. *Journal of Manufacturing Science and Production* 16 (3): 183-187

Sodha, M.S., Dang, A., Bansal, P.K., & Sharma, S.B. (1985). An Analytical and Experimental Study of Open Sun Drying and Cabinet Type Dryer. *Energy Conversion and Management.*25:263

Somasiri, N. P., Chen, X. & Rezazadeh, A. A. ((2004). Neural Network Modeller for Design Optimisation of Multilayer Patch Antennas. IEE Proceedings. Ieeexplore.iee.org/stamp/stamp.jsp?arnumber=1387753. Retrieved on 10th March 2017

Sukhatme, S.P. (1996). Solar Energy: Principles of Thermal Collection and Storage. 2nd Ed. Tata McGraw-Hill Publishing Company Ltd: New Delhi

Tahmasebi, M., Hashjin, T. T., Khoshtaghaza M. H. & Nikbakht, A. M. (2011). Evaluation of Thin-Layer Drying Models for Simulation of Drying kinetics of Quercus (*Quercus persica* and *Quercus libani*) *Journal of Agricultural Sciences* 13: 155-163

Tiwari, G.N. (2002). *Solar Energy: Fundamentals, Design, Modeling and Applications.* Parybourne: Alpha Science International Limited

Tiwari, G.N. (2016). A Review of Solar Drying of Agricultural Produce *Journal of Food Processing and Technology*. 7.623. doi.10.4172/2157- 7110.1000623

Twidell, J.W. & Weir, A.D. (2006).*Renewable Energy Resources*. English Language Book Society: London

Tzepelinkos, A. D., Vouros, A. P., Bardakas, A. V., Filios, A. E. & Margaris, D. P. (2014). Case Studies on the Effect of the Air Drying Conditions on the Convective Drying of Quinces. *Case Studies in Thermal Engineering* 3: 79-85

Umayal A.R.S., Neelamegam, P. & Subramanian, C.V. (2013).Performance of Evacuated Tube Collector Solar Dryer with and without Heat Sources. *Iranica Journal of Energy and Environment* 4(4):336-342

USDA (United States Department of Agriculture), USA (2018). Global Food Security. https://nifa.usda.gov/topic/global-food-security. Retieved on 16th November 2018

University of Wisconsin (2013). *Transient Systems Software*.www.trnsys.com, Retrieved on 14th, December 2015

Walubengo, D. (2007). *Community-led Actions in Building Resilience to Climate Change: a Kenya Case Study*.pubs.iied.org/pdfs/go2310pdf.Retrieved on 30th November 2015

Weiss W. & Buchinger, J. (2012). *Solar Drying.* Training Course within the Scope of the Project Establishment of a Production, Sales and Consulting Infrastructure for Solar Thermal Plants in Zimbabwe. Australian Development Cooperation, Institute of Sustainable Technologies, Australia

Wilcke, W.F. & Morey, R.V. (2015). *Selecting Fans and Determining Airflow for Crop Drying, Cooling and Storage*. http://www.extension.umn.edu/agriculture/crops. Retrieved on 15th September 2015

Williams, L .J. & Abdi, H. (2010). *Fisher's Least Significant Difference (LSD).* Encyclopaedia of Research Design. Sage: Thousand Oaks

Yadollahinia, A. R., Omid, M, & Rafiee, S. (2008). Design and Fabrication of Experimental Dryer for Studying Agricultural Products. *Journal of Agriculture and Biology* 10: 61-65

APPENDICES

APPENDIX I: SIMULATION AND SIZING

IA: AIR VELOCITY UP VARIOUS GRAIN LAYER THICKNESSES

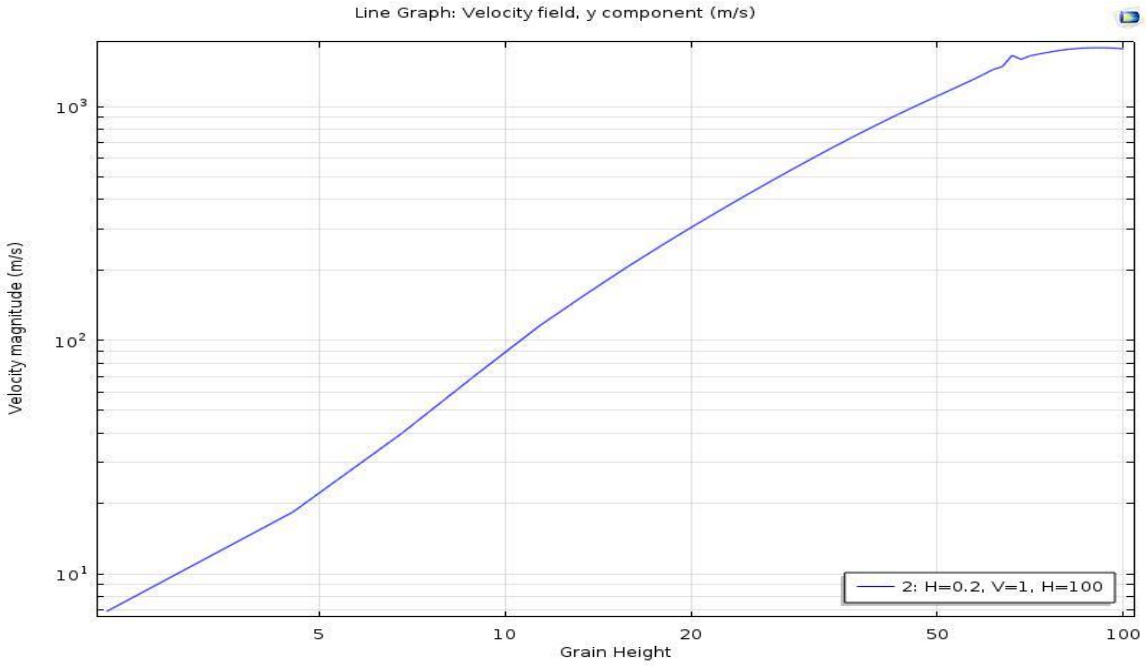

(mm)

Figure A 1: Air Velocity up Single Grain Layer of Height 0.1 m, inlet Velocity 1 m/s

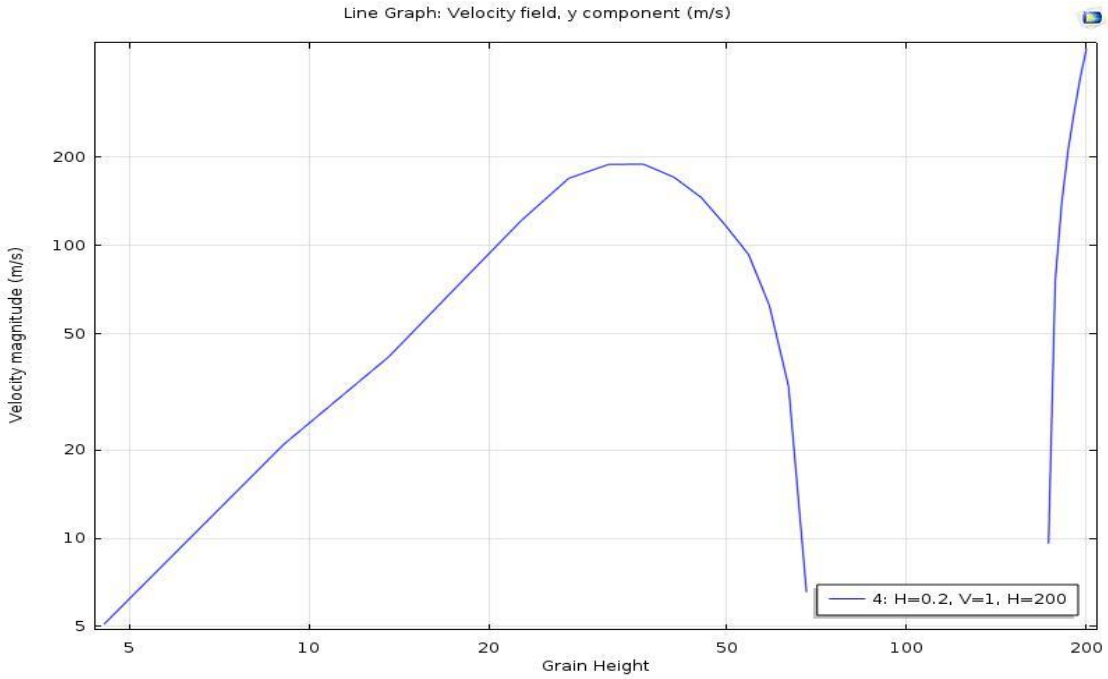

(mm)

Figure A 2: Air Velocity up Single Grain Layer: Height 0.2 m & inlet Velocity 1 m/s

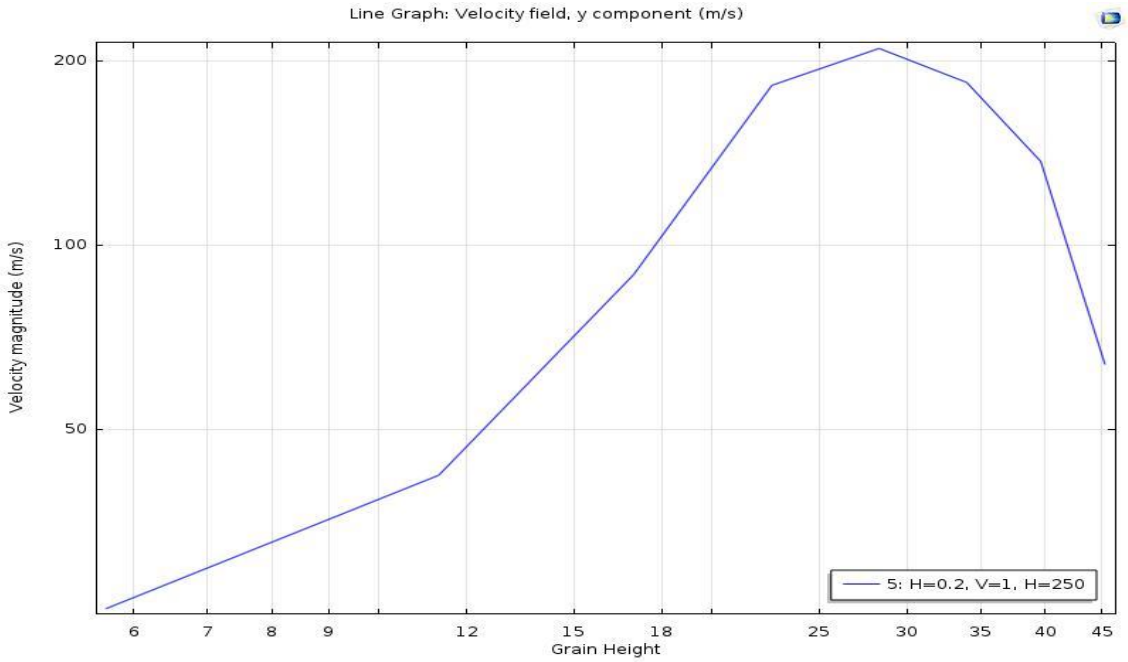

(mm)

Figure A3: Air Velocity up Single Grain Layer (Height 0.25 m & inlet Velocity 1 m/s)

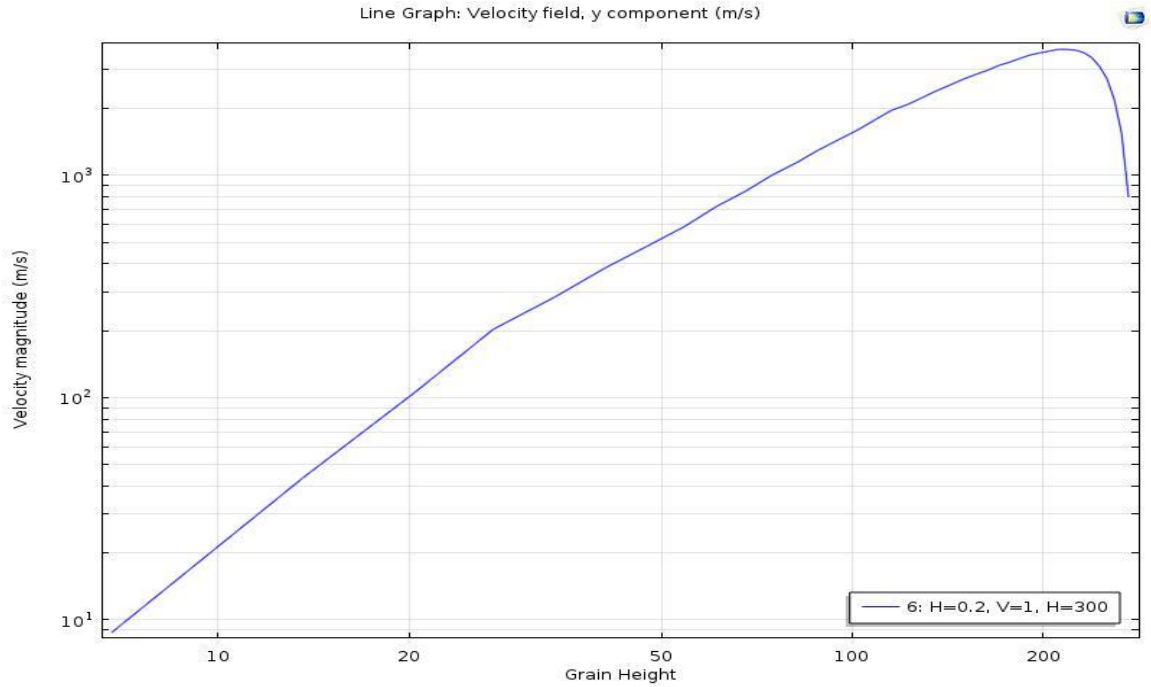

(mm)

Figure A4: Air Velocity up Single Grain Layer (Height 0.3 m & inlet Velocity 1 m/s)

1B: PRESSURE DROP FOR DIFFERENT GRAIN LAYER THICKNESSES

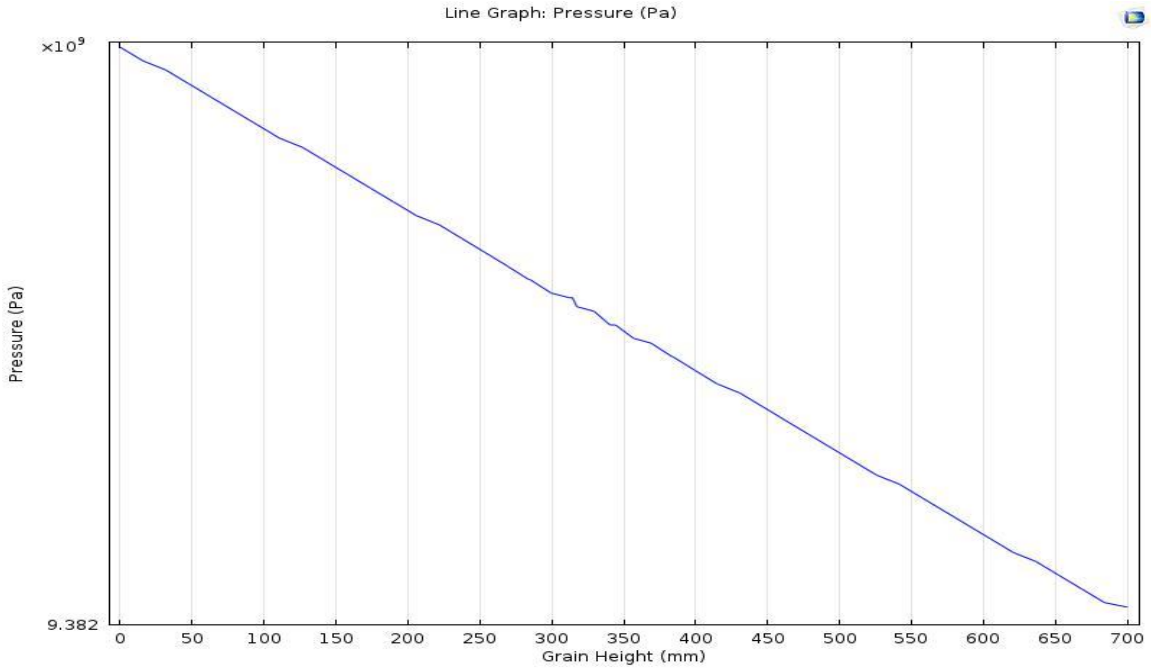

Figure A5: Variation of Pressure for Four (4) 0.1 m Thickness Grain Layers

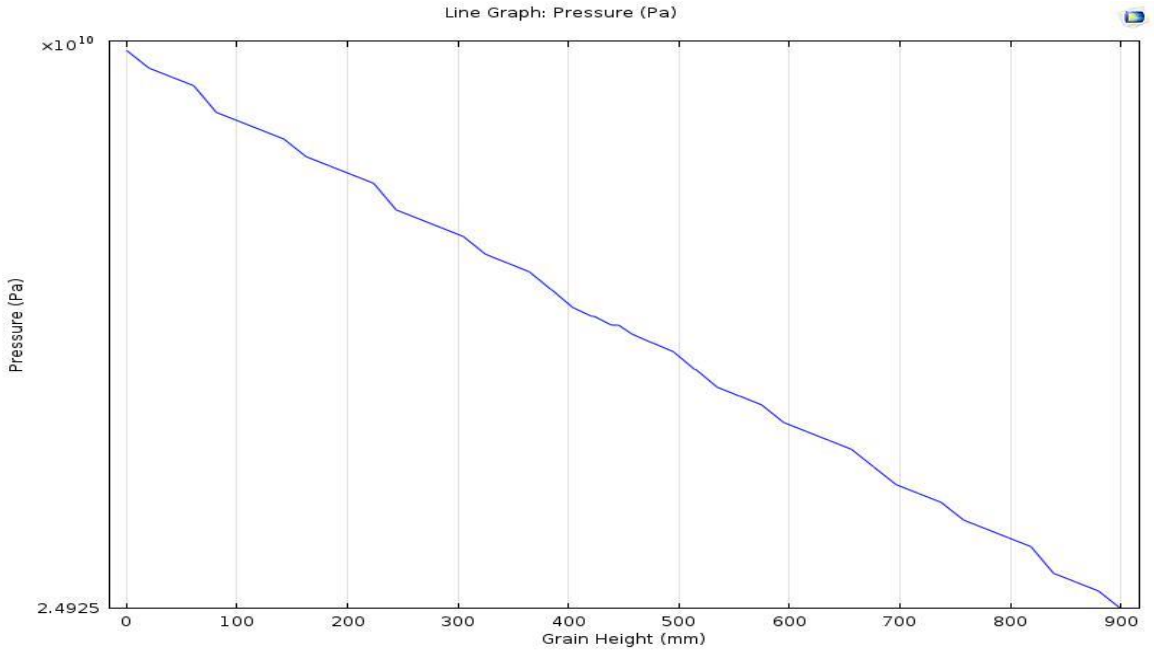

Figure A6: Variation of Pressure for Five (5) 0.1 m Thickness Grain Layers

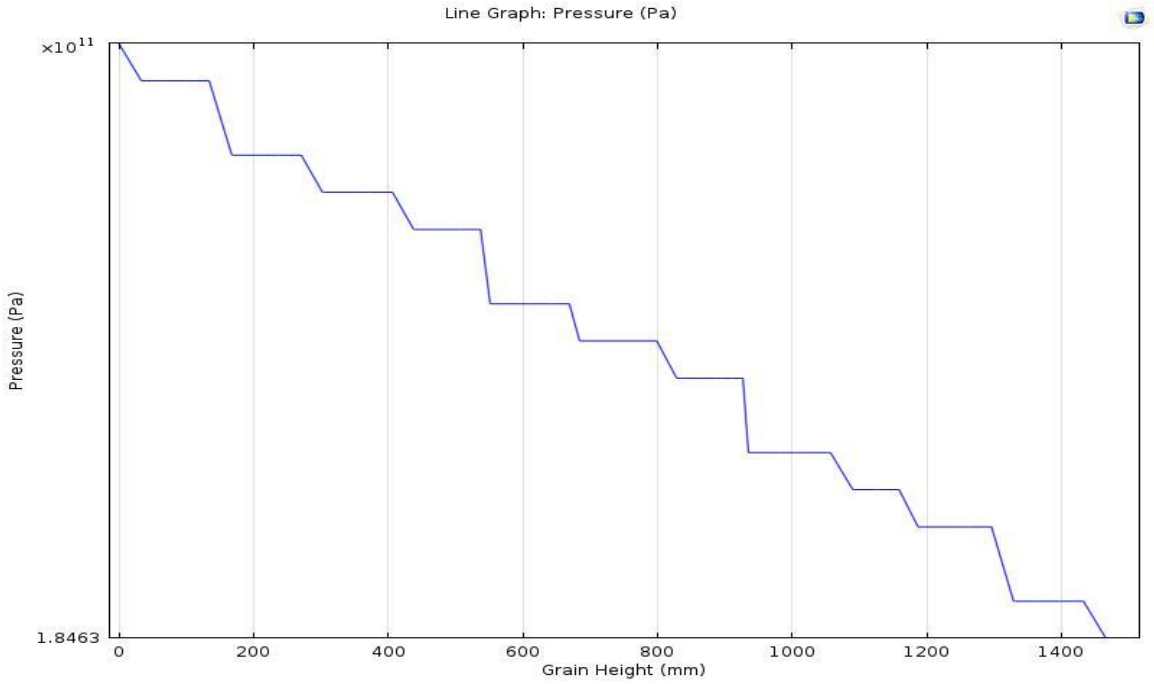

Figure A7: Variation of Pressure for Eight (8) 0.1 m Thickness Grain Layers

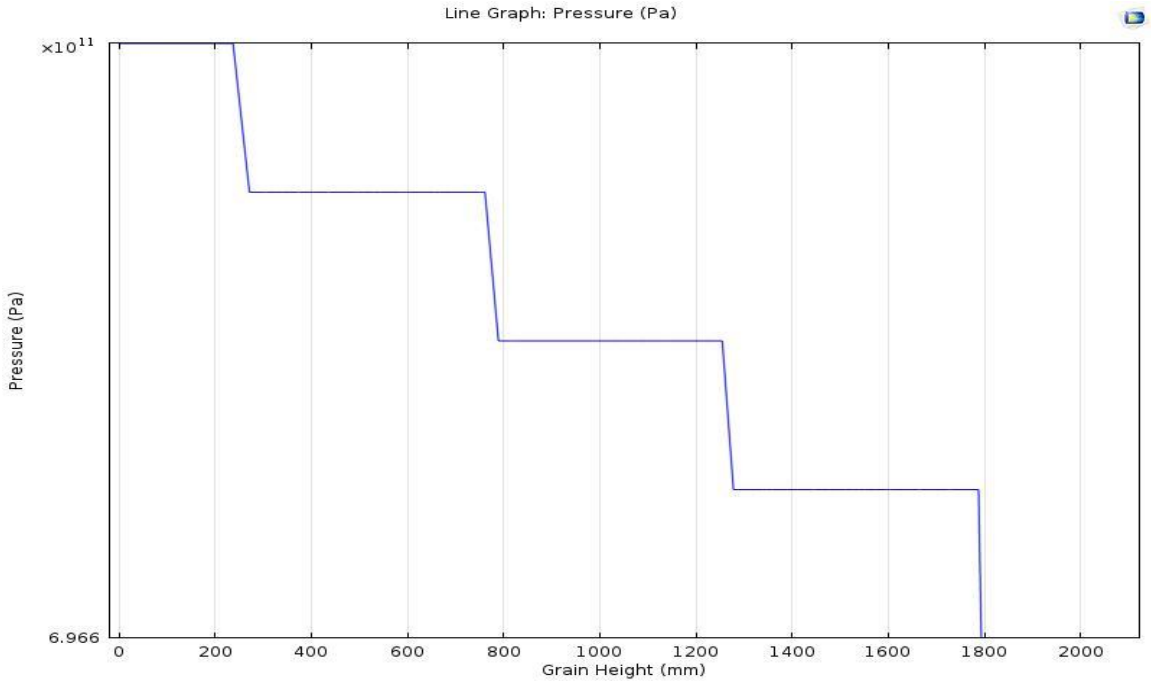

Figure A8: Variation of Pressure for Eleven (11) 0.1 m Thickness Grain Layers

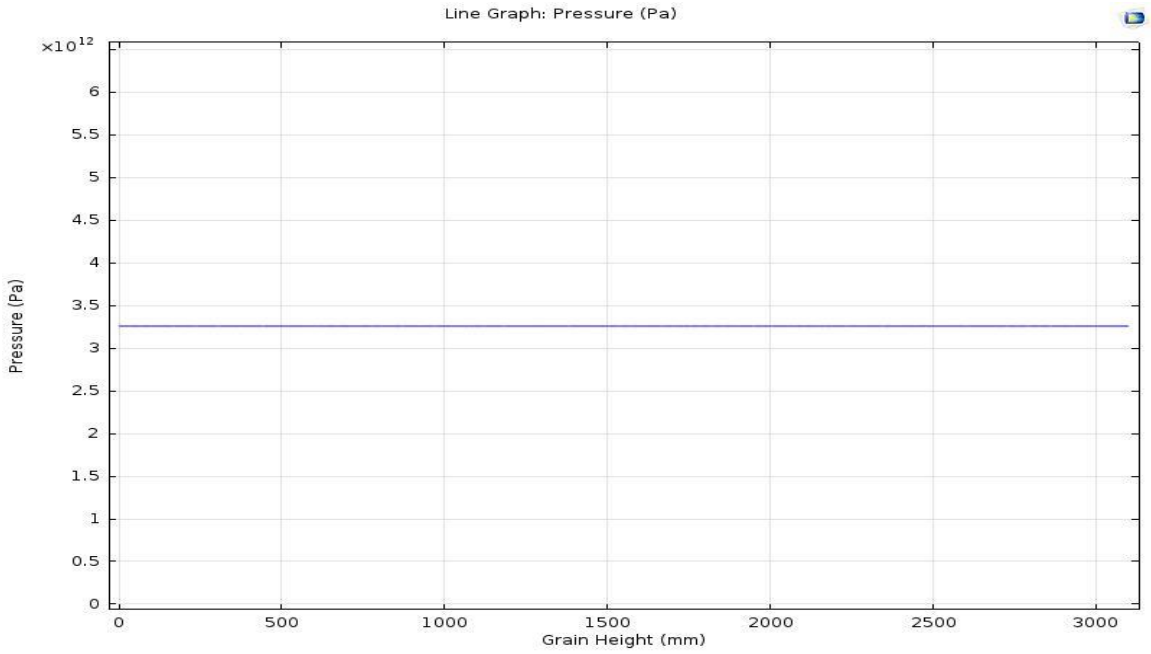

Figure A9: Variation of Pressure for Sixteen (16) 0.1 m Thickness Grain Layers

IC: SIZING OF FAN, DRYING CABINET AND SOLAR AIR HEATER

FAN SIZING

i. To find static pressure P_s in inches of water

249.082 Pa = 1 inch of water hence 25600 Pa = 25600/ 249.082 = 102.8 inches of water

Thus static pressure P_s = 102.8 inches of water

ii. To find air flow rate V_s in cfm:

Mass of grain per batch (2 trays) = 36 kg = 0.036 tonnes

Converting to bushels: 1 tonne = 39.368 bu hence 0.036 tonnes = 0.036 x 39.368 = 1.417 bu

Using a value of 1.4 cfm/bu as recommended for grains by Wilcke and Morey (2015),

1 bu = 1.4 cfm hence 1.417 bu = 1.4 x 1.417 = 1.984 cfm

Thus air flow rate V_s = 1.984 cfm

iii. To find fan power P_f in Hp:

Using eq. (2.5), $P_f = \frac{(V_s x\ P_s\ )}{3814}$ = $\frac{1.984\ x\ 102.8}{3814}$ = 0.053 Hp

But 1 Hp = 0.735 kW hence Fan power = 0.053 x 0.735 = 0.039 kW

DRYING CABINET SIZING

Required was a drying cabinet with two trays, each with a capacity of 18 kg of grain per tray. This was sized to be 0.5 m x 0.5 m x 1 m as shown below.

Mass of grain m_{gr} = 18000 g, grain density for maize ρ_{gr}= 0.76 g/cc

Using eq. (3.1) to find volume of grain V_{gr} ,

$V_{gr} = \frac{m_{gr}}{\rho_{gr}}$ = $\frac{18000}{0.76}$ = 23684.2 cm^3

For cross sectional area A_{cb} of drying cabinet, eq. (3.2) was used, assuming a layer thicknesst_{gr}= 10 cm.

$A_{cb} = \frac{V_{gr}}{t_{gr}}$ $\frac{23684}{10}$ = 2368.42 cm. Thus the required drying cabinet would have a square cross section 0.5 x 0.5 m.

The lowest tray was to be placed 0.3 m from the bottom to allow for the plenum chamber, and the second one 0.2 m above (0.1 m each for grain layer and void space). Leaving 0.3 m above the upper tray for fitting the fan, this resulted in a total drying cabinet height of 1 m.

SOLAR COLLECTOR SIZING

Using an air velocity, v of 0.3 m/s (the lowest recommended for drying of grains) and drying cabinet cross section 0.25 m^2, the volume flow rate Q, through the collector was determined to be $0.075\ m^3/s$ (mass flow rate $\dot{m}$ = 0.092 kg/s), using eqs. (3.3) and (3.4).

$Q = Av$ = 0.25 x 0.3 = 0.075 m^3/s

($\dot{m} = Q\rho$ = 0.075 x 1.225 = 0.092 kg/s)

The required solar collector area was then determined to be 3.25 m^2 as shown below.

Specific heat capacity of air c_{pa}= 1010 J/ (kg K)

Maximum temperature to maintain grain quality T_o= 58°C,
Ambient temperature from (measured in research area during drying period) T_i= 23°C
Highest insolation for 0930 hrs to 1300 hrs on a typical day in the drying period, I_c= 1200 W/m^2
Solar collector efficiency η = 83.28 % (Achieved by Aduewa *et al*., (2014) at Insolation =1199.46 W/m^2)

Hence from eq. (2.1), Solar collector area, $A_c = \frac{\dot{m}_a c_{pa}(T_o - T_a)}{I_c \eta}$ = $\frac{0.092\ x\ 1010\ x\ 35}{1200\ x\ 0.8328}$ = 3.25 m^2

APPENDIX II: EFFECTS ON DRYER PERFORMANCE

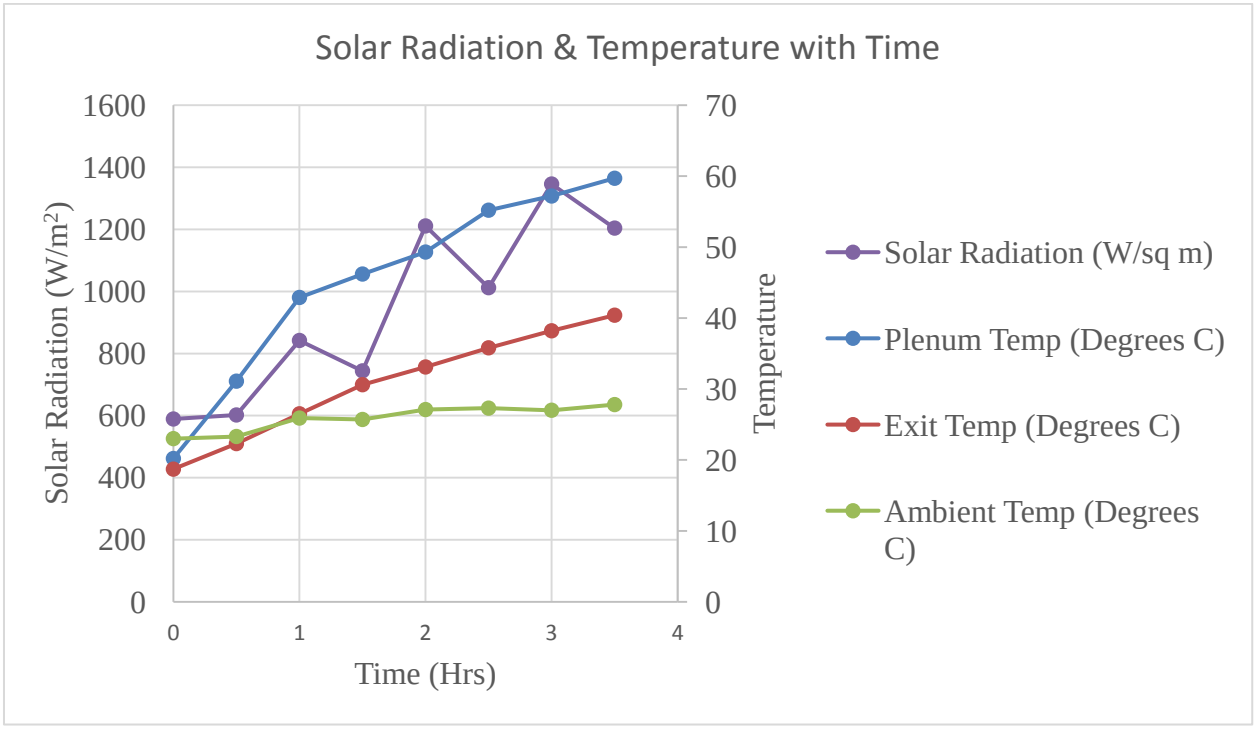

Figure A10: 60 mm Grain Layer Thickness at 0.8 m/s Air Velocity

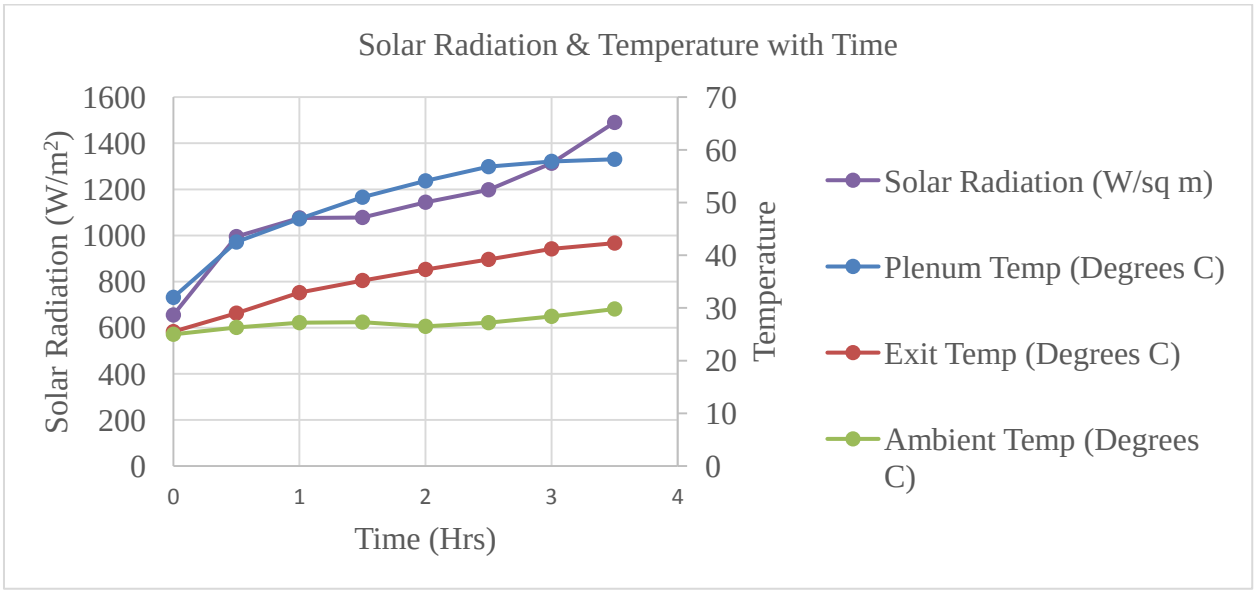

Figure A11: 80 mm Grain Layer Thickness at 0.9 m/s Air Velocity

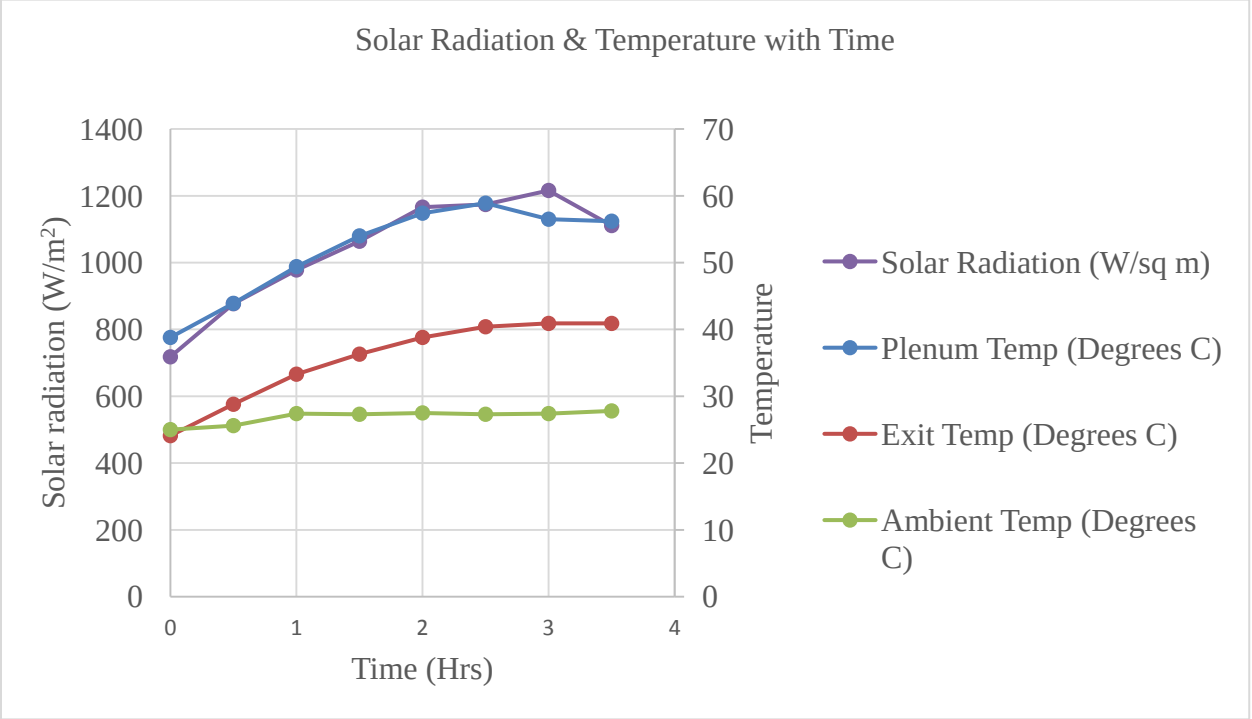

Figure A12: 40 mm Grain Layer Thickness at 2.5 m/s Air Velocity

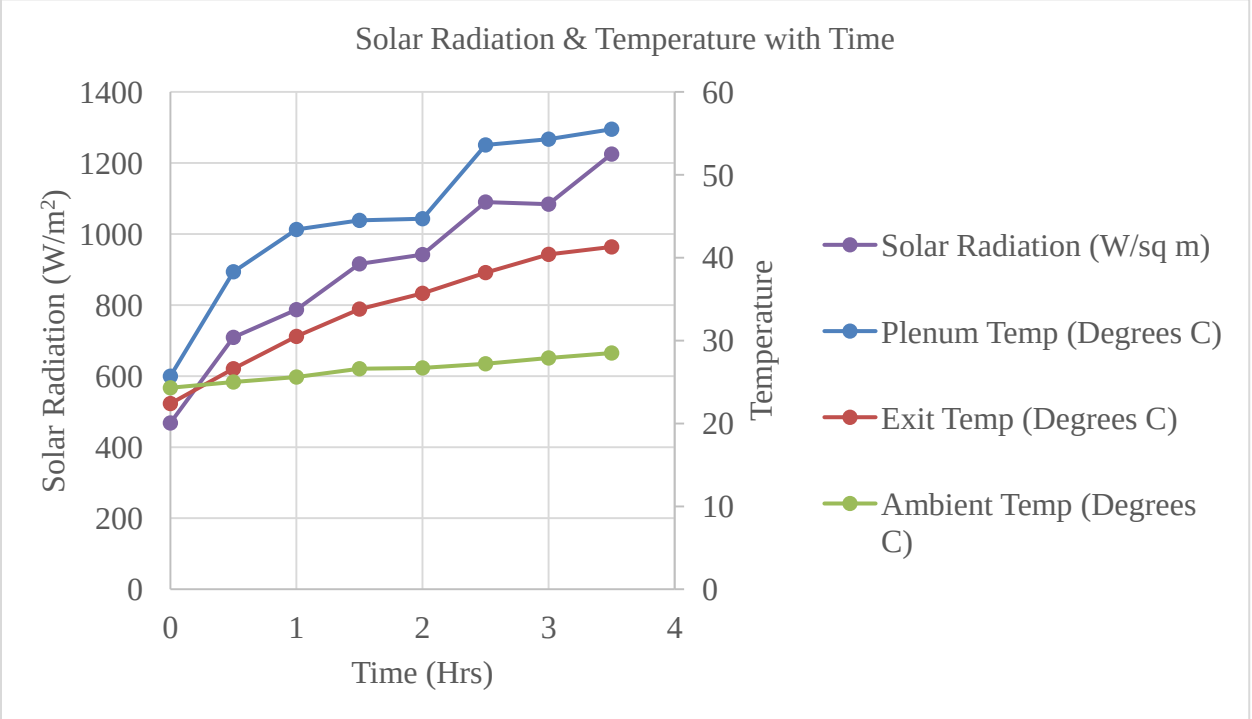

Figure A13: 60mm Grain Layer Thickness at 2.5 m/s Air Velocity

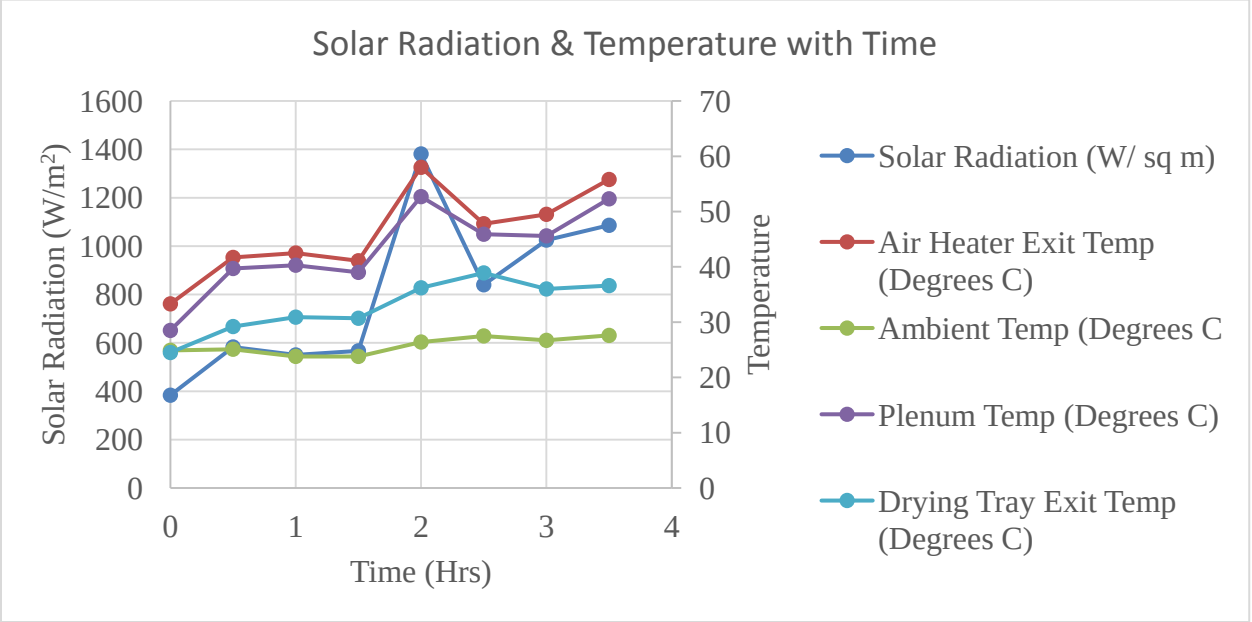

Figure A14: 100mm Grain Layer Thickness at 2.5 m/s Air Velocity

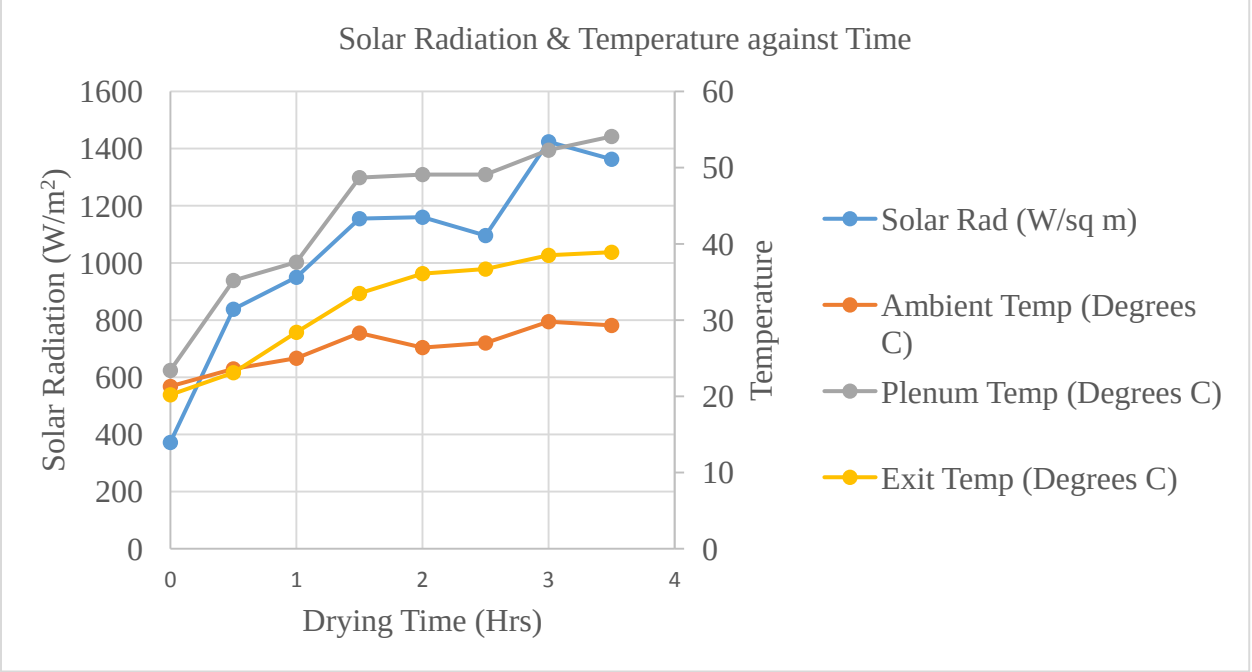

Figure A15: Variation for Air Velocity of 0.8 m/s & Grain Layer thickness of 40 mm

Table A2: Solar Radiation & Temperature against Time at 6.8 m/s Exit Velocity (Unloaded)

Time (Hrs)	1000	1030	1100	1130	1200	1230	1300	1330	1400	1430	1500
Plenum Temperature (°C)	26.7	29.7	28.8	36.7	33.7	34.3	35.6	29.4	30.0	35.5	38.3
Exit Temperature (°C)	26.8	29.1	28.7	35.5	33.5	34.1	35.5	30.1	30.0	34.2	37.6
Ambient Temperature(°C)	23.0	25.9	24.4	29.3	26.0	26.8	27.7	23.4	24.3	30.0	27.7
Solar Radiation (W/m^2)	438.0	710.0	436.0	1065.0	626.0	840.0	571.0	212.6	371.0	1513.0	872.0

Table A3: Solar Radiation & Temperature for 20 mm Thick Layer at 6.8 m/s Exit Velocity

Time (Hrs)	1300	1330	1400	1430	1500	1530	1600	1630
Ambient Temperature (ºC)	28.6	27.0	25.7	24.8	25.9	24.5	23.2	22.1
Air Heater Exit Temperature(ºC)	53.7	55.7	46.5	44.9	41.4	36.8	31.1	25.4
Plenum Temperature (ºC)	44.8	43.2	45.5	43.2	40.7	36.3	31.5	26.5
Tray 1 Exit Temperature (ºC)	36.9	34.6	31.0	31.1	30.9	29.6	27.5	24.7
Solar Radiation (W/m^2)	1168	832	739	670	412	354	151.8	69.0

APPENDIX III: OPTIMISATION AND MODELING

IIIA: TAGUCHI APPROACH

Table A1: Experimental Plan (L'16 Orthogonal Array)

Experiment	Parameter/Levels		Actual Values of Parameter/ Levels	
	Air Velocity	Grain Layer Thickness	Air Velocity	Grain Layer Thickness
1	1	1	0.212	0.02
2	1	2	0.212	0.04
3	1	3	0.212	0.06
4	1	4	0.212	0.08
5	2	1	0.272	0.02
6	2	2	0.272	0.04
7	2	3	0.272	0.06
8	2	4	0.272	0.08
9	3	1	0.344	0.02
0	3	2	0.344	0.04
11	3	3	0.344	0.06
12	3	4	0.344	0.08
13	4	1	0.408	0.02
14	4	2	0.408	0.04
15	4	3	0.408	0.06
16	4	4	0.408	0.08

IIIB: ANOVA RESULTS

Table A4: ANOVA Results for MRR

Anova: Two-Factor Without Replication

SUMMARY	*Count*	*Sum*	*Average*	*Variance*
0.02	4	0.22	0.055	0.000
0.04	4	0.152	0.038	0.000
0.06	4	0.085	0.021	0.000
0.08	4	0.057	0.014	0.000
MRR at 6.8 m/s	4	0.097	0.024	0.000
MRR at 8.6 m/s	4	0.092	0.023	0.000
MRR at 11.0 m/s	4	0.164	0.041	0.000
MRR at 13.0 m/s	4	0.161	0.040	0.000

ANOVA TABLE

Source of Variation	*SS*	*df*	*MS*	*Fcomputed*	*P-value*	*F critical*
Grain Layer Thickness	0.004	3.000	0.001	103.659	0.000	3.863
Air Velocity	0.001	3.000	0.000	30.202	0.000	3.863
Error	0.000	9.000	0.000			
Total	0.005	15.000				

Anova: Two-Factor Without Replication for Moisture Removal Rate

SUMMARY	*Count*	*Sum*	*Average*	*Variance*
0.02	4	41	10.25	2.917
0.04	4	45.7	11.425	7.529
0.06	4	36	9	4.860
0.08	4	32.7	8.175	13.109
η at 6.8 m/s	4	28.7	7.175	2.709
η at 8.6 m/s	4	32.4	8.1	5.680
η at 11.0 m/s	4	45.3	11.325	2.309
η at 13.0 m/s	4	49	12.25	1.737

ANOVA

Source of Variation	*SS*	*df*	*MS*	*Fcomputed*	*P-value*	*F critical*
Layer Thickness	24.373	3.000	8.124	5.654	0.019	3.863
Air Velocity	72.313	3.000	24.104	16.775	0.000	3.863
Error	12.933	9.000	1.437			
Total	109.618	15.000				

Table A5: ANOVA Results for Drying Efficiency

The SAS System 8:58 Monday, July 4, 2016

The ANOVA Procedure

Class Level Information

Class	Levels	Values
Thickness	4	0.02 0.04 0.06 0.08
velocity	4	11.0m/s 13.0m/s 6.8m/s 8.6m/s

Number of observations 16

The ANOVA Procedure

Dependent Variable: Efficiency

Source	DF	Sum of Squares	Mean Square	F Value	Pr > F
Model	6	96.6850000	16.1141667	11.21	0.0010
Error	9	12.9325000	1.4369444		
Corrected Total	15	109.6175000			

R-Square	Coeff Var	Root MSE	Efficiency Mean
0.882022	12.34210	1.198726	9.712500

Source	DF	Anova SS	Mean Square	F Value	Pr > F
Thickness	3	24.37250000	8.12416667	5.65	0.0186
Velocity	3	72.31250000	24.10416667	16.77	0.0005

Table A6: ANOVA Results for MRR

The SAS System 08:58 Monday, July 4, 2016

The ANOVA Procedure

Dependent Variable: mrr

Source	DF	Sum of Squares	Mean Square	F Value	Pr > F
Model	6	0.00514250	0.00085708	66.93	<.0001
Error	9	0.00011525	0.00001281		
Corrected Total	15	0.00525775			

R-Square	Coeff Var	Root MSE	mrr Mean
0.978080	11.13925	0.003578	0.032125

Source	DF	Anova SS	Mean Square	F Value	Pr > F
Thickness	3	0.00398225	0.00132742	103.66	<.0001
velocity	3	0.00116025	0.00038675	30.20	<.0001

Table A7: **ANOVA Results for Drying Efficiency**

The SAS System 08:58 Friday, July 4, 2016

The ANOVA Procedure

t Tests (LSD) for Efficiency

NOTE: This test controls the Type I comparisonwise error rate, not the experimentwise error
rate.

Alpha	0.05
Error Degrees of Freedom	9
Error Mean Square	1.436944
Critical Value of t	2.26216
Least Significant Difference	1.9175

Means with the same letter are not significantly different.

t Grouping	Mean	N	Thickness
A	11.4250	4	0.04
A			
B A	10.2500	4	0.02
B			
B C	9.0000	4	0.06
C			
C	8.1750	4	0.08
123			

Table A8: ANOVA Results for MRR

The SAS System 08:58 Friday, July 4, 2016

The ANOVA Procedure

t Tests (LSD) for mrr

NOTE: This test controls the Type I comparisonwise error rate, not the experimentwise error rate.

Alpha	0.05
Error Degrees of Freedom	9
Error Mean Square	0.000013
Critical Value of t	2.26216
Least Significant Difference	0.0057

Means with the same letter are not significantly different.

t Grouping	Mean	N	Thickness
A	0.055000	4	0.02
B	0.038000	4	0.04
C	0.021250	4	0.06
D	0.014250	4	0.08

The ANOVA Procedure

t Tests (LSD) for Efficiency

NOTE: This test controls the Type I comparisonwise error rate, not the experimentwise error rate.

Alpha	0.05
Error Degrees of Freedom	9
Error Mean Square	1.436944
Critical Value of t	2.26216
Least Significant Difference	1.9175

Means with the same letter are not significantly different.

t Grouping	Mean	N	velocity
A	12.2500	4	13.0m/s
A			
A	11.3250	4	11.0m/s
B	8.1000	4	8.6m/s
B			
B	7.1750	4	6.8m/s

The ANOVA Procedure

t Tests (LSD) for mrr

NOTE: This test controls the Type I comparisonwise error rate, not the experimentwise error rate.

Alpha	0.05
Error Degrees of Freedom	9
Error Mean Square	0.000013
Critical Value of t	2.26216
Least Significant Difference	0.0057

Means with the same letter are not significantly different.

t Grouping	Mean	N	velocity
A	0.041000	4	11.0m/s
A			
A	0.040250	4	13.0m/s
B	0.024250	4	6.8m/s
B			
B	0.023000	4	8.6m/s

Anova: Two-Factor Without Replication (Comparison of Performance for Trays & Temperature)

SUMMARY	*Count*	*Sum*	*Average*	*Variance*
2.0000	2.0000	36.8500	18.4250	675.2813
1.0000	2.0000	24.1220	12.0610	289.8750
2.0000	2.0000	39.9530	19.9765	793.8917
32.1000	3.0000	100.8000	33.6000	70.0900
0.0480	3.0000	0.1250	0.0417	0.0003

ANOVA

Source of Variation	SS	df	MS	F	P-value	F crit
No of Trays	70.3752	2.0000	35.1876	1.0082	0.4980	19.0000
Temperature	1689.2426	1.0000	1689.2426	48.3986	0.0200	18.5128
Error	69.8054	2.0000	34.9027			
Total	1829.4232	5.0000				

Anova: Two-Factor Without Replication for RH and Temperature

SUMMARY	*Count*	*Sum*	*Average*	*Variance*
RH =56 %	2	0.104	0.052	0
RH =62%	2	0.053	0.0265	0.001201
RRH=62	2	0.094	0.047	0.000072
MRR at 45 degrees C	3	0.156	0.052	0.000001
MRR at 40 degrees C	3	0.095	0.031667	0.00069

ANOVA

Source of Variation	*SS*	*df*	*MS*	*F*	*P-value*	*F crit*
Rows	0.00073	2	0.000365	1.119571	0.471794	19
Columns	0.00062	1	0.00062	1.90138	0.301888	18.51282
Res.Errors	0.000652	2	0.000326			
Total	0.002003	5				

APPENDIX IIIC: MODELING

Table A9: Simulated Air Velocity up Dryer Cabinet

Dryer Cabinet Height (m)	Air Velocity (m/s)
0	0.327268297
0.003511175	0.328888604
0.010095477	0.328604435
0.015066372	0.328077899
0.02	0.331452175
0.025734492	0.331525878
0.03	1.12E-05
0.033852347	1.12E-05
0.04	1.11E-05
0.045232004	2.88E-01
0.049999999	2.88E-01
0.054767994	2.86E-01
0.06	8.65E-06
0.065374618	8.51E-06
0.07	8.39E-06
0.076366019	0.258832932
0.083272131	0.258633457
0.089822713	0.258101351
0.096269323	0.258334668
0.1	0.257519848

IIID DRYING COEFFICIENTS

For 50 degree

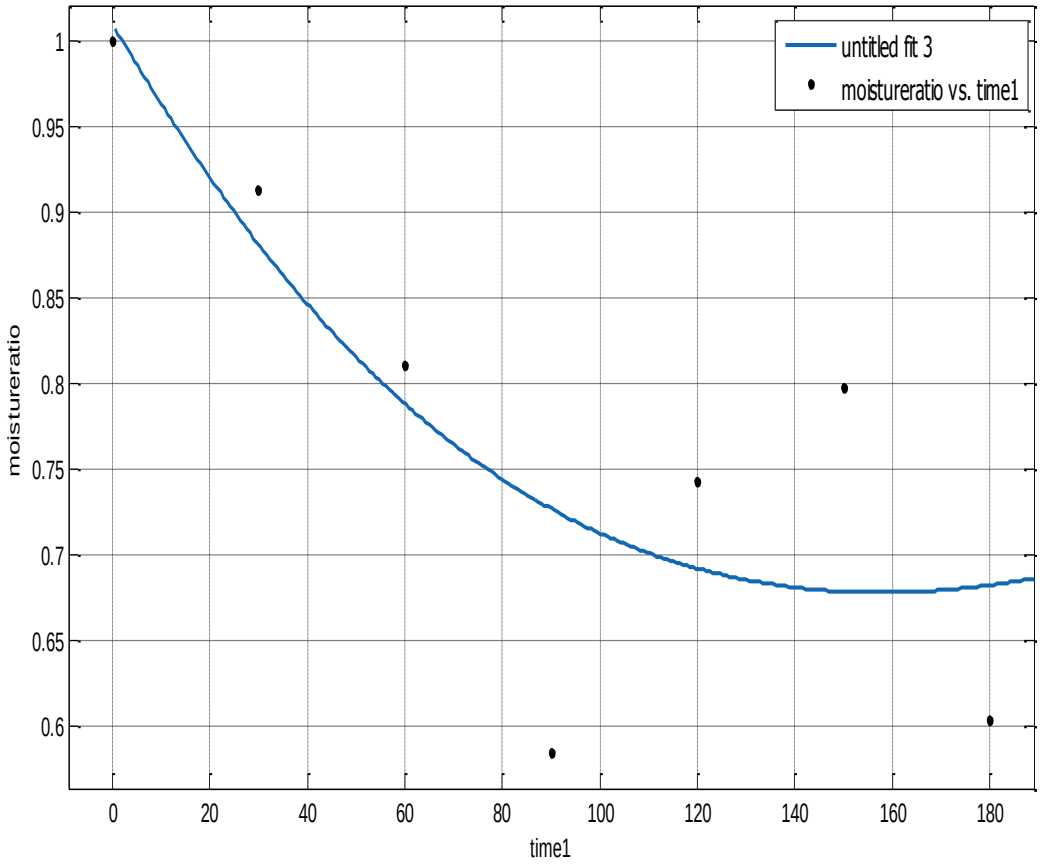

Figure A16: Simulated Drying Curve to Determine Drying Coefficients at 50 °C

Fit found when optimization terminated:

General model:

f(x) = a*exp(-b*x^n)+c*x

Coefficients (with 95% confidence bounds):

a = 1.009 (0.5929, 1.426)

b = 0.006806 (-0.0693, 0.08291)

c = 0.002366 (-0.009787, 0.01452)

n = 1.021 (-2.061, 4.104)

Goodness of fit:

SSE: 0.05183

R-square: 0.6237

Adjusted R-square: 0.2475

RMSE: 0.1314

f(x) = a*exp(-b*x^n)+c*x

Coefficients (with 95% confidence bounds):

a = 1.009 (0.5929, 1.426)

b = 0.006806 (-0.0693, 0.08291)

c = 0.002366 (-0.009787, 0.01452)

n = 1.021 (-2.061, 4.104)

For 40 degrees

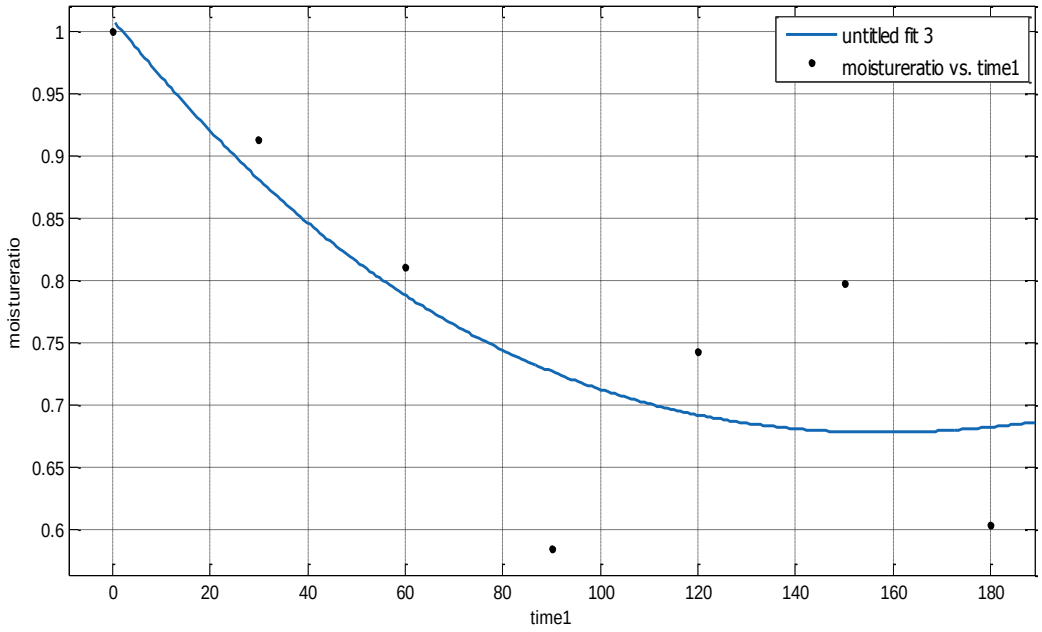

Figure A17: Simulated Drying Curve to Determine Drying Coefficients at 40 °C

Fit computation did not converge:

Success, but fitting stopped because change in residuals less than tolerance (TolFun).

Fit found when optimization terminated:

General model:

f(x) = a*exp(-b*x.^n)+c*x

Coefficients (with 95% confidence bounds):

a = 1 (0.5784, 1.422)

b = 0.006362 (-0.1141, 0.1268)

c = 0.0002749 (-0.03528, 0.03583)

n = 0.8719 (-6.074, 7.818)

Goodness of fit:

SSE: 0.05291

R-square: 0.6159

Adjusted R-square: 0.2317

RMSE: 0.1328

For 45 degree

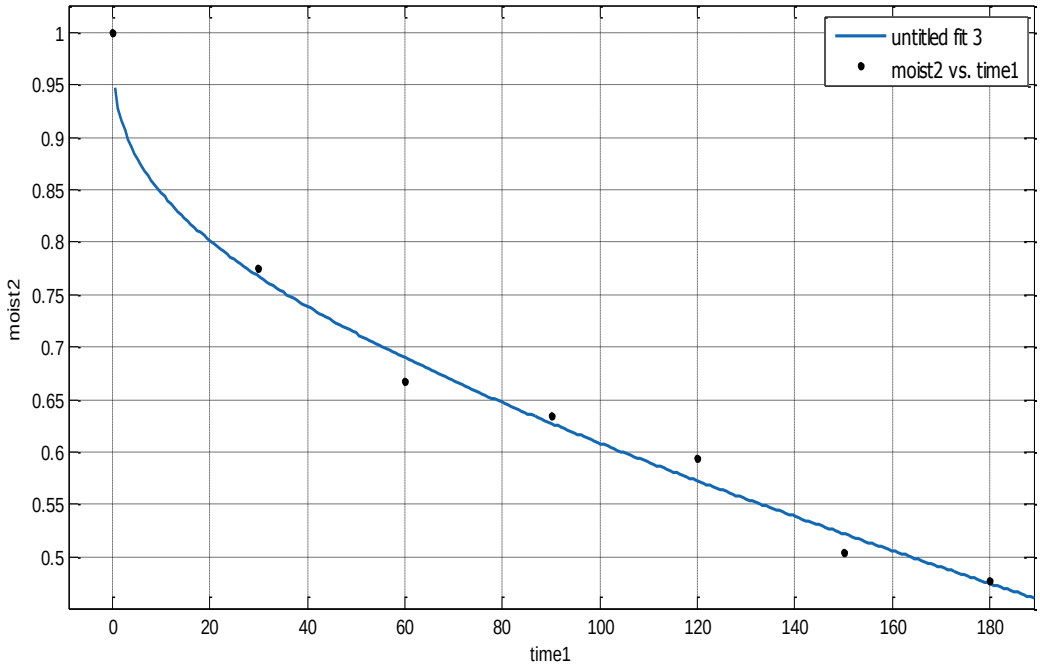

Figure A18: Simulated Drying Curve to Determine Drying Coefficients at 45 °C

General model:

f(x) = a*exp(-b*x^n)+c*x

Coefficients (with 95% confidence bounds):

a = 1 (0.9261, 1.074)

b = 0.06928 (-0.172, 0.3105)

c = -0.00101 (-0.004803, 0.002783)

n = 0.3476 (-0.753, 1.448)

Goodness of fit:

SSE: 0.001623

R-square: 0.9915

Adjusted R-square: 0.9831

RMSE: 0.02326

Degree 55

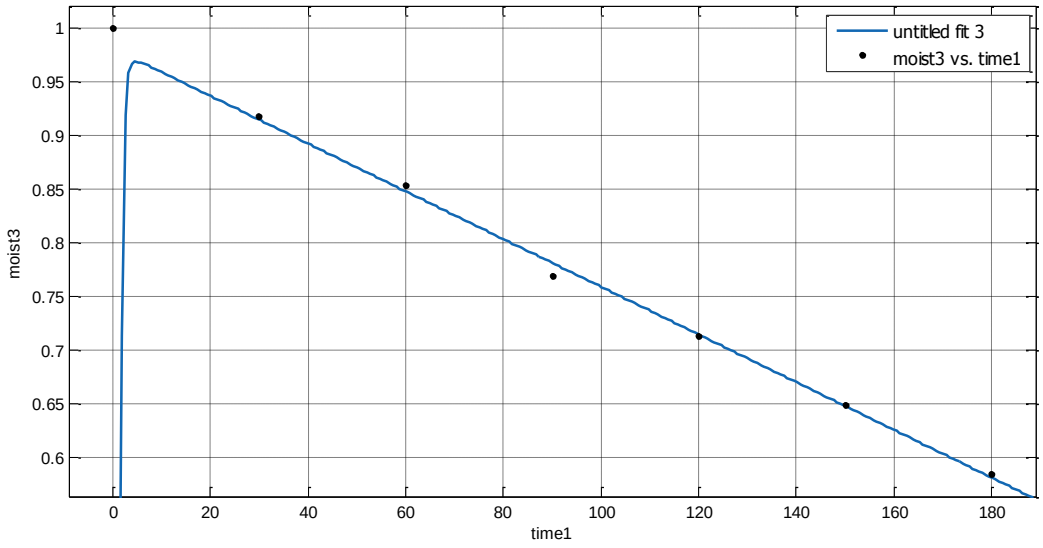

Figure A19: Simulated Drying Curve to Determine Drying Coefficients at 55 °C

General model:

f(x) = a*exp(-b*x^n)+c*x

Coefficients (with 95% confidence bounds):

a = 0.9812 (-3.234, 5.196)

b = 8.258 (-6.989e+09, 6.989e+09)

c = -0.002225 (-0.03135, 0.0269)

n = -5.318 (-2.53e+08, 2.53e+08)

Goodness of fit:

SSE: 0.7737

R-square: -4.824

Adjusted R-square: -10.65

RMSE: 0.5079

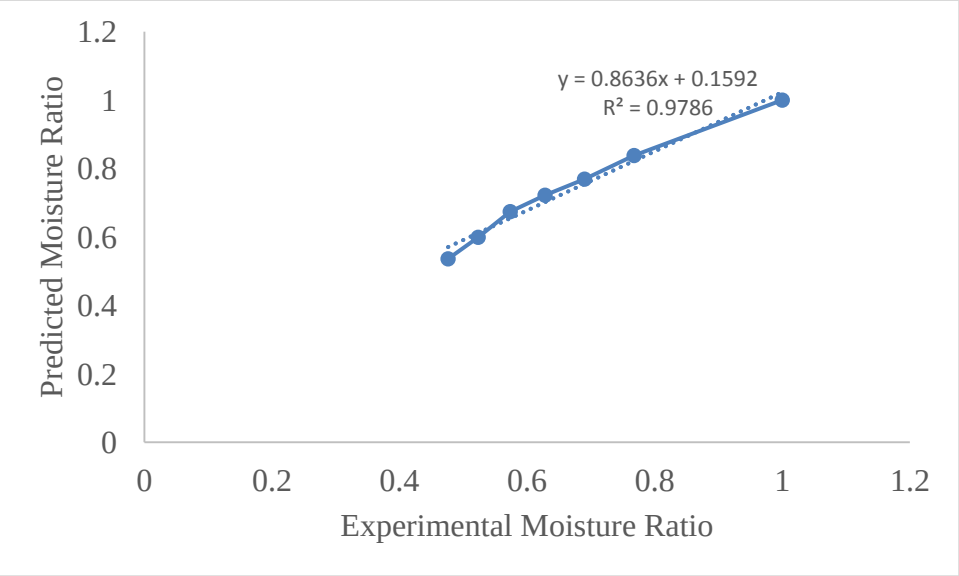

Figure A20: Predicted and Experimental Moisture ratios at 45 °C

APPENDIX IV: MOISTURE CONTENT DATA

IVA BEFORE AND AFTER SOLAR DRYING

Experiment	Moisture Content %		Grain Layer Thickness (m)	Air Velocity (m/s)	Mean Drying Air Temperature (°C)	Mode of drying
	Initial	Final				
1	38.1	19.4	0.02	0.41	36.8	Solar
2	37.5	21.9	0.02	0.41	33.5	Solar
3	42.9	31.6	0.02	0.34	37.8	Solar
4	40.1	32.5	0.04	0.41	32.1	Solar
5	37.2	25.4	0.04	0.34	38.7	Solar
6	39.4	35.9	0.06	0.41	36.4	Solar
7	37.7	35.2	0.06	0.34	38.3	Solar
8	35.8	33.0	0.08	0.41	30.8	Solar
9	38.4	34.5	0.08	0.34	39.6	Solar
10	35.9	22.0	0.02	0.27	36.4	Solar
11	38.0	36.4	0.04	0.27	24.1	Solar
12	38.0	36.7	0.06	0.27	27.0	Solar
13	35.9	22.0	0.02	0.27	36.4	Solar
14	35.7	21.8	0.06	0.27	26.9	Solar
15	35.2	27.6	0.02	0.15	38.4	Solar
16	35.2	27.6	0.02	0.15	38.4	Solar
17	38.5	34.9	0.06	0.15	48.9	Solar
18	38.2	36.5	0.10	0.15	41.8	Solar

IVB MOISTURE RATIO VARIATION DURING DRYING

Time (min)	Xr at 40 °C			Xr at 45 °C			Xr at 50 °C			Xr at 55 °C		
	Expt 1	Expt 2	Expt 3	Expt 1	Expt 2	Expt 3	Expt 1	Expt 2	Expt 3	Expt 1	Expt 2	Expt 3
0	1.000	1.000	1.000	1.000	1.000	1.000	1.000	1.000	1.000	1.000	1.000	1.000
30	0.911	0.901	0.912	0.840	0.855	0.819	0.947	0.961	0.973	0.897	0.878	0.965
60	0.841	0.837	0.812	0.778	0.745	0.784	0.895	0.876	0.859	0.808	0.834	0.919
90	0.813	0.802	0.785	0.721	0.728	0.717	0.859	0.777	0.818	0.713	0.846	0.720
120	0.755	0.738	0.727	0.661	0.671	0.690	0.792	0.739	0.755	0.703	0.650	0.754
150	0.655	0.675	0.689	0.594	0.605	0.598	0.709	0.652	0.688	0.647	0.629	0.687
180	0.640	0.655	0.622	0.540	0.546	0.522	0.682	0.615	0.656	0.609	0.646	0.585

APPENDIX V: ENGINEERING DRAWINGS OF SOLAR DRYER

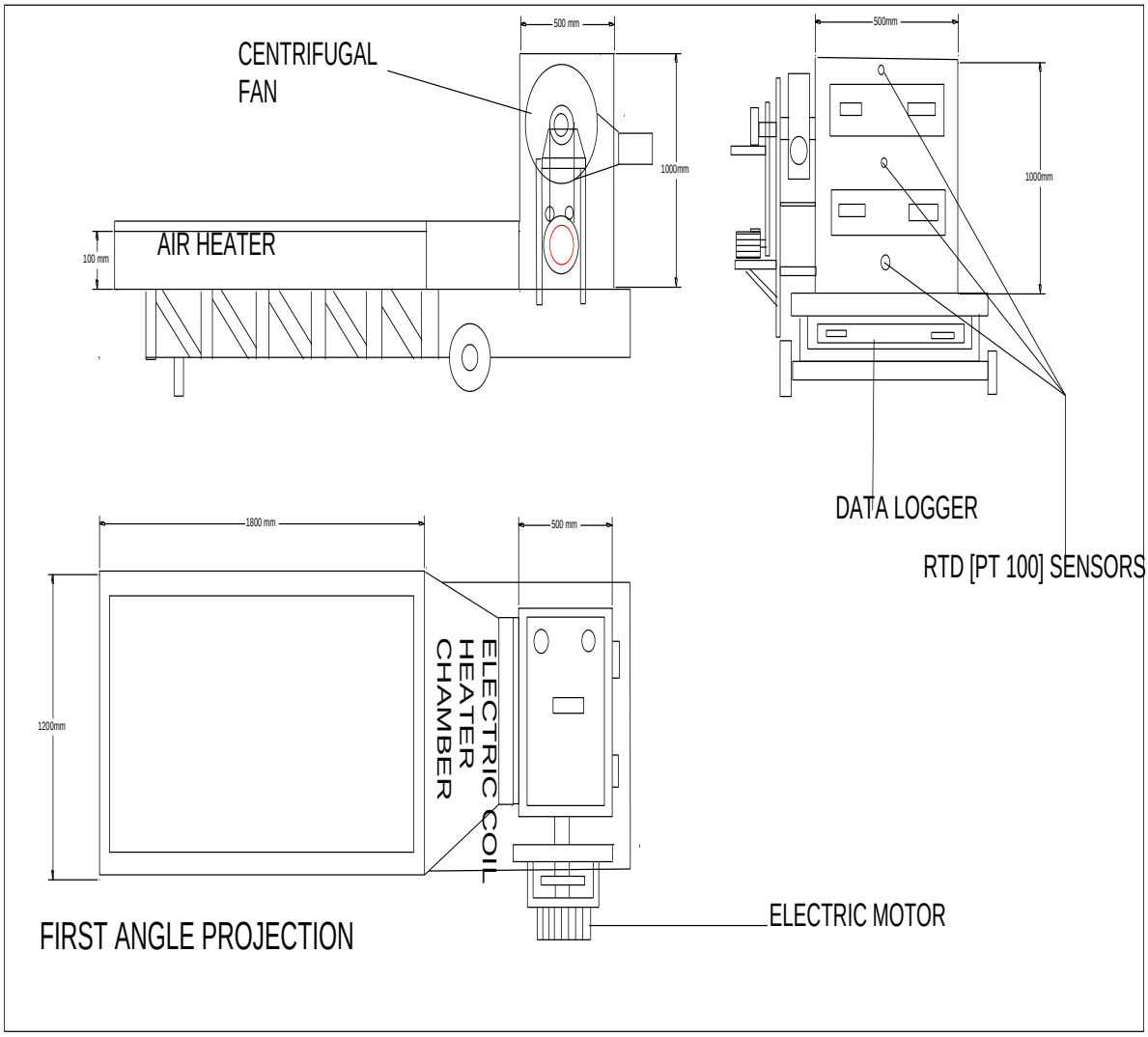

FIRST ANGLE PROJECTION OF SOLAR DRYER

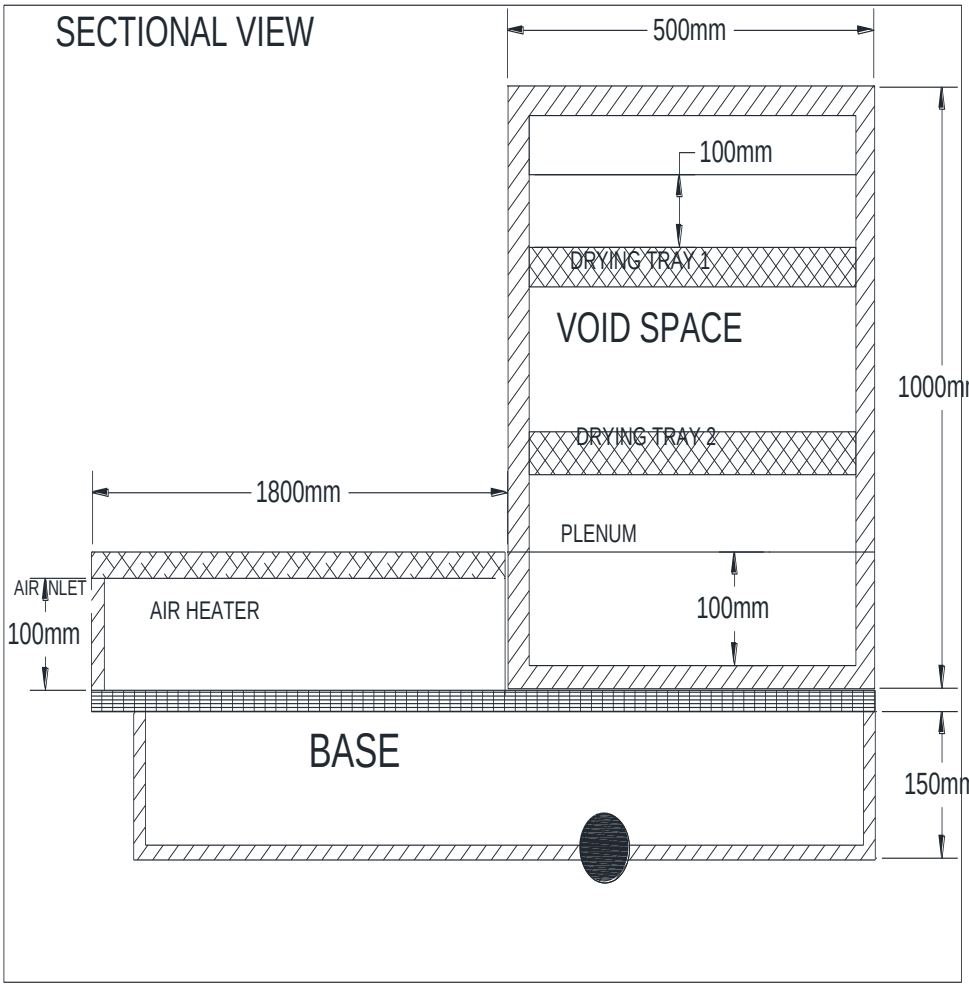

SECTIONAL VIEW OF SOLAR DRYER

APPENDIX VI: SOLAR ENERGY

The surface of the sun, called the photosphere, has a temperature of about 6000K, and behaves as a near perfect black body. It is the source of the solar energy that is incident on the earth. The energy flux received from the sun outside the earth's surface is essentially constant. The solar constant I_{sc} is the rate at which energy is received from the sun on a unit area perpendicular to the rays of the sun, at a mean distance of the earth from the sun. It has a value of approximately 1367 W/m^2 (Klaus *et al*., 2014). The distance between the earth and the sun varies a little through the year, hence the extra-terrestrial flux also varies, and its value I'_{sc} on any day is given by eq. (2.1) [Sukhtame, 1996].

$$I'_{sc} = I_{sc}[\,1 + 0.033cos\frac{360n}{365}\,] \qquad (2.1)$$

(n is the day of the year)

Solar radiation received at the earth's surface is in an attenuated form due to absorption and scattering as it passes through the atmosphere. Absorption is primarily due to ozone and water vapour (and to a lesser extent due to gases such as carbon dioxide, nitrogen dioxide, oxygen and methane) and particulate matter. Scattering is due to gaseous molecules as well as particulate matter. Solar radiation received on the earth's surface without scattering is called beam or direct radiation, while that received after scattering is called diffuse radiation. The sum of beam and diffuse radiation is called total or global radiation (Sukhatme, 1996; Klaus *et al*., 2014).

Due to difficulties in predicting variation with time of beam and diffuse radiation, designers of solar equipment resort to making measurements over a period of time in the location in question, or using available measurements for some other location with reasonably similar climate. A third option is to use empirical equations linking values of solar radiation with other meteorological parameters whose values are known for the location in question. For example, monthly average of global daily radiation on a horizontal surface ($\bar{H}_g$), is given by eq. (2.2) [Sukhtame, 1996], where

$\bar{H}_0$ is the mean value of H_0, the extra-terrestrial radiation which would fall on a horizontal surface of the location for each day of the month.

$$\frac{\bar{H}_g}{\bar{H}_0} = a + b\left[\frac{\bar{S}}{\bar{S}_{max}}\right] \quad (2.2)$$

(a and b are constants which have been obtained for various locations). For example, for Kisangane, Zaire, the ratio $\frac{\bar{S}}{\bar{S}_{max}}$ ranges between 0.34-0.56, a = 0.28, b= 0.39). H_0 is obtained from eq.(2.3) [Sukhtame, 1996].

$$H_0 = \frac{24}{\pi} I_{sc}\left[1 + 0.033cos\frac{360n}{365}\right](\omega_s sin\delta + cos\emptyset cos\delta sin\omega_s) \quad (2.3)$$

Declination (δ), hour angle (ω_s) and maximum possible day length or sunshine hours (S_{max}) are obtained from eqs. (2.4) - (2.6), respectively.

$$\delta = 23.45\sin\left[\frac{360}{365}(284 + n)\right] \quad (2.4)$$

$$\omega_s = cos^{-1}(-tan\emptyset tan\delta) \quad (2.5)$$

$$S_{max} = \frac{2}{15} cos^{-1}(-tan\emptyset tan\delta) \quad (2.6)$$

The calculation of $\bar{H}_0$ has been simplified by the determination that its value equals the value of H_0 on specific days of the month, namely January 17, February 16, March 16, April 15, May 15, June 11, July 17, August 16, September 15, October 15, November 14 and December 10. Monthly average daily diffuse radiation may be obtained using similar empirical equations (Sukhatme, 1996; Garg and Prakash, 2005).

To determine monthly average hourly global radiation, eq. (2.8) may be used.

$$\frac{I_g}{\bar{H}_g} = \frac{I_0}{\bar{H}_0}(a + bcos\omega) \quad (2.7)$$

Where

$a = 0.409 + 0.5016\sin(\omega_s - 60°)$ and $b = 0.6609 - 0.4767\sin(\omega_s - 60°)$.

Monthly average hourly diffuse radiation values may similarly be predicted using empirical equations (Sukhatme, 1996; Garg and Prakash, 2005).